Studies of viral entry and viral proteases of coronaviruses and caliciviruses

by

Krishani Dinali Imasha Perera

B.Sc., University of Peradeniya (Sri Lanka), 2014
M.S., Kansas State University, 2018

AN ABSTRACT OF A DISSERTATION

submitted in partial fulfillment of the requirements for the degree

DOCTOR OF PHILOSOPHY

Department of Diagnostic Medicine and Pathobiology
College of Veterinary Medicine

KANSAS STATE UNIVERSITY
Manhattan, Kansas

2022

Abstract

Rabbit hemorrhagic disease virus (RHDV) is a pathogenic lagovirus in the *Caliciviridae* family, which is associated with ongoing outbreaks in the US since 2020. Although vaccines are available, there is no specific treatment against RHDV. Lagovirus-encoded 3C-like protease (3CLpro) is a promising therapeutic target as it is critical for virus replication. In chapter 2, we identified 3CLpro inhibitors that are effective against pathogenic lagoviruses *in vitro* that could be developed into broad-spectrum antivirals to target multiple lagoviruses.

Feline infectious peritonitis virus (FIPV) is a virulent feline coronavirus that causes a fatal systemic infection in cats. FIPV also encodes a 3CLpro, which is essential for the replication of the virus. We passaged FIPV in the presence of 3CLpro inhibitors to investigate the generation of antiviral resistance in chapter 4. Our results showed that mutant FIPV reduce the susceptibility to 3CLpro inhibitors, which can be recovered by the addition of P-gp inhibitors in cell culture. Therefore, the role of P-gp activity in the generation of resistance to 3CLpro inhibitors in FIPV needs further investigations.

Severe acute respiratory syndrome coronavirus 2 (SARS-CoV-2) is the causative agent of COVID-19 pandemic. In chapter 6, we studied the entry of SARS-CoV-2 in cell lines expressing angiotensin-converting enzyme 2 (ACE2) from different animal species using a pseudovirus system. We identified that all the tested animal ACE2 receptors supported the entry of pseudoviruses at various levels. Combinations of spike mutations found in variants had various effects on the entry of pseudoviruses into ACE2 expressing cells. This study contributes to the understanding of the SARS-CoV-2 host range and the effect of spike mutations on the entry of the virus into human and animal ACE2 expressing cells.

Studies of viral entry and viral proteases of coronaviruses and caliciviruses

by

Krishani Dinali Imasha Perera

B.Sc., University of Peradeniya (Sri Lanka), 2014
M.S., Kansas State University, 2018

A DISSERTATION

submitted in partial fulfillment of the requirements for the degree

DOCTOR OF PHILOSOPHY

Department of Diagnostic Medicine and Pathobiology
College of Veterinary Medicine

KANSAS STATE UNIVERSITY
Manhattan, Kansas

2022

Approved by:

Co-Major Professor
Yunjeong Kim

Approved by:

Co-Major Professor
Kyeong-Ok Chang

Copyright

Abstract

Rabbit hemorrhagic disease virus (RHDV) is a pathogenic lagovirus in the *Caliciviridae* family, which is associated with ongoing outbreaks in the US since 2020. Although vaccines are available, there is no specific treatment against RHDV. Lagovirus-encoded 3C-like protease (3CLpro) is a promising therapeutic target as it is critical for virus replication. In chapter 2, we identified 3CLpro inhibitors that are effective against pathogenic lagoviruses *in vitro* that could be developed into broad-spectrum antivirals to target multiple lagoviruses.

Feline infectious peritonitis virus (FIPV) is a virulent feline coronavirus that causes a fatal systemic infection in cats. FIPV also encodes a 3CLpro, which is essential for the replication of the virus. We passaged FIPV in the presence of 3CLpro inhibitors to investigate the generation of antiviral resistance in chapter 4. Our results showed that mutant FIPV reduce the susceptibility to 3CLpro inhibitors, which can be recovered by the addition of P-gp inhibitors in cell culture. Therefore, the role of P-gp activity in the generation of resistance to 3CLpro inhibitors in FIPV needs further investigations.

Severe acute respiratory syndrome coronavirus 2 (SARS-CoV-2) is the causative agent of COVID-19 pandemic. In chapter 6, we studied the entry of SARS-CoV-2 in cell lines expressing angiotensin-converting enzyme 2 (ACE2) from different animal species using a pseudovirus system. We identified that all the tested animal ACE2 receptors supported the entry of pseudoviruses at various levels. Combinations of spike mutations found in variants had various effects on the entry of pseudoviruses into ACE2 expressing cells. This study contributes to the understanding of the SARS-CoV-2 host range and the effect of spike mutations on the entry of the virus into human and animal ACE2 expressing cells.

Table of Contents

List of Figures

List of Tables

Acknowledgements

My heartfelt gratitude extends to my major advisor Dr. Kyeong-Ok Chang and my co-major advisor Dr. Yunjeong Kim. I feel blessed to have met them and the time I spent as a graduate student in their labs will always remain as one of my most successful periods in life. I am forever grateful for their constant advice, unending support and guidance that nurtured me to be who I am today.

My gratefulness also goes to my committee members, Dr. Waithaka Mwangi and Dr. Rollie Clem for their guidance, advice, and words of encouragement during my study.

My sincere gratitude and appreciation go to David George for teaching me, being extremely patient with my all mistakes, and bearing with me for six years. This study would not be possible without his support and motivation each day.

My sincere thanks go to my lab mates Alexandria Zabiegala and Luija Nathali for their companionship and making my lab-life enjoyable. I am thankful to all my friends and colleagues at K-State for being sources of motivation for me throughout these years at Manhattan.

Finally, the tribute of all my achievements goes to my ever-loving husband Kenath, my parents, sister, family, and pets for having faith in me. Their words of encouragement, support, love, and affection made it possible for me to come this far. I am truly blessed to have you all in my life.

Dedication

I dedicate this dissertation to my husband Kenath, and my family for their love, encouragement, and unending support.

Chapter 1 - Review of Literature on rabbit hemorrhagic disease viruses

1.1 Lagoviruses

Lagoviruses are a group of viruses that infect lagomorphs and belong to the family *Caliciviridae*. The name *Caliciviridae* derives from the cup-like (*calyx*) surface of the virions, and the family comprises of viruses that can cause a wide array of diseases in multiple animal species including mammals. However, no zoonotic transmission has been reported in caliciviruses so far. Notable caliciviruses include human noroviruses that cause gastroenteritis, murine noroviruses that causes encephalitis or gastroenteritis in mice, feline caliciviruses causing upper respiratory infections or systemic disease in cats, and lagoviruses infecting rabbits and hares. The lagovirus species include pathogenic and non-pathogenic lagoviruses. Rabbit hemorrhagic diseases viruses (RHDV) and European brown hare syndrome viruses (EBHSV) are pathogenic lagoviruses, whereas rabbit caliciviruses (RCV) and hare caliviruses (HaCV) are considered non-pathogenic lagoviruses.

1.2 Classification of lagoviruses

The nomenclature of lagoviruses and the placement on the phylogenetic tree were based initially on the pathogenicity, antigenic properties, and the host of the virus strains. However, naming the same variants differently, frequent recombination between strains, cross-species infection, and the lack of a cell culture system for serotyping and neutralization assays further complicated this nomenclature schemes. This caused difficulty in distinguishing between subtypes. Thus, a new nomenclature system was proposed by Le Pendu and colleagues based on the gene sequences of

major capsid protein VP60 (1) (Fig. 1.1). According to this proposed nomenclature system, *Lagovirus europaeus* is the virus species within the *Caliciviridae* family that infects lagomorphs. There are two genogroups consisting of lagoviruses, GI and GII (1). GI group is sub-divided into genotypes indicated as GI.1, GI.2, etc. (1). Letters, such as GI.1a, denote the subgroups within genotypes. GII is subdivided into genotypes GII.1 and GII.2 consisting of HaCV (1). The new nomenclature system also proposed the strain name to be written in order of the genogroup, genotype, the Latin name of the species from which the virus was first detected, the country where it was first detected, year of isolation and the identification of the strain from the submitting laboratory (1). The given example for this would be as follows, *Lagovirus europaeus*/GI.1d/*O cun*/FR/2003/03–24 (1).

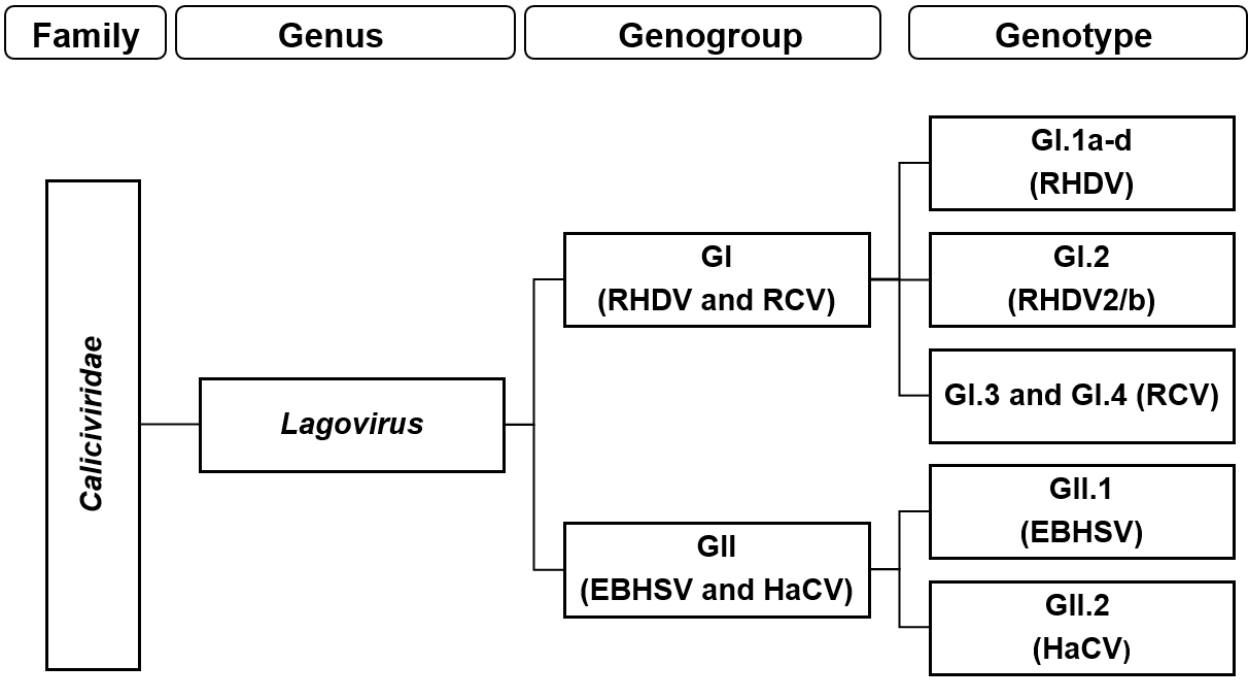

Figure 1.1 Classification of lagoviruses

The proposed classification of lagoviruses according Le Pendu and colleagues (1). *Lagovirus europaeus* is the virus species within the *Caliciviridae* family that infects lagomorphs. Two main genogroups GI and GII further divide into several genotypes, and these genotypes subdivide into variants. GII.2 genotype consist of hare caliciviruses.

1.3 Genome organization of lagoviruses

The characterization of lagovirus genome has been mainly investigated using GI.1/RHDV strains. Lagoviruses were initially categorized as a small, non-enveloped, single stranded RNA virus showing icosahedral symmetry with a diameter of 33-37nm (2–6). Later, it was further characterized as a calicivirus (2,4) with a 7-8 kb long RNA genome (7,8). Lagovirus genomes differ from other caliciviruses by its two open reading frames (ORFs), distinctly based on the ORF1 region that also contains the major capsid protein VP60 (Fig. 1.2). The ORF1 of the genome

encodes a single major polypeptide of 63 kDa (2,4) which is processed into non-structural proteins and the major capsid protein VP60 (7,9) by the virus 3C-like protease (3CLpro) (10). The ORF2 encodes a small (10 kDa) minor capsid protein known as VP10 (11,12). VP10 interacts with VP60 and viral RNA, thereby encapsidating the viral genome (12). The GI.1/RHDV genomic RNA and subgenomic RNA that encodes structural proteins are covalently linked to the viral protein VPg at the 5' end (7). GI.2/RHDV2/b, EBHSV (13,14), RCV (15) and HaCV (16) also have the same genomic organization and characteristics as GI.1/RHDV.

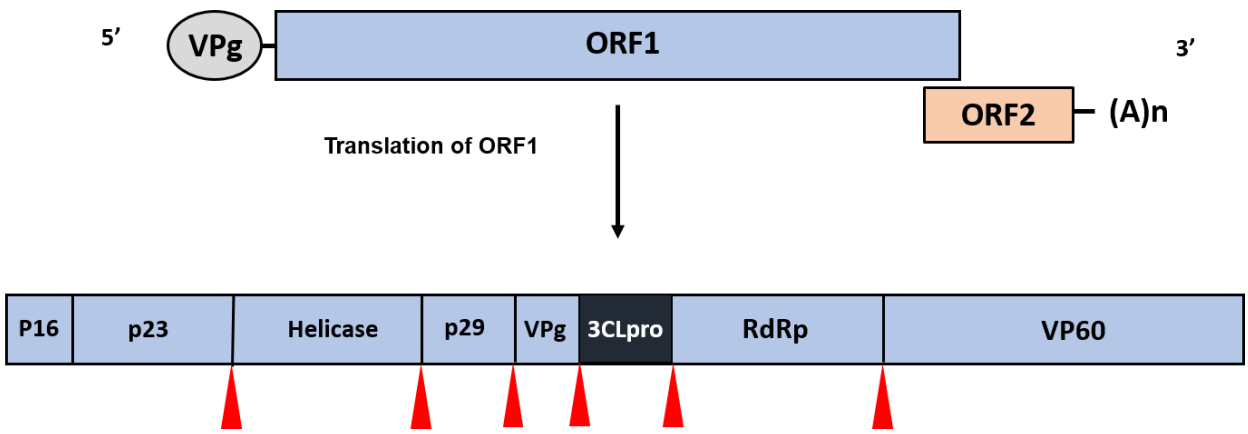

Figure 1.2 Genome organization of lagoviruses

Lagoviruses contain an RNA genome composed of two ORFs: ORF1 that encodes a large polyprotein containing non-structural proteins and the major capsid protein, and ORF2 encoding the minor capsid protein. The polyprotein translated from ORF1 is proteolytically processed by 3CLpro. The confirmed 3CLpro cleavage sites in the polyprotein encoded by ORF1 are indicated as red arrows, and 3CLpro is highlighted in black.

1.4 3CLpro of lagoviruses

A putative protease region was first identified upstream of the RNA polymerase region in the GI.1/RHDV genome (7,17). Further characterization showed that it is functionally similar to picornavirus 3C protease while its size correlated with that of picornavirus 2A protease (10). The GI.1/RHDV 3CLpro specifically cuts GI.1/RHDV polyprotein substrates both in *cis* and *trans* conformations (Fig. 1.2) (10). The predicted catalytic triad was confirmed as H27, D44 and C104, and these residues are crucial for lagovirus 3CLpro activity (10,18). Generally, GI.1/RHDV 3CLpro shows a preference for E, Q or D at P1 site and G, A or S (larger side chain containing substrates) residues at P1' of the polyprotein substrate (12,19,20). No experimental data exists regarding the ability of the EBHSV 3C-like protease to cleave the ORF1-encoded polyprotein. Nevertheless, comparison with GI.1/RHDV sequence indicated that multiple 3CLpro cleavage sites are conserved among EBSHV strains (13,14). Apart from polyprotein processing, GI.1/RHDV 3CLpro may also play a role in inhibition of IFN expression in host cells by cleaving the interferon promoter stimulated 1 (IPS-1) protein (21).

1.5 Rabbit hemorrhagic disease viruses

1.5.1 GI.1/Rabbit hemorrhagic disease virus (RHDV)

The oldest record of GI.1/RHDV dates back to rabbit sera collected in 1955 from different regions in the UK (22). The first description of GI.1/RHDV was as a causative agent of acute viral hepatitis or viral hemorrhagic fever in rabbits (23). However, GI.1/RHDV became more recognized in 1984 after the major outbreak in China which spread among Angora rabbits imported from Germany (3,22,24). Subsequent GI.1/RHDV outbreaks in rabbits (*Oryctolagus sp.*) were reported from

multiple continents across the world. GI.1/RHDV received more attention in the 1990s when the GI.1/RHDV strain Czech V351 virus was used in Australia and New Zealand as a biocontrol agent (32–34). However, rabbits slowly became resistant to the virus and the virus eventually established in the Australian continent (32–34). In the US, GI.1/RHDV was first reported in a rabbit farm in Iowa in 2000 (35).

GI.1/RHDV can be divided into several subtypes, from GI.1a to GI.1d (36–39). The genetic differences between these subtypes are mainly clustered within the major capsid protein VP60 (40), where recombination between strains occur frequently (41). Recombination may also occur rarely in regions of non-structural genes, which could still impact evolution, epidemiology and diversity of GI.1/RHDV (42,43). High level of nucleotide homology (89-100%) within GI genotype has been reported for GI.1/RHDV (44,45), but the mortality and morbidity rates alter with the strains (46).

Transmission of GI.1/RHDV occur predominantly during the breeding season of rabbits (47) and the virus spread through the fecal-oral route (30). Mosquitoes and insects such as fleas and bush flies were also suggested as mechanical vectors (11,48,49). Young rabbits (less than 8 weeks old) are rarely susceptible to the disease but can act as carriers (47). The virus infects both hepatocytes and macrophages, and macrophages are implicated in the systemic spread of infection (50). The GI.1/RHDV associated disease is known as rabbit hemorrhagic disease (RHD). An incubation period of 48-72 hours is followed by an infection period of up to 2 days where the infected animal remains either asymptomatic or show signs of epistaxis associated with the peracute form of RHD (3). The peracute form that leads to sudden death with no clinical signs is the predominant form

of RHD (51,52). The acute form of RHD is also common where rabbits may display signs of anorexia, respiratory distress, hemorrhage, and epistaxis before death (51,52). Necropsy studies have indicated hemorrhage mainly in the liver, spleen, epistaxis, digestive system and kidneys (3,28,29) as a result of terminal disseminated intravascular coagulopathy. Furthermore, the most common pathological finding in the infected and dead rabbits is acute liver necrosis (53). The less common subacute form results in similar but milder clinical signs than the acute form and the infected rabbits usually survive (51,52). During outbreaks, a low percentage of rabbits may experience the chronic form of RHD where they may show signs of severe jaundice, anorexia and lethargy for 1-2 weeks before death (54,55). Rabbits that survive subacute or chronic infections may develop antibodies that confer protection upon re-infection (51,54). Mortality and morbidity rates of natural infections could reach up to 80-99.5% in domestic rabbits (27,28) or around 45-55% in wild rabbits (56,57). Experimental infection of the virus results in mortality rates of 60-100% in infected rabbits within 27-96 hours post infection (5,27,58–60). Prior infection with antigenically similar non-pathogenic rabbit caliciviruses may also provide cross protection in rabbits against GI.1/RHDV infection (61,62).

GI.1 tends to be highly species-specific and infects wild and domestic rabbits (*Oryctolagus* sp.). However, GI.1/RHDV and EBSHV antibodies have been detected in free ranging red foxes (63,64) and predators of rabbits such as feral cats (65). It is possible that this could be antigenic reactions after a meal. GI.1/RHDV strains were also identified in wood mice (*A. sylvaticus*), and Algerian mice (*M. spretus*) that were in the vicinity sharing habitats during GI.1/RHDV outbreaks in rabbits (66). Experimental inoculation of kiwis also generated serological response (67), while 4-6 week old piglets showed low level of RNA replication and low antibody titers (68). However, there are

no indications of natural GI.1/RHDV infections in these species. GI.1/RHDV does not infect or cause disease in humans (69). Yet, RHD is a model for acute fulminant liver disease in humans as RHDV related necrotic and apoptotic mechanisms can provide further insight in to pathogenesis of liver disease in humans and other species (70).

1.5.2 GI.2/RHDV2/b

A new variant of GI.1/RHDV associated with high mortality rates in domestic and wild rabbit populations were first reported from France in 2010 (71). This new variant was classified as GI.2/RHDV2/b, and it quickly became dominant over GI.1/RHDV in multiple regions of the world, including Europe and Australia (72–77). The GI.2/RHDV2/b viruses are recombinants consisting of non-structural genes from pathogenic or benign GI strains and orphan capsid regions (78–81).

GI.2/RHDV2/b causes fatal hepatitis in both wild and domestic rabbits similar to GI.1/RHDV associated RHD. The pathological findings resemble those of RHD and include epistaxis, necrosis or apoptosis, pulmonary congestion, edema, and acute renal tubular injury (82,83). Likewise, peracute form is seen most often where the affected rabbits die without any signs or display reduced appetite and lethargy for a short period immediately prior to death (83). The mortality rates associated with GI.2/RHDV2/b may vary depending on the virus isolate (76,84,85) and other associated factors. GI.2/RHDV2/b infections have been reported less in adult rabbits (76) in contrast to GI.1/RHDV where age plays a major role (86). However, unlike in GI.1 infections, young rabbits are highly susceptible to disease GI.2/RHDV2/b with high mortality (50%) especially in new born and baby rabbits (84,85). One underlying reason could be the inefficient

innate immune response against GI.2/RHDV2/b in young rabbits, that does not prevent the development of fatal necrotic hepatitis (85,87). However, the mechanism underlying the disease susceptibility between GI.1 vs GI.2 has not been understood.

GI.2/RHDV2/b can be introduced into rabbit populations during the annual breeding cycles where extensive replication occurs in young rabbits, causing increased shedding of the virus, clinical disease, and mortality (88). The virus laden carcasses further promote virus transmission leading to outbreaks and eventual removal of the susceptible rabbit populations (88). Experimental infection of GI.2/RHDV2/b has shown poor seroconversion, persistence of the virus, and shedding of infectious virus particles by asymptomatic rabbits (89), indicating another mode of virus transmission via carriers. GI.1 and GI.2 RHDVs are antigenically different, thus, GI.1/RHDV infected rabbits or rabbits receiving vaccination against GI.1/RHDV do not develop immunity against GI.1/RHDV2 (90).

There are reports of GI.2/RHDV2/b infection in hare species. These hare species include mountain hares (*Lepus timidus*), Sardinian Cape hares (*Lepus capensis mediterraneus*), Italian hares (*Lepus corsicanus*) and European brown hares (61,91–94). The infected mountain hares (*Lepus timidus*) showed lesions and tissue distribution similar to EBHSV that infects hares (*Lepus timidus*) (85). Co-infection of EBHSV and GI.2/RHDV2/b has also been reported (93). Additionally, infectious GI.2/RHDV2/b virus was also detected in the carcasses of a Mediterranean pine vole (*Microtus duodecimcostatus*) and two white-toothed shrews (*Crocidura russula*), that were able to cause experimental infections in rabbits (95). GI.2/RHDV2/b has also been detected in a diseased Alpine musk deer (*Moschussifanicus*) that indicated signs of hemorrhage and peracute disease (96) and in

a Eurasian badger (*Meles meles*) (97). However, it is unknown if these animals may serve as reservoirs for the virus in the wild.

The initial detection of GI.2/RHDV2/b in North America was in Canada in 2016 (98) followed by reports of sporadic infections in domestic and feral rabbits from Ohio in 2018 (99), and Washington State in 2019 (100). During the most recent outbreaks across the US, the virus was first detected in March 2020 in New Mexico and subsequently spread through Arizona, Texas, Colorado, Nevada, California, Utah, and eventually across the country. These most recent outbreaks starting from 2020 were the first time that the disease was detected in wild rabbits and hares in the United States. In addition to the rabbits of European origin (*Oryctolagus cuniculus*), desert cottontail rabbits (*Sylvilagus audubonii*), mountain cottontails (*Sylvilagus nuttallii*), black-tailed jackrabbits (*Lepus californicus*), and antelope jackrabbits (*Lepus alleni*) are among the lagomorph species that were affected in the US (82).

1.6 GII.1/European brown hare syndrome virus (EBHSV)

Hares are a minor pest species, and their economic and agricultural impacts are less well understood. However, the increasing population numbers have contributed to them being considered as an undesirable ‘sleeper species’ (61). EBHSV infect hare species and has been circulating in Europe since 1980s (101–103) eventually spreading into other countries. Virions of EBHSV show the typical morphological and genomic characteristics of the *Caliciviridae* family (13,14,54,101,103). The VP60 based homology within strains of EBHSV are high (92-100%), while the homology between G1.1/RHDV and EBHSV strains are 63-69.4% (13,45).

EBHSV is placed in a different branch within lagoviruses (101). Still, the clinical and pathological manifestations of European brown hare syndrome (EBHS) are remarkably similar to RHD despite the genetic and serological differences (104). EBHS is uncommon in young hares but common in adults (104) similar to GI.1/RHDV disease in rabbits. The infected hares usually display the peracute form of disease, where the animals show signs of lethargy and depression a few hours before sudden death (104). Histopathological changes of EBHS include necrotizing hepatitis in hares, however, disseminated intravascular coagulation or hemorrhage occur only rarely (105). EBHSV infects different hare species including mountain hares (*Lepus timidus*) and European brown hares (*Lepus europaeus*) (106,107). Although evidence of natural cross-infection of EBSHV between hares and rabbits is rare, cross-infection can be achieved experimentally (30) and has been detected in the field. One instance is the susceptibility of Eastern cottontail (*Sylvilagus floridanus*) rabbits to EBHSV. Eastern cottontails develop and EBHS-like disease, but is considered a dead-end host (108).

1.7 Non-pathogenic lagoviruses

Rabbit calicivirus (RCV) is a non-pathogenic lagovirus (15) which may have played an important role in the evolution of RHDV strains (54,109). The genomic organization of RCV is the same as RHDV (15) and is more homologous to GI.1/RHDV (~91.5% amino acid identity) than to EBHSV (~75% amino acid identity) (15). RCV infection is asymptomatic and does not result in histopathological lesions. Interestingly, the tissue tropism of RCV is in the intestines unlike in RHDV where the virus shows tropism towards liver or spleen (15,110,111). This tissue tropism is evident in classic RCV strains such as GI.3/06-11/RCV-E1 (71), Michigan rabbit calicivirus (MRCV) (110) and GI.4/ RCV-A1 (111). RCV and GI.1/RHDV also share similar antigenic

epitopes, thus, rabbits pre-exposed to RCV may develop protection against GI.1/RHDV (15). However, RCV infection does not seroconvert or protect hares from EBHSV infections (15).

Hare calicivirus (HaCV) is another nonpathogenic lagovirus, which causes asymptomatic infections in hares. The main site of replication appears to be the intestine similar to RCV (112,113). The first full-genome sequence of a hare calicivirus shows the same genomic organization of other lagoviruses, and is highly homologous to EBHSV (~79% nucleotide identity) (16) indicating a possible role in the evolution of EBSHV.

1.8 Vaccines and therapeutics against lagovirus infections

Vaccines for RHDV are licensed to use in European countries where the virus is endemic. Recently, a recombinant GI.2/RHDV2/b subunit vaccine was developed by Medgene in the US, which was authorized for emergency use by the United States Department of Agriculture (USDA) (114).

Lagoviruses do not grow in cell culture and many of the attempts to culture the virus in primary rabbit kidney cells and primary rabbit hepatocytes have failed (5,115). This has greatly hindered the efforts to study RHDV in cell culture and the discovery of antivirals against RHDV. A few studies investigated the effect of antiviral compounds against RHDV. Non-nucleoside inhibitors (NNIs) such as JTK-109, TMC-647055, Beclabuvir, and PPNDS have been tested against recombinant lagovirus RdRp *in vitro* (116,117). A cocktail consisting of baicalin, linarin, icariin, and notoginsenoside R1 (BLIN) flavonoids was shown to improve survival and alleviate hepatic and oxidative injury in rabbits experimentally infected with G1.1/RHDV (118). Although

decreased RHDV capsid protein expression was observed in BLIN treated experimentally infected rabbits, direct antiviral activity of these compounds has not been tested so far (118). In summary, there are no licensed therapeutics for lagovirus diseases, and no previous reports are available on the effects of compounds targeting 3CLpro of RHDV so far.

Chapter 2 - Potent protease inhibitors of highly pathogenic lagoviruses: Rabbit hemorrhagic disease virus and European brown hare syndrome virus

2.1 Abstract

Rabbit hemorrhagic disease (RHD) and European brown hare syndrome (EBHS) are highly contagious diseases caused by lagoviruses in the *Caliciviridae* family. These infectious diseases are associated with high mortality and a serious threat to domesticated and wild rabbits and hares, including endangered species such as riparian brush rabbits (*Sylvilagus bachmani riparius*). In the United States (U.S.), only isolated cases of RHD had been reported until Spring 2020. However, RHD caused by GI.2/rabbit hemorrhagic disease virus (RHDV)2/b was unexpectedly reported in April 2020 in New Mexico and has subsequently spread to several U.S. states, infecting wild rabbits and hares and making it highly likely that RHD will become endemic in the U.S. Vaccines are available for RHD; however, there is no specific treatment for this disease. Lagoviruses encode a 3C-like protease (3CLpro), which is essential for virus replication and a promising target for antiviral drug development. We have previously generated focused small-molecule libraries of 3CLpro inhibitors and demonstrated the in vitro potency and in vivo efficacy of some protease inhibitors against viruses encoding 3CLpro, including caliciviruses and coronaviruses. Here, we report the development of the enzyme and cell-based assays for the 3CLpro of GI.1c/RHDV, recombinant GI.3P-GI.2 (RHDV2/b), and GII.1/European brown hare syndrome virus (EBHSV) as well as the identification of potent lagovirus 3CLpro inhibitors, including GC376, a protease inhibitor being developed for feline infectious peritonitis. In addition, structure-activity

relationship study and homology modeling of the 3CLpro and inhibitors revealed that lagovirus 3CLpro share similar structural requirements for inhibition with other calicivirus 3CLpro.

This chapter is a published article (119) and can be accessed through the following links.

Citation - Perera, K. D., Johnson, D., Lovell, S., Groutas, W. C., Chang, K.-O., & Kim, Y. (2022). Potent Protease Inhibitors of Highly Pathogenic Lagoviruses: Rabbit Hemorrhagic Disease Virus and European Brown Hare Syndrome Virus. Microbiology Spectrum, e0014222. DOI: https://doi.org/10.1128/spectrum.00142-22

Other accessible links to this publication

PMCID: PMC9430360

https://journals.asm.org/doi/10.1128/spectrum.00142-22

Chapter 3 - Review of Literature on Coronaviruses

3.1 Classification of coronaviruses

Coronaviruses are RNA viruses that infect a wide range of species. As members of the family *Coronaviridae* in the group *Nidovirales,* coronaviruses display the characteristic features of Nidoviruses. These features include large polyproteins (120) and characteristic nested sub-genomic mRNAs that are produced during replication (121,122). Coronaviruses are further divided into four genera within the subfamily of *Coronavirinae*: alpha, beta, gamma and delta (Fig. 3.1). Of these genera, alpha and beta coronaviruses mainly consist of viruses that are known to infect humans. Alpha coronaviruses include human coronaviruses 229E and NL63, and viruses that infect animals such as feline coronavirus (FCoV), ferret coronavirus (FRCoV), mink coronavirus (MCoV), canine coronavirus (CCoV), porcine epidemic diarrhea virus (PEDV), transmissible gastroenteritis virus (TGEV) and many bat coronaviruses including HKU8, and HKU10. Beta coronaviruses that include severe acute respiratory syndrome coronaviruses (SARS-CoV) and SARS-CoV-2 received worldwide attention during the recent COVID-19 pandemic. Beta coronaviruses also include other human coronaviruses that infect the respiratory tract such as Middle East Respiratory Syndrome coronavirus (MERS-CoV), HKU1, and OC43, and animal coronaviruses such as murine hepatitis virus (MHV) and bat coronaviruses such as HKU4, HKU5 and HKU9. A majority of gamma coronaviruses such as infectious bronchitis virus (IBV) infect avian species (123). Delta coronaviruses include a variety of avian coronaviruses (124) and porcine coronaviruses such as HKU15 (125), and some porcine delta coronavirus strains that may also infect humans (126).

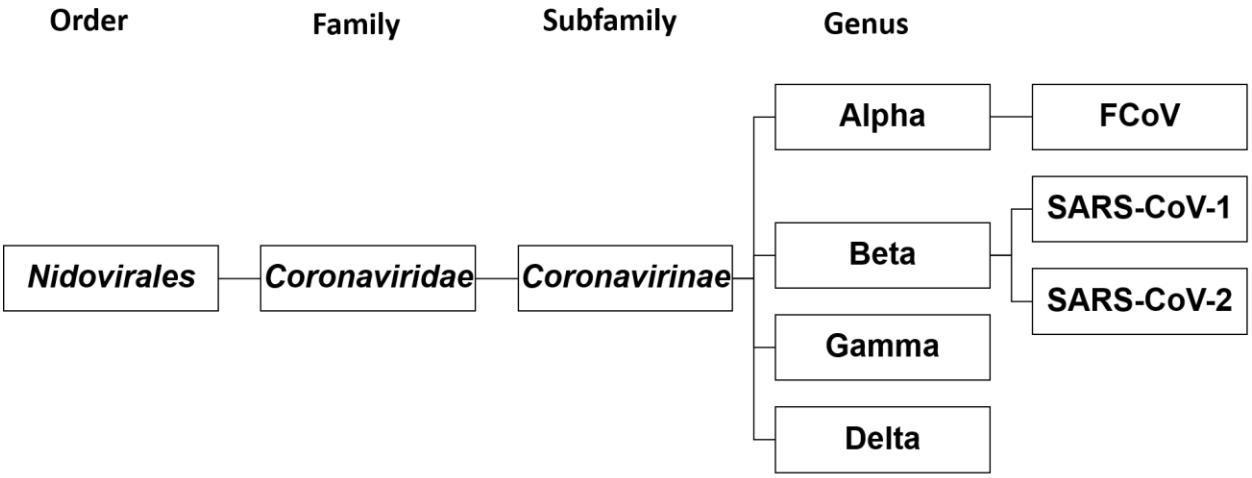

Figure 3.1 Classification of coronaviruses

Classification of the *Coronaviridae* family by the International Committee on Taxonomy of Viruses (127).

3.2 Genome organization of coronaviruses

Coronaviruses are the largest among RNA viruses and the virions display a characteristic 'corona' with its spike proteins under the electron microscope (128–130). The ~ 30kb long positive sense, single stranded, non-segmented RNA genome of coronaviruses contains ~10 ORFs (131) (Fig. 3.2). Of these, ORF1 is the largest and encodes a larger ORF1a and a comparatively smaller ORF1b. ORF1a encodes the polyprotein pp1a and ribosomal frameshifting between ORF1a and ORF1b results in a larger polyprotein pp1ab (128,132–134). The polyprotein ppla may contain 1-11 non-structural proteins and pp1ab may consist of 1-16 non-structural proteins depending on the genera. These polyproteins are processed into non-structural proteins by endogenous virus proteases, papain-like protease (PLpro) and the main protease or 3C-like protease (3CLpro). The remaining ORFs encode the structural proteins, spike (S), envelope (E), membrane (M) and

nucleocapsid (N) (128,135). S protein of coronaviruses are trimeric glycoproteins on the virion surface that mediate entry into the host (136). The heavily phosphorylated N proteins form the nucleocapsid and binds to viral RNA, while the small M proteins interact with the N proteins (130,137,138). The E proteins form the envelope, and E protein of SARS-CoV is reported to have ion channel activity (139). The arrangement of accessory genes within the genome and their functions differs between virus genera (Fig. 3.2).

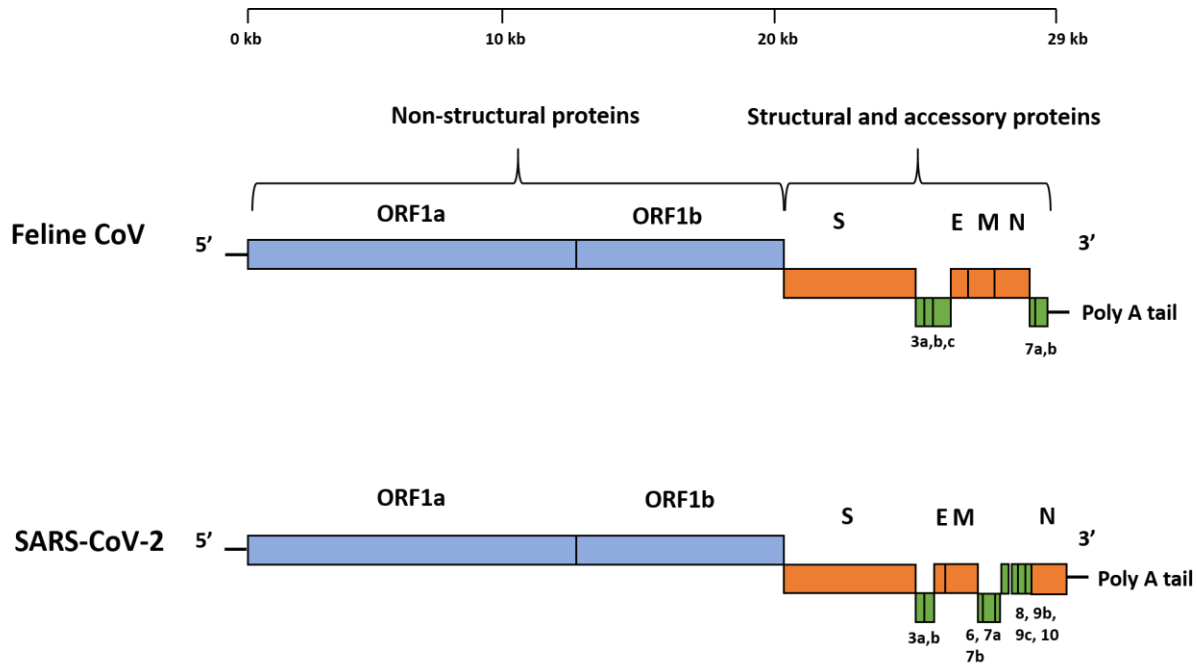

Figure 3.2 Genome organization of coronaviruses

In coronaviruses, ORF1 is translated into pp1a and pp1ab, which are subsequently processed by viral proteases to generate non-structural proteins. ORFs S, E, M and N generate structural proteins and ORFs encoding accessory proteins are in between the structural genes.

3.3 Replication of coronaviruses

Interaction of the coronavirus S protein with its cognate receptor on the host cells initiates the virus entry into the cell. Coronaviruses are known to utilize different receptors. These include angiotensin-converting enzyme 2 (ACE2) used by HCoV-NL63 and SARS-CoV and SARS-CoV-2 (140–144), dipeptidyl peptidase 4 by MERS-CoV (145), and aminopeptidase N by TGEV, PEDV, HCoV-229E, and type II FCoV (146–148). The spike protein of coronaviruses is a class I fusion protein comprising of three domains: ectodomain, transmembrane domain and endodomain. The endodomain consists of S1 and S2 domains (136,149). The receptor-binding domain (RBD) is within the S1 domain, and the fusion peptide is contained within the S2 domain. Binding of the S protein to its receptor triggers a cascade of reactions. Subsequent cleavage between S1 and S2 domains exposes the fusion peptide initiating membrane fusion and uncoating of the virus (150–152).

The RNA genome of the virus is translated within the host cell. PLpro and 3CLpro proteolytically process these translated polyproteins. PLpro processes 1-4 of the N terminal cleavage sites of the non-structural proteins while the remaining 8-11 sites are processed by 3CLpro (153) (Fig. 3.3). The assembly of these non-structural proteins forms a membrane attached replication-translation complex where genomic and subgenomic mRNAs are synthesized (154–158). Translation of subgenomic mRNA generates structural and accessory proteins. These structural proteins undergo maturation while transporting through the endoplasmic reticulum-associated secretory pathway (158,159). Subsequently, the assembled virions are transported and released at the cell surface.

3.4 Coronavirus 3CLpro

3CLpro is the main protease of coronaviruses, which cleaves a majority of the cleavage sites in the virus polyprotein (Fig. 3.3). 3CLpro is a chymotrypsin like serine protease that resembles the 3C protease of the viruses in the picornavirus-like superfamily (160). The active 3CLpro is a dimer of monomers. Each monomer consists of three domains, I, II and III. The active site of coronavirus 3CLpro is between domains I and II and is composed of a catalytic dyad consisting of residues Cys and His (160–164) (Fig. 3.5). During the processing of coronavirus polyprotein, a nucleophilic attack is initiated by nucleophilic Cys, while His functions as the proton acceptor (164,165). Domain III is important for the dimerization of 3CLpro (160,161,164–168). Coronavirus 3CLpro cleaves the polyprotein substrate at P2-P1-P1’ residues where cleavage occurs specifically between the P1 and P1’ residues. Thus, the amino acids in the locations P2, P1 and P1’ in the virus polyprotein are important for substrate specificity. In feline coronavirus 3CLpro, the preferred amino acids in the sites are as follows, Lys at P2, Gln at P1 and small aliphatic residue such as Ser or Ala at P1’ (153,165,169,170) (Fig. 3.4).

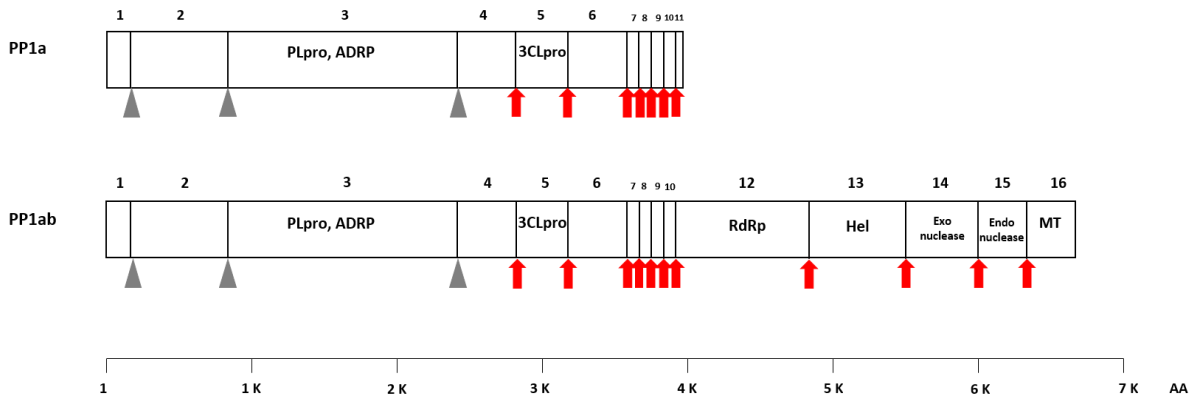

Figure 3.3 3CLpro cleavage sites of feline coronaviruses

Schematic cleavage map of feline coronavirus polyproteins (adapted from (133)). Proteolytic processing of PP1a generates 1-11 non-structural proteins while pp1ab generates the non-structural proteins 1-10 and 12-16. The cleavage sites of PLpro (grey) and 3CLpro (red) are indicated in the map. The putative functions of several non-structural proteins are designated in the diagram (abbreviations: ADRP - ADP-ribose 1"-phosphatase; RdRp - RNA-dependent RNA polymerase; Hel - helicase; Exo. N – exonuclease; Endo. N – endoribonuclease; MT - 2'-O-methyltransferase).

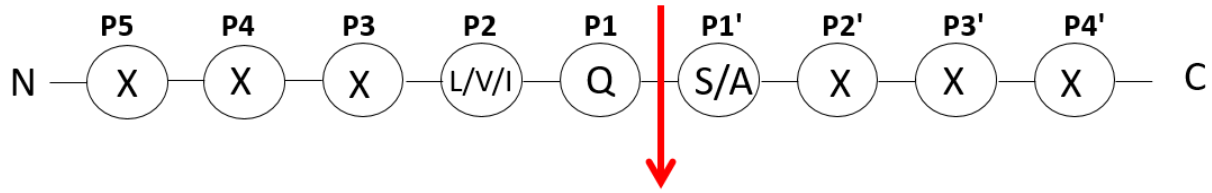

Figure 3.4 Substrate preferences of FIPV 3CLpro

The amino acid specificity at the 3CLpro cleavage sites in the polyprotein are marked P5 to P4' from the N to C termini (adapted from (170). Cleavage occurs between the residues P1 (Glutamine) and P1' (Serine or Alanine) as indicated by a red arrow.

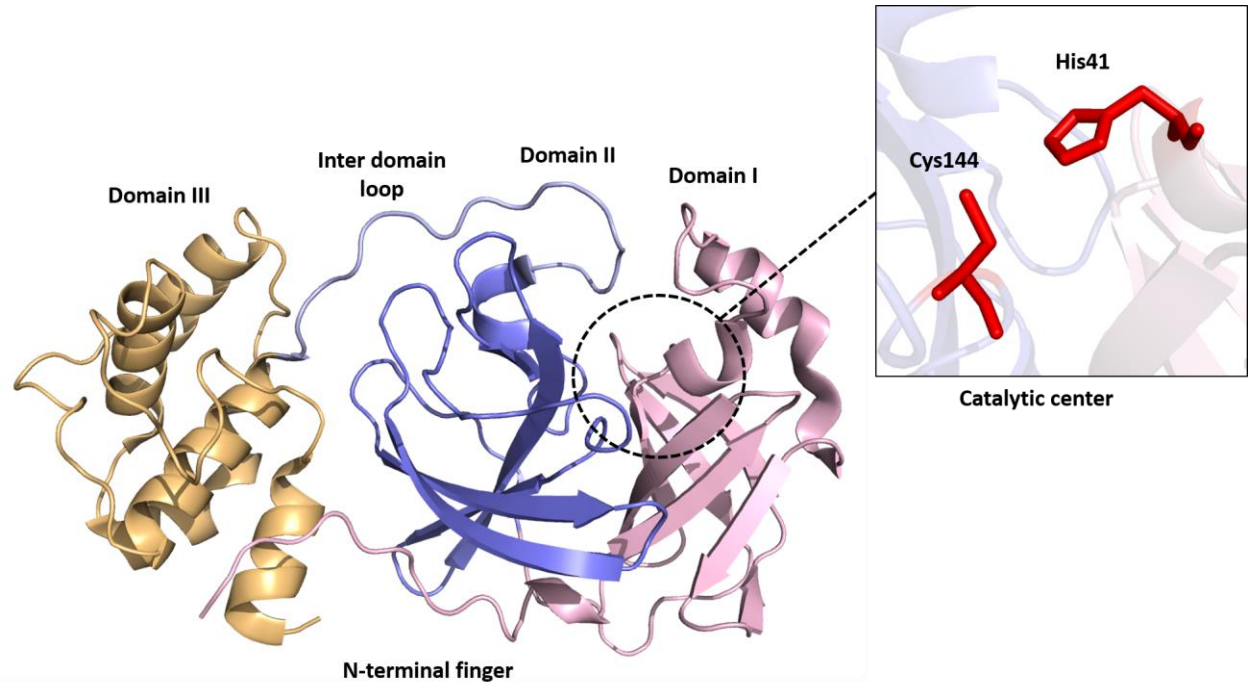

Figure 3.5 3CLpro crystal structure of FCoV (PDB accession 4ZRO)

The 3CLpro monomer of FCoV consists of domains I, II and III. The catalytic residues His41 and Cys144 are indicated in red (zoomed in) at the catalytic center between domain I and II. An inter domain loop connects domains II and III. The active form of 3CLpro is a dimer, and dimerization requires interactions between the C terminal residues in domain III and the N terminal residues in domain I of two monomers. This is modified from the figure 1-4 of the MS dissertation chapter 1 of Perera, 2018 (171).

3.5 Feline coronavirus (FCoV)

FCoVs infect felids and have the classic features of other coronaviruses. An interesting feature of FCoVs is the existence of two serotypes (I and II) and two biotypes (feline enteric coronavirus or FECV and feline infectious peritonitis virus or FIPV). The serotypes I and II are based on the S protein, where the S gene of type I is of feline origin and type II S gene is a recombinant of FCoV

with CCoV (172–174). Type I is the predominant serotype in the field (175–178). Occasional co-infection of both serotypes has also been reported (175,176,178). The two serotypes use different cellular receptors. The receptor for type I is unknown, while type II FCoV uses feline aminopeptidase N (fAPN or CD13) (179,180). Type II FcoV is reported to interact with feline cell-specific intracellular adhesion molecule-3-grabbing non-integrin (DC-SIGN) to enhance entry into host cells (181,182). Type I FCoV does not grow well in cell culture, but cell culture systems have been established for type II FCoVs (183). Thus, laboratory-based research on FCoVs is mainly based on the type II FCoV strains.

As mentioned in the above paragraph, there are two biotypes of FCoVs based on the clinical disease. Feline enteric coronavirus (FECVs) are FCoVs that cause mild enteritis or no symptoms. FECV infect enterocytes (183–185) causing villous atrophy (186,187), but mortality is rare. The infected cats often recover completely, however, may also show intermittent or persistent shedding of the virus for a prolonged time (187,188). This facilitates infections of naïve cats or re-infections in multi cat households, shelters and catteries via the oral-fecal route (188,189). Co-infection with different FECV strains has also been reported (188,190).

3.5.1 Feline infectious peritonitis virus (FIPV)

Feline infectious peritonitis virus (FIPV) is the virulent biotype of FCoV and causes a fatal, systemic disease known as feline infectious peritonitis (FIP) in ~5% of infected cats (191). FIP is common in 6 months to 2 years old cats (192–197), and certain breeds such as Abyssinians, Bengals, Birmans, Himalayans, Ragdolls and Rexes (197–199) are genetically predisposed to FIP. Increased FIP prevalence is seen in sexually intact males, cats living in multi cat households, and

with stress and co-infections with feline leukemia virus or feline immunodeficiency virus (194,200,201). However, FIP rarely transmits between cats.

Unlike FECV, FIPVs show a tropism towards macrophages (202,203), which could be a key feature leading to systemic infection or FIP (204). Two main clinical forms of FIP have been characterized based on the development of effusion in the body cavities. These are the wet/effusive form and the dry/non-effusive form. As the name suggests, dry form shows no to little effusion but can progress into the wet form, where protein and fibrin rich effusions accumulate in the chest and/or abdomen of the infected cats. The host immune response appears to play a major role in the development of FIP. The dry form results from a partial immune response, and poor cellular immune response is associated with the wet form (204). Thus, a potent cellular immune response appears to be important for protection against FIP. Poorly neutralizing antibody response does not offer effective protection, and is associated with antibody dependent enhancement *in vitro* (194,205–209). In addition to effusions, FIP-associated lesions include characteristic granulomatous lesions (consisting of macrophages, neutrophils, lymphocytes and plasma cells), and vasculitis in multiple organs such as the liver, kidneys and the central nervous system (204,210–213).

The mechanism of development of FIPV is not very clear. One of the proposed theories is that FIPV is circulating among cats, which is distinct from FECV (214). The other widely accepted 'internal mutations theory' is that FIPV evolves from internal mutations in FECV that eventually acquire macrophage tropism in the infected cats (194,195,215–218). Accessory proteins have been studied to understand their involvement in the shift in tropism to macrophages and evolution of

FIPV. An intact 3c protein supports replication in intestinal cells while the truncated versions allow the switch into macrophages (195,216). The intact form of 7b protein is important for FIPV replication in macrophages (219) and deletions result in a loss of virulence (220). Nevertheless, the exact mechanism for internal mutation theory is still unclear.

3.6 Vaccines and therapeutics against FCoV infections

Felocell FIP (Zoetis US) is available for FIPV but it is not licensed for young kittens (<16 weeks) (211,221), and is not effective against various field strains. Thus, it is not recommended by the American Association of Feline Practitioners (AAFP). Treatment options are currently limited to symptomatic care (213). Different antiviral compounds such as nucleoside analogs (222–229), small interfering RNA (siRNA) (230,231), synthetic peptides and monoclonal antibodies to inhibit attachment and membrane fusion (232–240) have been tested against multiple coronaviruses. Host factors have also been studied as targets to design inhibitors for coronaviruses (241). Still, none has received authorization for use for FIPV by FDA.

3.6.1 3CLpro inhibitors

Protease inhibitors that target PLpro (242–245) and 3CLpro are attractive antiviral choices among the different inhibitors for coronaviruses. Of these two viral proteases, coronavirus 3CLpro has been studied extensively. The 3CLpro inhibitors reported include natural compounds (246–248), synthetic compounds such as metal conjugates (249–252), nucleoside analogs (253), keto-glutamine analogues (254), and inorganic compounds and their derivatives (161,237,255–261).

Peptidomimetic inhibitors have also been developed as 3CLpro inhibitors. These peptidomimetic inhibitors target the active site and interact with the catalytic Cys residue by closely resembling the coronavirus polyprotein (164,170,262–270), or the dimeric interface to block dimerization of the 3CLpro (271,272). Our lab group has identified and characterized peptidomimetic 3CLpro inhibitors that target the active site of 3CLpro of different coronaviruses infecting humans as well as animals such as FIPV (263,268,273–278). GC376 is one such 3CLpro inhibitor that is highly potent against FIPV in experimental (279) as well as natural infections (280), which was the first demonstration of validity of coronavirus 3CLpro as a drug target *in vivo*, and is currently under clinical development. Furthermore, the efficacy of GC376 and its structural derivatives were also demonstrated against SARS-CoV-2 and multiple human coronaviruses (281–286). Among other tested 3CLpro inhibitors is Paxlovid (PF-00835231), which is a clinical antiviral drug combination of nirmatrelvir and ritonavir developed by Pfizer that shows potent inhibition of SARS-CoV-2 (287,288).

3.7 Antiviral resistance to 3CLpro inhibitors

Antiviral resistance is a global concern in antiviral therapy as it compromises the clinical efficacy of antiviral drugs, especially in treating RNA viruses. RNA viruses can evolve rapidly due to the general lack of intrinsic proof reading activity in the virus replicase protein, which generates genetic variants or quasispecies within a single host (289,290). Exposure to antivirals may select drug-resistant variants among quasispecies. *De novo* genetic variants can also arise in response to selective pressures such as exposure to antiviral treatment. Emergence of antiviral resistance is influenced by the potency and genetic barrier to resistance of a compound. Genetic barrier is the number and type of mutations that is required for the virus to develop resistance against an antiviral

compound while maintaining replicative fitness. Thus, antiviral compounds with a high genetic barrier are preferred. The resistant variants with a higher replication fitness may eventually establish as the dominant variant in the population leading to antiviral resistance (291,292). Emergence of antiviral resistance can also be enhanced by hosts (293,294). Failure to adhere to a treatment regime or prolonged treatment, or a compromised immune response are additional host derived factors that may increase the emergence of antiviral resistance (291,295). To mitigate emergence of antiviral resistance in antiviral treatment, combinations of antiviral drugs of different mechanisms have been used in some viral diseases such as HIV and HCV (293–297).

Studying the mechanism of antiviral resistance expands our understanding on the molecular basis of resistance against antivirals and benefits the development and optimization of antiviral treatment. Unlike other RNA viruses, coronavirus has proof-reading function or unique 3′ to 5′ exonuclease activity in the nsp14 protein (298). Despite a lower error rate compared to other RNA viruses, the error rate of coronaviruses is still higher than that of DNA viruses (299). Six SARS-CoV-2 lineages (C.37 Lambda, B.1.1.318, B.1.2, B.1.351 Beta, B.1.1.529 Omicron, P.2 Zeta) have naturally occurring changes within the 3CLpro gene (G15S, T21I, L89F, K90R, P132H, L205V) (300) compared to the parental SARS-CoV-2 strain. The 3CLpros carrying K90R, G15S and P132H showed comparatively similar activity as the 3CLpro of parental SARS-CoV-2 and remained susceptible to nirmatrelvir, a 3CLpro inhibitor in Paxlovid (300). Similar studies on the 3CLpro of SARS-CoV-2 variants including alpha, beta, gamma, and omicron carrying 3CLpro mutations such as K90R, G15S and P132H showed comparatively similar susceptibility to nirmaltrelvir as the parental SARS-CoV-2 (301–304,304). Multiple studies conducted on the parental SARS-CoV-2 passaged in the cell culture in the presence of nirmatrelvir showed

mutations both close or distal to the nirmatrelvir binding site in the 3CLpro (305–307). These *in vitro* generated mutations were also identified in low levels among the circulating SARS-CoV-2 isolates (305,306). Among these mutations, E166V mutation within the substrate binding site conferred a ~80-100-fold resistance to nirmatrelvir but showed low viral replicative fitness (306,307). However, combination of L50F and T21I with E166V rescued the replicative fitness of the E166V mutant virus (306). Still, these SARS-CoV-2 3CLpro mutant viruses were susceptible to remdesivir (306,307) suggesting the importance of combining antivirals targeting different viral proteins to mitigate antiviral resistance. Nevertheless, SARS-CoV-2 resistance to nirmatrelvir in patients receiving Paxlovid has yet to be reported.

Antiviral resistance has also been investigated for MHV, another beta coronavirus. MHV passaged in the presence of a 3CLpro inhibitor GRL-001 generated resistance within four passages resulting in variants containing single (T26I or D65G) and double (T26I/D65G, T26I/D65A, or T26I/A298D) mutations (308). The single and double mutants increased the 50% effective concentration (EC_{50}) of GRL-001 against MHV by ~3 and ~6 folds, respectively. Among identified mutations in 3CLpro, T26I was particularly close to the active site (308). Nevertheless, these mutants showed a delay in replication *in vitro* and an attenuated phenotype *in vivo* compared to the parental virus (308).

Only a limited number of studies have been published on antiviral resistance of 3CLpro inhibitors against feline coronaviruses. Passaging FIPV in the presence of NPI52 increased the EC_{50} of NPI52 by 15 folds by 10 passages (279), and the resistant FIPV variant showed amino acid changes at S131C, which is located within domain II of 3CLpro (279). However , FIPV did not generate

resistance against GC376 even at 20 passages in cell culture (279). Nevertheless, N25S, A252S and K260N mutations were identified in the 3CLpro of FIPV sequenced from a feline FIP patient that received GC376 treatment for a prolonged period, but did not show clinical resistance (309). Among these mutations, N25S was close to the active site whereas A252S and K260 N were located in the domain III of 3CLpro (309). Only N25S containing recombinant 3CLpro conferred a slight increase in fold change (~1.68-fold increase in the 50% inhibitory concentration) in fluorescence resonance energy transfer (FRET) based enzyme assay (309). This suggests that these amino acid changes have minimal effect on the susceptibility of FIPV to GC376. Another recent study investigated mutations in FIPV in response to viral passaging with GC376 (310). The EC_{50} of FIPV passaged 50 times with GC376 showed an 8-fold increase against GC376, and the genomes of the passaged viruses showed mutations at multiple sites: nsp2 (A403V, A431V), nsp3 (Y891N), nsp4 (P384L, M476K), nsp8 (V159D), nsp12 (T421K, S925P), nsp14 (I262T), and nsp15 (N15V) (310). However, no mutation was observed in 3CLpro. Nsp12-S925P, one of the mutations identified, was partially responsible for conferring the increase in EC_{50} for both GC376 and nirmatrelvir (310). The mutant containing nsp12-S925P were also able to replicate efficiently and reach high titers (10 fold increase) compared to the WT virus (310). The mutant FIPV with nsp12-S925P also showed reduced susceptibility to GC376 in experimentally infected cats (310). The authors reveal that serine to proline mutation causes tighter binding of 3CLpro and increased cleavage efficiency at nsp12-13 cleavage site, thereby, resulting in increased replication fitness of the mutant virus (310). This study indicates that non-target site mutations can affect virus replication and virulence. Thus, combination of multiple inhibitors such as 3CLpro and RdRp inhibitors (310) would be a more prudent and potent antiviral treatment approach against FIPV.

3.8 The role of P-glycoprotein in antiviral resistance

3.8.1 P-glycoprotein

The permeability glycoprotein (P-gp) is a host protein that contributes to multidrug and antibiotic resistance. The multidrug resistance protein (MDR1/ABCB1) or P-gp is an efflux transporter in the ATP-dependent transport protein superfamily (311). The highly polymorphic ATP binding cassette subfamily B (Abcb1) genes encode P-gp. Homologs of P-gp can be found in prokaryotes as well as eukaryotes (312), and many animal species express P-gp in multiple tissues including the liver, intestines, kidneys, and the blood-brain barrier, especially on the apical membrane of enterocytes, hepatocytes, and endothelial cells of the blood-brain barrier (313,314). P-gp on the plasma membrane typically interacts with hydrophobic and cationic compounds and has a broad substrate specificity that includes HIV protease inhibitors, calcium channel blockers and most importantly, many anticancer drugs (315,316). P-gp uses ATP hydrolysis to transport these interacting compounds back to extracellular domains (311). Therefore, P-gp functions as a natural barrier and causes multi drug resistance, especially in antiviral therapy and cancer chemotherapy. The expression level and activity of P-gp increases with age (317) and fluctuates in response to the cell type and hormone levels in different tissues (311). Genetic or extrinsic factors could also change the function of P-gp that could greatly affect its interactions with drugs, altering drug efficacy, safety, and toxicity.

Still, it is unknown whether P-gp is indispensable for normal physiological responses in humans, and the role of P-gp may be species specific. Murine multiple drug resistance (mdr) gene, mdr1a is not essential for normal physiological responses in mice (318). However, the lack of mdr1a

results in increased susceptibility to severe, spontaneous intestinal inflammation that resembles inflammatory bowel disease in humans (319). This highlights its protective role in the GI tract. Interestingly, mdr1 gene deletion in collie dogs results in increased ivermectin sensitivity (320). Feline MDR1 gene is homologous to those of other species and show a similar distribution in cats as humans (314). A majority of feline cancers such as feline lymphoma display a strong expression of P-gp (321) and thus, show resistance to anti-cancer drugs (322,323). Feline P-gp expression level does not correlate with the prognosis of feline lymphoma (324), however, P-gp expression level is considered as a prognostic factor of certain human and canine cancers (325).

3.8.2 The role of P-gp in virus replication

The influence of P-gp in virus replication has been widely studied in HIV infections. Expression of P-gp results in suboptimal penetration of anti-retroviral drugs, thus, limiting their therapeutic effects and creating sanctuaries such as in the brain and the testes for virus persistence (326). HIV-1 infected patients show an increased number of CD4+ T cells expressing P-gp compared to healthy individuals, and progression of HIV-1 further enhances P-gp expressing cell populations (327). However, P-gp function appears to be defective in these cells despite the increased expression levels (327). Similarly, HIV infection also increased P-gp expression in H9 (T cell line) and U937 (monocytic cell line) cells that decreased the accumulation of antiretroviral agents compared to uninfected cells (328). However, HIV infection in human astrocytes, which are cellular reservoir of HIV-1, has a down regulatory effect on P-gp expression (329). Contrastingly, overexpression of P-gp in human CD4+ T-leukemic cells (without changes in the expression levels of HIV receptors CD4 or CXCR4) results in marked decrease of HIV replication (330). HIV may use glycolipid-enriched membrane domains that also harbor P-gp for entry and egress (331). Thus,

this observation could be due to the virus gp41 interacting with P-gp through the hydrophobic fusion domain instead of its cognate receptor, thereby restricting the entry into cells (330). Collectively, these observations indicate the possible existence of cell populations that overexpress P-gp and resist HIV infections (330). Still, the effects of P-gp expression on the clinical outcome of HIV are unknown and requires further investigations using larger study groups. Therefore, differential expression of P-gp in different cell subsets and the use of P-gp expression as a marker of HIV-1 progression requires more extensive studies (327,332).

P-gp is known to affect the metabolism/clearance of some antiviral drugs for HIV and hepatitis C virus (HCV) infections (333,334). For instance, HIV protease inhibitors amprenavir, and indinavir are recognized as substrates of P-gp, increasing drug clearance (335). P-gp levels can be induced by antiretorviral therapy (ART) as HIV patients on ART show enhanced levels of P-gp expression compared to ART-naïve group (336). Thus, targeted inhibition of P-gp using highly specified and potent agents may improve the efficacy of antiviral therapeutics (333,335).

3.8.3 P-gp inhibitors

P-gp inhibitors modulate P-gp function by competitive or no-competitive inhibition. Competitive inhibitors bind P-gp and block the transport of the drug, while non-competitive inhibitors bind either the drug interaction site or another modulator binding site on P-gp causing allosteric changes (reviewed by (337)). There are three groups of P-gp inhibitors or modulators. The first group of inhibitors are therapeutic agents but could be toxic as high concentrations are required for efficacy. The second group of P-gp modulators are analogues of the first group of modulators, but they are

less toxic than the first group. The third group of modulators are developed and targeted against specific MDR mechanisms.

Inhibition of P-gp with compounds such as verapamil, ritonavir, cyclosporine, PSC833 and ivermectin, and the concomitant usage with the drugs that are P-gp substrates could greatly improve their bioavailability and tissue penetration, especially in cancer therapy (313,338–340). Inhibition of P-gp expression with P-gp inhibitors could also increase the bioavailability of HIV protease inhibitors (333,341). Furthermore, P-gp inhibitors could inhibit replication of several viruses. CP100356 hydrochloride (CP100356) is one such P-gp inhibitor that can moderately suppress lassa virus (LASV) and lymphocytic coriomeningitis virus (LCMV) infections by inhibiting low-pH-dependent membrane fusion with minimal cytotoxicity (342). Thus, CP100356 could be used as an effective virus entry inhibitor for LASV and other highly pathogenic mammarenaviruses (342). Apart from the applications in cancer therapy and virus replication, P-gp inhibitors could also alleviate antibiotic resistance (343).

Chapter 4 - In vitro studies of viral resistance to FIPV protease inhibitors

4.1 Abstract

Feline infectious peritonitis virus (FIPV) is a virulent feline coronavirus that causes a fatal systemic infection known as feline infectious peritonitis (FIP) in cats. 3C-like protease (3CLpro) is a virus-encoded protein, which is essential for the replication of viruses within the picornavirus-like superfamily. We have previously developed small molecule inhibitors against 3C-like protease (3CLpro) of multiple coronaviruses including SARS-CoV-2 and FIPV, and GC376 is a clinical candidate for FIP. Here, we passaged FIPV WSU 79-1146 in CRFK cells in the presence of GC376, or its structural derivative GC1003. After eight or twenty passages, we observed a reduction in the susceptibility of passaged FIPV to GC1003 and GC376, respectively, FIPV passaged in GC376 showed no mutations in the 3CLpro region, however, mutations in 3CLpro (G23V and G298S) were identified in FIPV passaged with GC1003. Both passaged viruses also showed mutations in other genomic locations. The 3CLpro with G23V and G298S moderately affected the effectiveness of GC376 and GC1003 against FIPV in fluorescence resonance energy transfer (FRET) assay. Interestingly, incubating the mutant FIPV infected cells with inhibitors of P-glycoprotein (P-gp), a drug efflux pump, restored the susceptibility of mutant FIPV to GC376. In summary, our results showed that passaging FIPV in GC376 and GC1003 led to the identification of mutations outside or within the 3CLpro region, which reduces the susceptibility to 3CLpro inhibitors in cell culture. The effectiveness of 3CLpro inhibitors against the mutant FIPV can be recovered by the addition of P-gp inhibitors in cell culture. Therefore, it is important

to investigate the effect of P-gp activity in the generation of resistance of FIPV to 3CLpro inhibitors.

4.2 Introduction

Feline infectious peritonitis virus (FIPV) is the virulent biotype of feline coronavirus that causes highly fatal systemic disease known as feline infectious peritonitis (FIP) in cats (202). Kittens are more susceptible to FIP and the incidence increases in multi cat households (194,200). Despite the high fatality, there are no commercially available effective vaccines or antiviral drugs for FIP. However, multiple efforts have been made to identify antiviral targets and develop antiviral drugs against FIPV. Virus-encoded 3C-like protease or 3CLpro is one of these targets for developing antivirals against FIPV as well as human coronaviruses including SARS-CoV-2 and MERS-CoV. 3CLpro is the main protease of coronaviruses and plays an essential role in processing the virus polyproteins to release non-structural proteins for virus replication. Our group has reported the efficacy of peptidomimetic 3CLpro inhibitors against multiple coronaviruses including SARS-CoV-2 (281,282,285) and FIPV (273–275,279). GC376 is one such highly potent 3CLpro inhibitor, that has shown efficacy against FIPV in experimentally (279) and naturally infected cats (280) and is a clinical drug candidate for FIPV.

The error-prone replication of RNA viruses contributes to emergence of antiviral resistance which may reduce the efficacy of antiviral drugs and treatment strategies. Although the mutation rate of coronaviruses is comparatively lower than many other RNA viruses owing to the inherent proof-reading activity (344,345), the single-stranded, positive-sense RNA genome of coronaviruses generate virus variants. This was quite evident during the COVID-19 pandemic where multiple

SARS-CoV-2 variants with different transmission, virulence and immune evasion features have emerged. Therefore, it is important to investigate the generation of antiviral resistance in FIPV against 3CLpro inhibitors. Our previous studies have shown that passaging FIPV up to 20 passages in the presence of GC376 did not generate mutations in the 3CLpro region nor antiviral resistance in cell culture (279). Still, mutations were identified in the 3CLpro of FIPV isolated from a feline FIP patient that received GC376 as treatment for a prolonged time although no signs of clinical resistance were identified (280,309). Another recent study identified mutations in multiple sites of the FIPV genome except in 3CLpro region in response to passaging the virus with GC376 for up to 50 passages. In that study, a mutation in nsp12 increased the viral replication in cell culture and virulence in experimentally infected cats (310).

In this study, we passaged FIPV in the presence of GC376 and its structural derivative GC1003, to investigate the generation of antiviral resistance in FIPV. Passaging FIPV in GC376 for 8 times (P8 GC376) resulted in reduced viral susceptibility to GC376 and GC1003 with increased EC_{50}s of GC376 and GC1003 by 13.2 and 3.2-folds, respectively. P8 GC376 had mutations in nsp12 and spike protein but none in the 3CLpro region. Similarly, passaging FIPV in GC1003 for 20 times (P20 GC1003) also reduced susceptibility to both GC1003 and GC376 by increasing the EC_{50}s by 5.6 or 30.2-folds, respectively. P20 GC1003 showed multiple mutations within the genome including the 3CLpro region, and the mutations on the 3CLpro only moderately affected the inhibitory activity of GC1003 in the FRET assay. Because P-glycoprotein (P-gp or ABCB1) plays crucial roles in maintaining intracellular concentrations of antivirals, we examined if P-gp inhibitors could influence antiviral activities of GC376 or GC1003 and/or restore the inhibitory activities of GC376 or GC1003 against P8 GC376 and P20 GC1003 viruses. First, we found that,

in the presence of P-gp inhibitor (Elacridar or CP100356), EC_{50}s of GC376 were not changed, but those of GC1003 and remdesivir were significantly reduced against FIPV in CRFK cells. Interestingly, the antiviral effects of GC376 against P8 GC376 and P20 GC1003 were restored to the levels comparable to the parental virus. These results show that multiple factors are involved in the resistance of FIPV against 3CLpro inhibitors, which includes the involvement of P-gp.

4.3 Materials and methods

4.3.1 Compounds

Synthesis of GC376 (273) and GC1003 were previously described and were synthesized in the laboratory of W. C. Groutas (Department of Chemistry, Wichita State University). Remdesivir was included for comparison purposes. P-glycoprotein inhibitors Elacridar and CP 100356 hydrochloride were purchased from Sigma-Aldrich (St Louis, MO).

4.3.2 Viruses and Cells

Crandell Rees feline kidney (CRFK) cells were maintained in modified Eagle's medium (MEM) supplemented with 5% heat-inactivated fetal bovine serum (FBS), 1% penicillin-streptomycin, and 1% glutamine. FIPV WSU-79-1146 strain was propagated in CRFK cells.

4.3.3 Cytotoxicity assay

To investigate the cytotoxicity of each inhibitor, CRFK cells were treated with each inhibitor at different concentrations up to 150 μM and the cells were left at 37 °C for 36hrs. Then the cell cytotoxicity was measured using the CytoTox 96 nonradioactive cytotoxicity assay kit following

the manufacturer's protocol (Promega, Madison, WI). The 50% cytotoxic concentration (CC_{50}) of each compound was determined using non-linear regression analysis in GraphPad Prism software.

4.3.4 *In vitro* selection of FIPV variants and genetic analysis

To determine the generation of resistance, FIPV WSU 9-1146 was passaged in CRFK cells with gradually increasing concentrations of 3CLpro inhibitors: GC376 or GC1003. Briefly, confluent cells were infected with virus at 0.01-0.1 MOI with the inhibitors at EC_{90}, simultaneously. The infected cells were incubated up to 48hrs at 37 °C. The cells were freeze-thawed after 100% CPE development was observed, centrifuged to remove debris, and kept at -80 °C or passaged into fresh CRFK cells in the presence of increased inhibitor concentration. At each passage, the 50% effective concentration (EC_{50}) for each compound was determined by 50% tissue culture infective dose (TCID50) method (346), and the EC_{50}s were compared with that of the mock passaged virus (Mock) and parental strain (PA). EC_{50} is the concentration of the inhibitor required to decrease the virus titer by 50% in cell culture. At passages eight (P8) or 20 (P20) in the presence of GC376 or GC1003, respectively, the virus mRNA was isolated using Qiagen RNeasy kit and the whole genome sequences of the passaged viruses and PA were determined using NextGen RNAseq. In parallel with the virus passages in the presence of each compound, viruses were also passaged without any compound (Mock) for eight (P8 Mock) and 20 times (P20 Mock). These Mock passaged viruses were used for some experiments as controls.

To investigate the replication of the passaged viruses, CRFK cells were infected with FIPV (passaged viruses or PA) at 1 MOI and incubated at 37 °C for 1hr. Then the media was replaced followed by further incubation, and cell lysates were collected at different time points. RNA were

extracted from these cell lysates using Qiagen RNeasy kit according to the manufacturer's protocol and the RNA were amplified using qRT-PCR. The TCID50s of the virus at each time point were determined using a previously established standard curve for FIPV replication.

4.3.5 Inhibition assay of FIPV replication

The EC_{50}s of 3CLpro inhibitors against the PA or passaged viruses were determined as follows. Serial dilutions of 3CLpro inhibitors or Remdesivir in the presence/absence of P-glycoprotein inhibitors were added to confluent CRFK cells and the cells were simultaneously infected with FIPV at a MOI of 0.01-0.1. Then the cells were incubated at 37 °C until extensive CPE were observed. Next, the cells were freeze-thawed and the virus titers were determined using TCID50 method. Briefly, 10-fold serial dilutions were prepared from each well and the dilutions were added to confluent CRFK cells in 96 well plates followed by incubation at 37 °C until no CPE progression was observed. Then, TCID50 was calculated using the standard TCID50 method (346). The EC_{50} was determined using non-linear regression analysis in GraphPad Prism software version 6 (GraphPad Software, La Jolla, CA).

4.3.6 Multiple amino acid sequence alignment and structural models of passaged FIPV 3CLpro

The amino acid sequences of the FIPV whole genome sequences were aligned using Clustal Omega (https://www.ebi.ac.uk/Tools/msa/clustalo/) (347). Additionally, 66 feline coronavirus strains that include 3CLpro sequences were also obtained from genbank for comparison of the amino acid sequences and their conservation.

3D homology models of 3CLpros of the passaged viruses were generated by using FIPV crystal structures (PDB accessions 4ZRO and 5EU8), and TGEV-GC376 crystal structure (PDB accession 4F49) as templates in SWISS-Model program (https://swissmodel.expasy.org/) (348). The generated models and crystal structures were visualized in PyMol or Chimera.

4.3.7 Recombinant 3CLpro and protein purification

In order to determine the effect of the amino acid changes identified in 3CLpro on the 3CLpro activity and response to the inhibitors, we generated recombinant mutant 3CLpros. 3CLpro regions from the P20 viruses including the mock and PA were amplified using RT-PCR and cloned into pET-28a+ vector (GenScript, Piscataway, NJ). The presence of the amino acid changes in the clones were confirmed by Sanger sequencing. The recombinant 3CLpros were expressed with an N-terminus 6His tag in BL21-DE3 (Invitrogen, Carlsbad, CA) cells and purified according to a previously established protocol by our lab group (273).

4.3.8 Fluorescence resonance energy transfer (FRET) assay

The activity of each recombinant 3CLpro was investigated using FRET assay following a standard procedure previously described by our group (273,349). Briefly, each recombinant 3CLpro was diluted in assay buffer consisting of 120 mM NaCl, 4 mM DTT, 50 mM HEPES and 30% Glycerol at pH 6.0. Next, these mixtures were incubated with a fluorogenic substrate consisting of the coronavirus 3CLpro cleavage site FAM-SAVLQ/SG-QXL520 (AnaSpec, Fremont, CA) for 30min at RT. Following this incubation, fluorescence readings were measured on a fluorescence microplate reader (FLx800, Biotek, Winnooski, VT) at an excitation and an emission wavelength of 485 nm and 516 nm, respectively. The 50% inhibitory concentration (IC_{50}) was calculated for

each 3CLpro using non-linear regression analysis in GraphPad Prism software version 6 (GraphPad Software, La Jolla, CA). For inhibition assays, serial dilutions of each 3CLpro inhibitor were prepared in DMSO and added into the enzyme-buffer mixture and incubated for 30min at RT before the addition of the fluorogenic substrate.

4.3.9 Analysis of P-glycoprotein expression and function

To investigate the mRNA expression levels of P-glycoprotein in cells, CRFK cells were infected with passaged, mock or PA FIPV at 10 MOI with or without 3CLpro inhibitors or remdesivir at concentrations >10-fold higher than EC_{50}s. Remdesivir was used for inhibiting virus replication in some experiments. Then the cells were incubated at 37 °C for 1hr. Following incubation, the media was replaced with or without inhibitors and the cells were further incubated for 12hrs at 37 °C. After 12hrs, RNA was extracted by Qiagen RNeasy kit, and amplified in qRT PCR with primers and probe for feline P-gp (to amplify the *Felis catus* ATP binding cassette subfamily B member 1 or ABCB1 - forward 5'-CACAGATGGCATGGTCAGTAT, reverse 5'-GTGGCAAACAACACAGGTTC, and the probe 5'-TCGGGAAATCATTGGTGTGGTGAGT). To determine the function of P-glycoprotein, CRFK cells were similarly treated and further incubated up to 24hrs following the media replacement. Function of P-gp was determined using the multidrug efflux transporter P glycoprotein (MDR1/P-gp) ligand screening kit (abcam, MA, USA- ab284553) according to the manufacturer's protocol.

4.3.10 Statistical analysis

Data from at least three independent experiments were used to compare statistical significance. Statistical analysis of data using one-way analysis of variance (ANOVA) with Tukey's post hoc

test or two-tailed student's t-test was performed using GraphPad Prism Software version 6 (GraphPad Software, La Jolla, CA).

4.4 Results

4.4.1 Identification of mutations in 3CLpro coding regions of FIPV passaged in the presence of 3CLpro inhibitors.

FIPV was passaged in the presence of 3CLpro inhibitors GC376 and GC1003, which is a structural derivative of GC376 (Fig. 4.1). The concentration of each inhibitor was increased gradually at each passage to induce the generation of antiviral resistance. Then the fold changes in the EC_{50} for each inhibitor was compared to PA at selected passages to determine the presence of resistance (Table 4-2). At the eighth passage, FIPV passaged in GC376 (P8 GC376) increased the EC_{50} of GC376 by 13.2-folds and the EC_{50} of GC1003 by 3.2-folds (Fig. 4.2) compared to PA. Both P8 Mock and P8 GC376 replicated more efficiently and showed slightly increased virus titers compared to PA at 24hpi (Fig. 4.3A). Although the virus titer of P8 GC376 increased during 6-12hpi compared to P8 Mock, it was apparent that P8 GC376 does not show marked replication efficiency over P8 Mock or PA. Sequencing of the entire genome of P8 GC376 revealed no mutations in the 3CLpro region. However, nsp12 RNA-dependent RNA polymerase had a mutation at T926I (T4949I in polyprotein), which is close to the nsp12/13 cleavage site by 3CLpro. Another mutation was identified in the C terminus of spike protein (I1301T).

FIPV passaged in GC1003 (P20 GC1003) caused a 5.6-fold increase in EC_{50} of GC1003 at 20 passages (Fig. 4.2 and Table 4-2) compared PA. P20 GC1003 also substantially increased the EC_{50}

of GC376 by 30.2-folds (Fig. 4.2 and Table 4-2). While P20 GC1003 and P20 Mock viruses replicated efficiently than PA, the titers of P20 GC1003 was only slightly higher than PA but less than P20 Mock virus after 24hpi (Fig. 4.3B). Whole genome sequences of P20 viruses showed multiple mutations in regions including 3CLpro, compared to PA (Table 4-1). A majority of these mutations were within ORF1 that encodes the polyprotein, while the structural proteins also showed mutations (Table 4-1). P20 GC1003 contained two mutations, G23V close to the active site and G298S in the C terminus of domain III (Fig. 4.4). P20 Mock virus also showed a mutation of F58S in 3CLpro. Multiple sequence analysis of 3CLpro sequences of 66 feline coronavirus strains available in Genbank showed that the 3CLpro residues G23, S58 and G298 are highly conserved among feline coronaviruses.

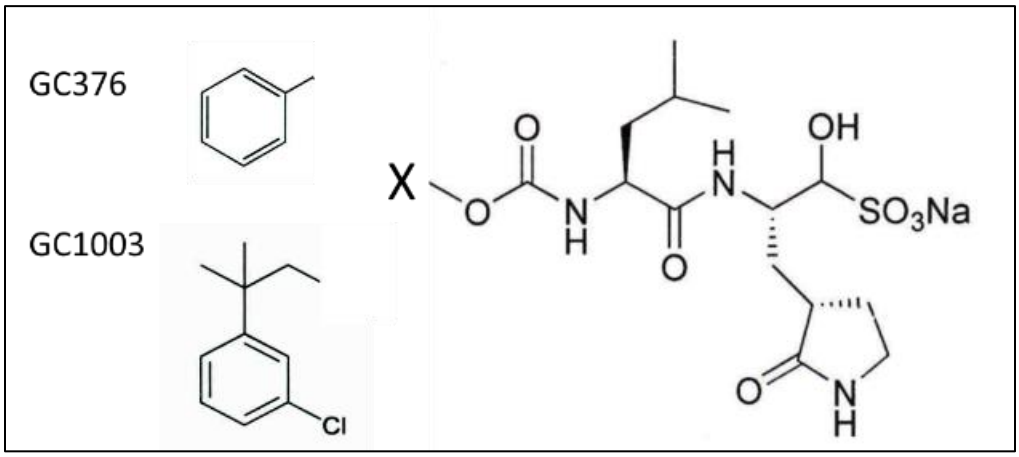

Figure 4.1 Structures of GC376 and GC1003.

Both GC376 and GC1003 share the same backbone with a glutamine surrogate at the P1 position and bisulfite adduct warhead that interacts with the cysteine residue (C104) at the catalytic site. The cap moiety (marked as X) differs between these inhibitors.

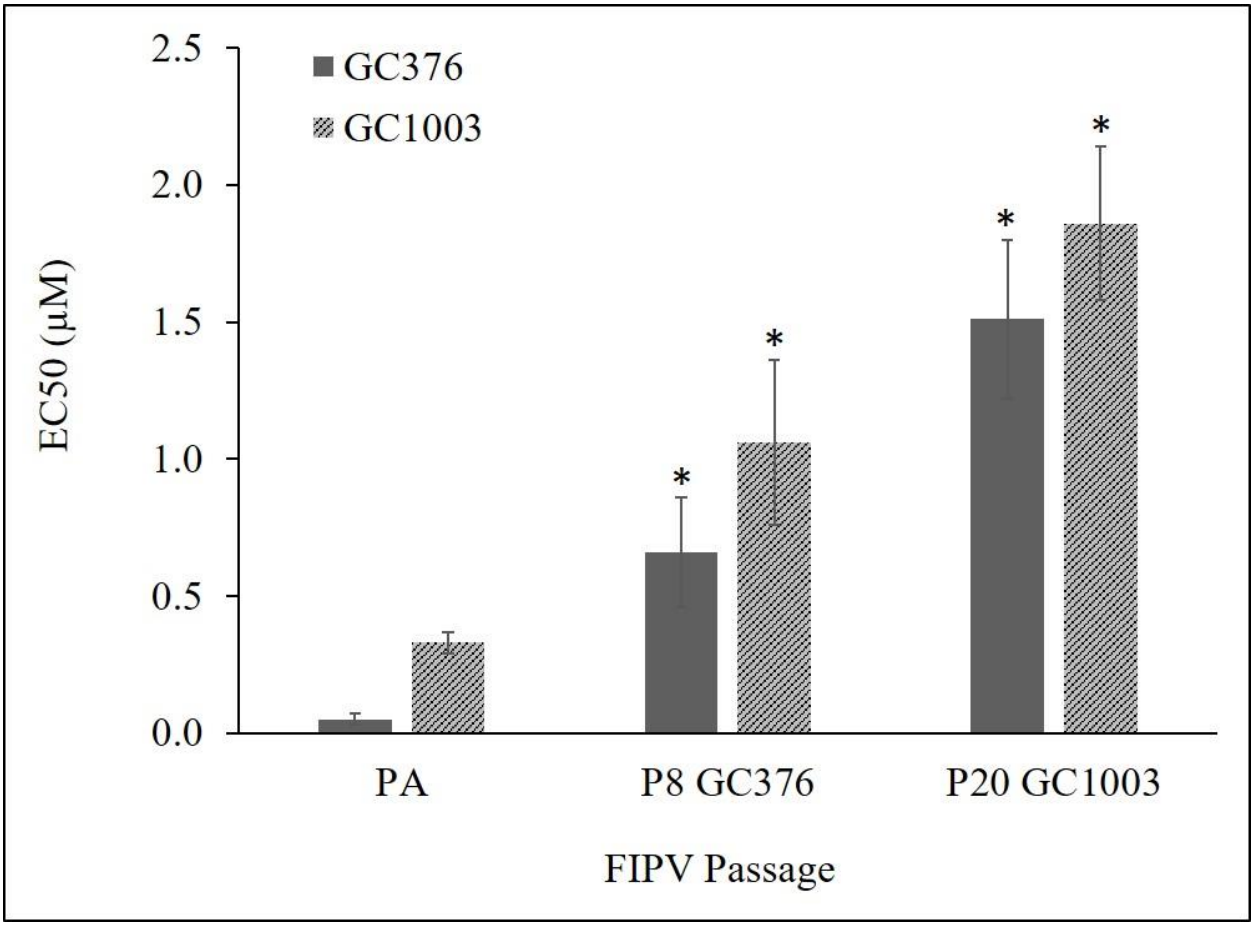

Figure 4.2 EC_{50}s of FIPV passaged in GC376 or GC1003 in CRFK cells.

The EC_{50}s of each inhibitor was determined in CRFK cells using the standard TCID50 method. Statistical significance comparing the EC_{50}s of passaged viruses against PA is indicated with an asterisk (*); $P < 0.05$. Error bars represent standard error of the mean (SEM).

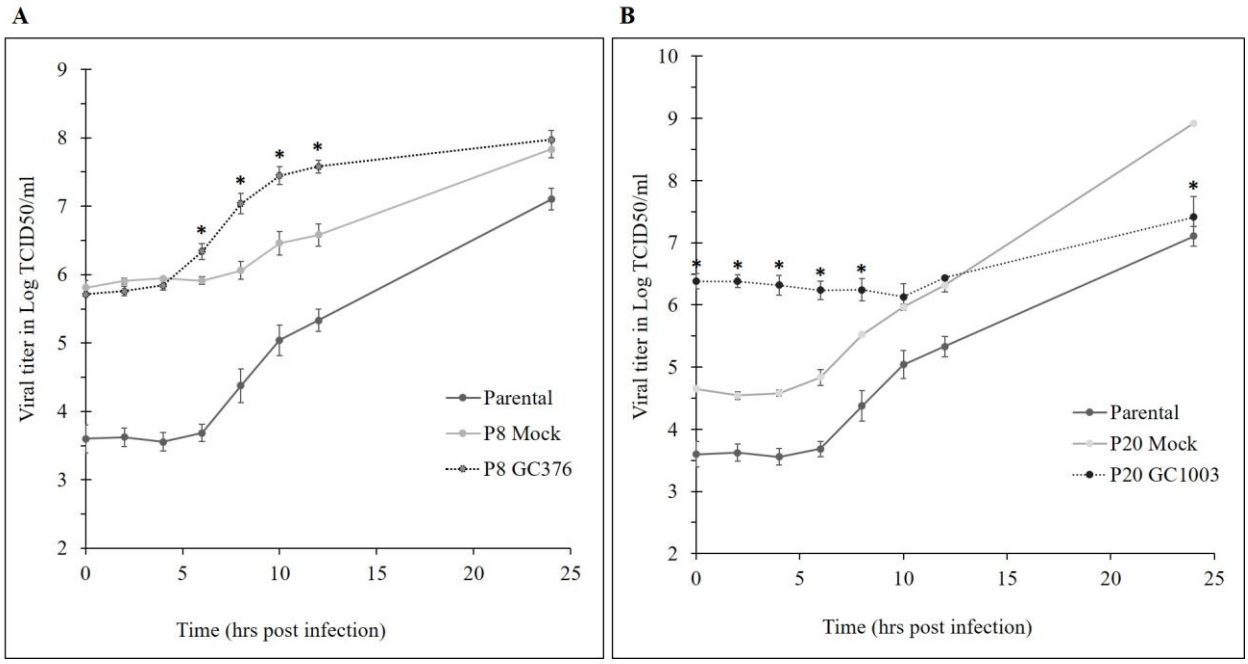

Figure 4.3 Growth kinetics of passaged FIPV.

The replication of (A) P8 viruses and (B) P20 viruses in CRFK cells up to 24hpi is indicated in terms of TCID50/ml compared to parental and mock passaged viruses. Error bars represent standard error of the mean (SEM). Statistical significance in virus titers compared to the mock passaged virus is indicated with an asterisk (*); $P < 0.05$.

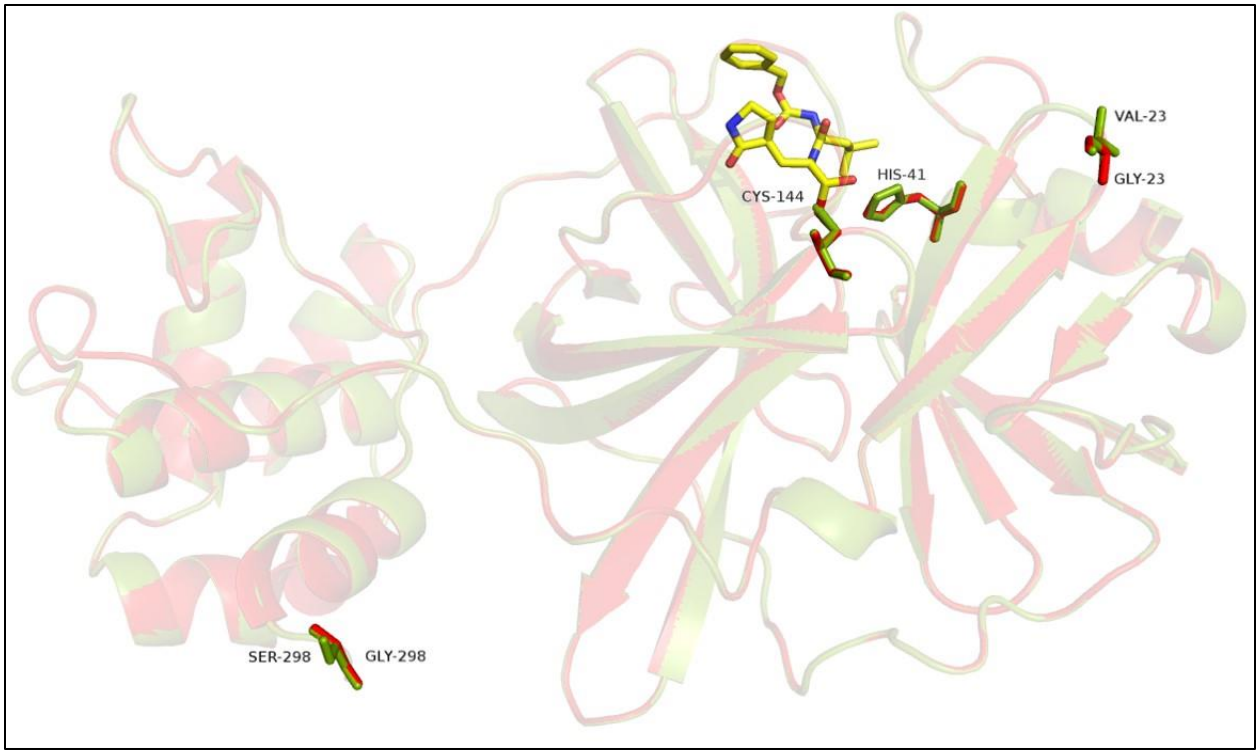

Figure 4.4 The locations of mutations G23V and G298S in the 3CLpro.

The 3CLpro homology model of P20 GC1003 was superposed with the FIPV 3CLpro crystal structure (PDB accession 4ZRO) to investigate the locations of mutations within 3CLpro. The active site of FIPV 3CLpro consists of H41 and C144. GC376 is also shown to indicate the interactions with the active site residues. The P20 GC1003 showed two mutations in 3CLpro, G23V in domain I close to the active site and G298S in domain III.

Table 4-1: Mutations in the genome sequence of P20 GC1003 virus compared to PA.

Passaged virus	Mutation	Location in the polyprotein	Location in the genome
P20 GC1003	**G23V**	**G2926V**	**3CLpro**
	G298S	**G3201S**	
	H112N	H232N	Nsp2
	S288A	S398A	
	G183E	G1062E	Nsp3
	L482F	L1361F	
	S519N	S1398N	
	E701K	E1580K	
	G765D	G1644D	
	A788D	A1667D	
	H1051Y	H1930Y	
	M410K	M2823K	Nsp4
	L138F	L3720F	Nsp8
	D431E	D4454E	Nsp12/RdRp
	D823G	D4846G	
	I208M	I6278M	Nsp15
	119,120 YI insertion (S1 domain)		Spike
	T773I (RBD)		
	D1341N (HR2)		
	N1374T (HR2)		
	C74Y		Envelope
	A22V		Membrane protein
	R66Q		Nucleocapsid

* The 3CLpro mutations are highlighted in black. The mutations shared with the P20 Mock are shown in grey.

4.4.2 The effects of mutations in FIPV 3CLpro against 3CLpro inhibitors in enzyme assay.

We investigated the 3CLpro mutations that were present in P20 GC1003 by generating recombinant 3CLpro bearing these amino acid changes. Recombinant 3CLpro of PA and P20 Mock were also generated for comparison. All the generated recombinant 3CLpro were active in

FRET assay and showed an increase in percent activity over time following a similar trend (Fig. 4.5A). The recombinant 3CLpro of P20 GC1003 increased the IC_{50s} of GC1003 and GC376 by 3.4-folds and 2-fold, respectively (Fig. 4.5B). The presence of G23V and G298S in P20 GC1003 3CLpro appears to marginally reduce the inhibitory activities of GC376 and GC1003 in FRET assay, still, these fold changes in IC_{50}s were comparatively less than that observed in CRFK cells. These results show that the tested 3CLpro inhibitors are still moderately effective against the recombinant mutant 3CLpro of P20 GC1003 in FRET assay.

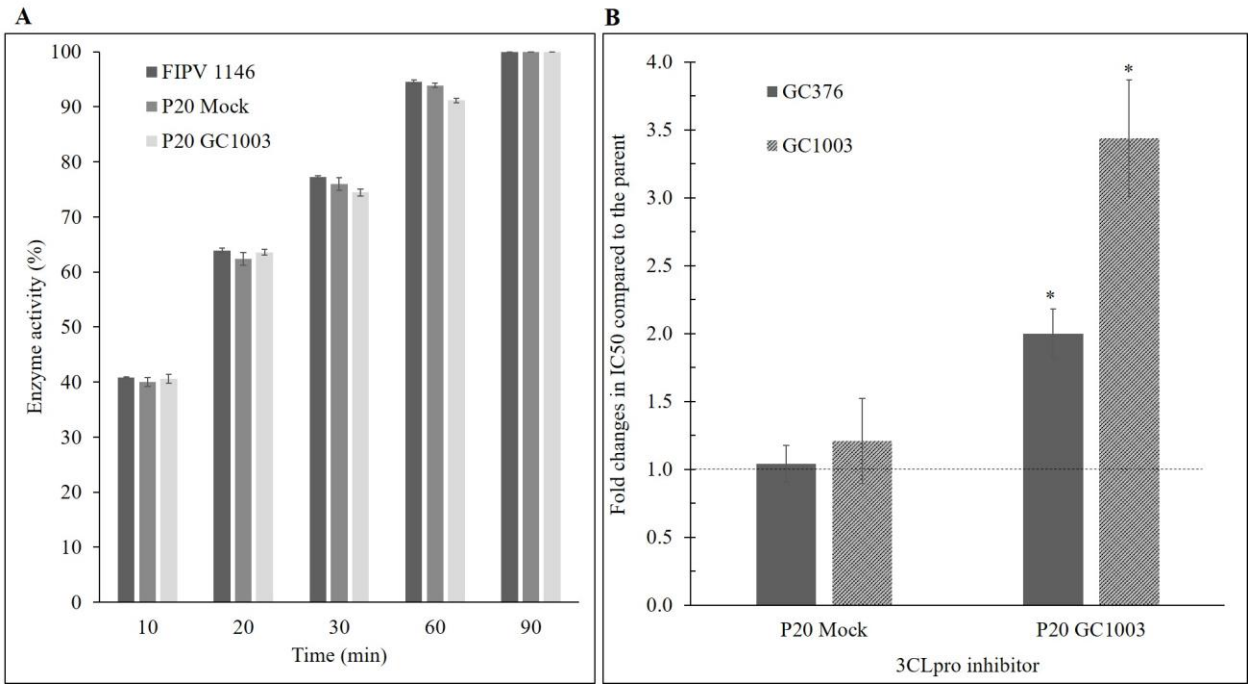

Figure 4.5 The effect of 3CLpro mutations in FRET assay.

(A) The percent activities of recombinant 3CLpro in FRET assay. (B) The fold changes in IC_{50} of the 3CLpro inhibitors against the recombinant 3CLpro in FRET assay. Error bars represent standard error of the mean (SEM). Statistical significance in IC_{50}s compared to PA is indicated with an asterisk (*); $P < 0.05$.

4.4.3 The effect of P-glycoprotein on FIPV and antiviral resistance.

Because P-glycoprotein (P-gp or ABCB1) plays crucial roles in maintaining intracellular concentrations of antivirals, we examined if P-gp inhibitors could influence antiviral activities of GC376 or GC1003 and/or restore the inhibitory activities of GC376 or GC1003 against P8 GC376 and P20 GC1003 viruses. We used Elacridar and CP100356 in the virus replication assay as P-gp inhibitors. These P-gp inhibitors were added at concentrations that showed minimal cytotoxicity and did not affect virus replication compared to the virus infected untreated cells. Addition of Elacridar did not change the EC_{50} of GC376 against PA but decreased the EC_{50}s for GC1003 or remdesivir by 16.5 and 6.5-folds, respectively (Table 4-2). Importantly, treating P8 GC376 infected CRFK cells with Elacridar markedly reduced the EC_{50}s of GC376 (5.5-folds) (Table 4-2), to a level comparable to PA. Similarly, when P20 GC1003 infected CRFK cells were treated with Elacridar, substantial decrease in the EC_{50} of GC376 (12.6-folds) was observed (Table 4-2). In the presence of Elacridar, the EC_{50}s of GC1003 reduced against P8 GC376 or P20 GC1003 by 7.5- or 4.1-folds, respectively, compared to EC_{50}s against the untreated mutant FIPV. Similar results were observed when CP100356 was used as a P-gp inhibitor.

Table 4-2: The effect of P-gp efflux on the inhibitory activity of 3CLpro inhibitors against FIPV.

FIPV	EC_{50} (μM)		
	GC376	**GC1003**	**Remdesivir**
PA	0.05±0.01	0.33±0.04	0.13±0.02
P8 GC376	0.66±0.20	1.06±0.30	NT
P20 GC1003	1.51±0.29	1.86±0.28	NT
PA + Elacridar	0.03±0.01	0.02±0.01	0.02±0.01
P8 GC376 + Elacridar	0.12±0.02	0.14±0.04	NT
P20 GC1003 + Elacridar	0.12±0.02	0.45±0.13	NT

*NT- Not tested.

We examined if the expression of viral proteins changes P-gp expression in the infection with PA and the passaged viruses. We infected CRFK cells with PA or the passaged viruses (P8 GC376 and P20 GC1003) at 10 MOI with or without remdesivir to study the effect of virus replication on P-gp RNA expression. Subsequent treatment of the infected cells with GC376 to block the processing of non-structural proteins did not markedly change the RNA expression of P-gp even at 12hpi compared to the untreated, virus only control (Fig. 4.6A). Furthermore, we investigated the changes in the activity of P-gp in CRFK cells infected with PA or passaged viruses at 10 MOI. Still, P-gp activity did not show marked changes in the virus infected cells at 24hpi compared to the control (Fig. 4.6B). These observations suggest that neither PA nor the passaged viruses alter RNA expression or the activity of P-gp in CRFK cells upon infection.

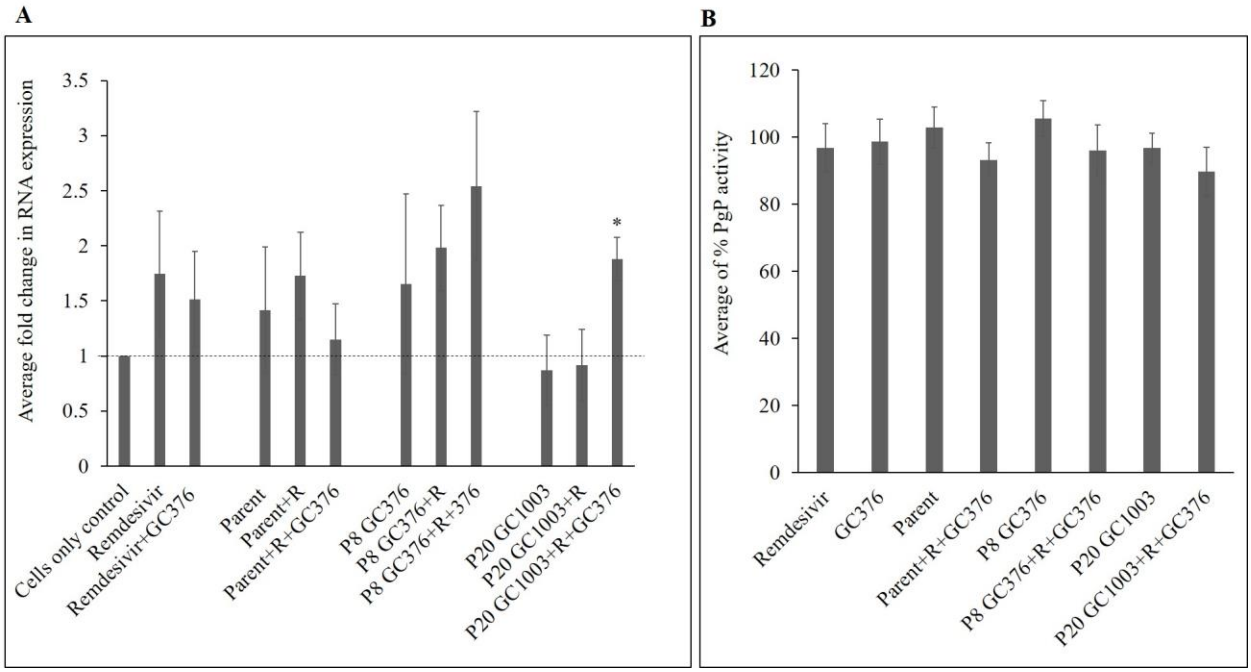

Figure 4.6 The changes in RNA expression of P-gp and percent activity of P-gp in response to FIPV infection in CRFK cells.

(A) Feline P-gp expression in CRFK cells in response to FIPV infection at 10 MOI with or without the treatment of remdesivir or GC376 after 12hpi. Statistical significance in fold change compared to the cells-only control is indicated with an asterisk (*); $P < 0.05$. (B) The percent activity of P-gp in CRFK cells in response to FIPV infection at 10 MOI after 24hpi. Remdesivir is also indicated as R. Error bars represent standard error of the mean (SEM).

4.5 Discussion

The 3CLpro of coronaviruses is an attractive target to develop antiviral drugs for coronaviruses. Recently, nirmatrelvir, a 3CLpro inhibitors combined with ritonavir (Paxlovid; Pfizer) received emergency use authorization for the treatment of COVID-19 in eligible patients (350) marking an important milestone for 3CLpro targeted antivirals. Study of molecular basis of antiviral resistance in coronaviruses greatly benefit the development of antiviral drugs that have a high genetic barrier

to resistance. This information is also crucial to understand the evolutionary dynamics of coronaviruses that would further improve preventive and therapeutic measures to control highly pathogenic coronaviruses. Therefore, we investigated the generation of resistance of FIPV to 3CLpro inhibitors GC376 and GC1003 in this study.

Passaging FIPV in the presence of GC376 reduced the susceptibility of FIPV (at P8) against both GC376 and GC1003 in cell culture in the absence of mutations in 3CLpro. This observation is consistent with recent studies on passaging FIPV in cell culture in the presence of GC376, where no mutation was observed in 3CLpro (279,310). Jiao *et al* reported mutations at non-3CLpro locations including nsp12- S925P, which is highly conserved among feline coronaviruses (310). Jiao *et al* reported that the mutant FIPV carrying nsp12-S925P showed reduced susceptibility to GC376 in cells and increased virulence and decreased response to GC376 in experimentally infected cats (310). The amino acids 925-926 in nsp12 are located close to the 3CLpro cleavage site between nsp12/13. Thus, it can be speculated that T926I, which we identified in our study, may contribute to the reduced 3CLpro inhibitory activity against P8 GC376 in cell culture. However, further investigations are necessary to study the exact role of nsp12-T926I in the generation of antiviral resistance.

Similarly, passaging FIPV in GC1003 reduced the susceptibility of the passaged virus (P20) to GC1003 as well as GC376 in cell culture. P20 GC1003 had mutations in 3CLpro and in other regions of the genome, some of which are shared with the mock passaged virus. The 3CLpro mutations (G23V and G298S) are in close proximity to 3CLpro mutations identified in our previous study (N25S, A252S, K260N) (280,309). In our previous study, FRET assay showed that

the presence of N25S, which was near the active site, slightly lowers the inhibitory activity of GC376, while A252S or K260N had no effect (309). The proteolytic activity of recombinant P20 GC1003 3CLpro carrying G23V and G298S mutations appeared unaffected in FRET assay. The combination of G23V and G298S in the recombinant mutant 3CLpro of P20 GC1003 moderately decreased the activity of 3CLpro inhibitors in FRET assay (<3.5-folds in IC_{50}s for GC376, GC1003). Because these IC_{50} fold changes were comparatively lower than observed EC_{50} fold changes in cells (30.2- or 5.6-fold for GC376 or GC1003, respectively), the mutations in 3CLpro alone could not explain the reduced susceptibility of P20 GC1003 to the inhibitors in cell culture. Further studies are needed to understand how these multiple mutations throughout the genome affect the resistance as well as virus replication and pathogenicity.

One of the key findings in this study is the effect of inhibiting host P-gp on the activity of 3CLpro inhibitors in cells. P-gp is a multi-drug resistant efflux transporter protein (311,312) that is expressed in multiple tissues including the liver, intestines, kidneys, and the blood-brain barrier (313,314). P-gp functions as a natural barrier that transports toxic substances as well as antiviral (333–335) and anticancer drugs back to extracellular domains (311,315,316). Thus, elevated P-gp activity could greatly affect drug efficacy, safety, and toxicity. P-gp is known to limit the therapeutic efficacy of anticancer drugs, and cause suboptimal penetration of many anti-retroviral drugs creating sanctuaries for virus persistence (326). Therefore, simultaneous inhibition of P-gp with compounds such as verapamil could greatly improve the bioavailability and tissue penetration of therapeutics (313,338–340) including antivirals such as HIV protease inhibitors (333,341). Importantly, ritonavir in the combination of nirmatrelvir and ritonavir (Paxlovid; Pfizer) that target

3CLpro of SARS-CoV-2 is also known to inhibit P-gp (351,352), and is a pharmacokinetic booster used in HIV and HCV treatments.

The results of P-gp inhibitors suggest that GC376 is not susceptible to the P-gp efflux activity, while the effectiveness of GC1003 and remdesivir are influenced by the P-gp efflux system in CRFK cells (Table 4-2). The inhibitory effects of both GC1003 and remdesivir significantly increased against PA in the presence of P-gp inhibitors (Table 4-2). On the other hand, there was no difference on the EC_{50}s of GC376 against PA with or without the P-gp inhibitor (Table 4-2). Because the antiviral effects of GC376 against P8 GC376 and P20 GC1003 were restored to the levels comparable to the parental virus in the presence of P-gp inhibitors (Table 4-2), the P-pg efflux system is involved in the resistant phenomenon against GC376 in P8 GC376 and P20 GC1003. For GC1003, the EC_{50}s were reduced in the presence of the P-gp inhibitor against P8 GC376 and P20 GC1003 at similar (or lower) levels against PA (Table 4-2). Since P8 GC376 did not show mutations in 3CLpro, this decrease in EC_{50} with P-gp inhibitor may be explained by the involvement of P-gp system in the resistant phenomenon of this mutant virus. It is possible that both 3CLpro mutations and P-gp system contribute to the resistant phenomenon observed with the P20 GC1003.

When the RNA expression or activity of P-gp in response to the infection with PA, P8 GC376 or P20 GC1003 in CRFK cells was examined, we did not observe significant changes. Neither FIPV replication nor virus non-structural proteins resulted in different P-gp activity or expression at RNA level in CRFK cells. A previous study indicates that CP100356 can moderately suppress virus replication by inhibiting low-pH-dependent membrane fusion with minimal cytotoxicity

(342). We did not observe marked changes in virus replication in the presence of Elacridar or CP 100356 at the tested concentrations. Overall, these results show that P-gp expression or activity was not related to the P-gp inhibitor-mediated restoration of inhibitory activity of GC376 against P8 GC376 and P20 GC1003. The cellular efflux system is complicated with multiple systems composed of several proteins (Reviewed by (353,354)), and it is possible that the 3CLpro inhibitors influence other efflux proteins than P-gp. These results suggest that multiple factors are involved in the resistance of FIPV against 3CLpro inhibitors, which includes the involvement of P-gp. Further investigation is important in understanding the function of efflux system in coronavirus replication and antiviral resistance.

Chapter 5 - Review of Literature on SARS-Coronavirus-2

5.1 SARS-Coronavirus-2

A novel human coronavirus was first identified in Wuhan, China in December 2019 with epidemiological ties to the Huanan seafood market in Wuhan (355). Based on its similarity of symptoms and severe respiratory illness as SARS-CoV (356) as well as the sequence similarity, the causative coronavirus was named as SARS-Coronavirus-2 (SARS-CoV-2), and the associated disease was named as COVID-19. Subsequently, efficient person-to-person transmission (357) of SARS-CoV-2 led to a global pandemic. It has claimed the lives of ~10 million individuals across the world since 2020 (358), and is still ongoing at the time of writing this dissertation. The declaration of the COVID-19 pandemic resulted in the implementation of strict control measures including mandatory facemasks and national lockdowns in many countries. Multiple vaccines were rapidly developed and authorized for use, and the use of new mRNA technologies was a breakthrough in vaccine development. Immunocompromised individuals and individuals with underlying diseases are more susceptible to severe SARS-CoV-2 infections, while acute SARS-CoV-2 infection causes minimal complications and is often cleared by the immune system in healthy individuals. Some SARS-CoV-2 infected individuals can experience long-term effects that include a wide range of health problems including general symptoms such as fatigue to digestive, respiratory, and neurological symptoms.

5.2 Origin of SARS-CoV-2

SARS-CoV-2 is classified as a sarbecovirus within the beta coronavirus genus in the family *Coronaviridae* (359). As other beta coronaviruses, SARS-CoV-2 also encodes large polyproteins

containing non-structural proteins from ORF1 (360) followed by ORFs that encode the structural proteins and six accessory proteins (361,362) (Fig. 3.2). The genome identity between SARS-CoV and SARS-CoV-2 is 79.6% (144), and there is a notable difference in the antigenicity between SARS-CoV and SARS-CoV-2 (143).

SARS-CoV-2 may have originated from bat coronaviruses and eventually transmitted into humans via an intermediate host. This stems from studies that revealed the high sequence similarity between SARS-CoV-2 and some bat coronaviruses, including RmYN02, bat-SL-CoVZC45 and bat-SL-CoVZXC21(355,363–365).

5.3 Spike protein of SARS-CoV-2

SARS-CoV-2 S glycoprotein is a type I viral fusion protein (366) which comprises the receptor binding S1 subunit (143) and the S2 subunit that contains the fusion domain (Fig. 5.1). Interactions of coronavirus S protein and the cellular receptor is dependent on the receptor-binding domain (RBD) in S1. The RBD of SARS-CoV-2 is composed of five-stranded antiparallel β sheets with short helices and loops that form the core. The receptor-binding motif (RBM) is contained within the RBD. It is composed of four pairs of disulfide bonds that stabilize the structure and other residues that bind the receptor (367). The overall structure of the SARS-CoV-2 RBD is similar to that of the SARS-CoV RBD (363,367). SARS-CoV-2 utilizes the same receptor, ACE2, as SARS-CoV (142–144) (Fig. 5.2). However, RBD of SARS-CoV-2 S protein has a higher binding affinity to human ACE2 (368), and shows more atomic interactions compared to SARS-CoV (143). Neuropilin-1 (NRP1) (369,370) and Tyrosine-protein kinase receptor UFO (AXL) (371) could be additional host factors involved in the entry of SARS-CoV-2. For example, NRP1 is expressed

abundantly in the respiratory and olfactory epithelium, and co-expression of ACE2, TMPRSS2 and NRP1 could even further potentiate infection of SARS-CoV-2 (369,370).

In contrast to SARS-CoV, SARS-CoV-2 S contains a polybasic cleavage site at the S1/S2 boundary (142,372), which may enhance the efficiency of entry into host cells and infectivity (373,374). Proteolytic processing of the polybasic cleavage site at S1/S2 and S2' by cellular proteases including transmembrane protease, serine 2 (TMPRSS2) triggers membrane fusion and SARS-CoV-2 virus entry into the host cell (368,375–379).

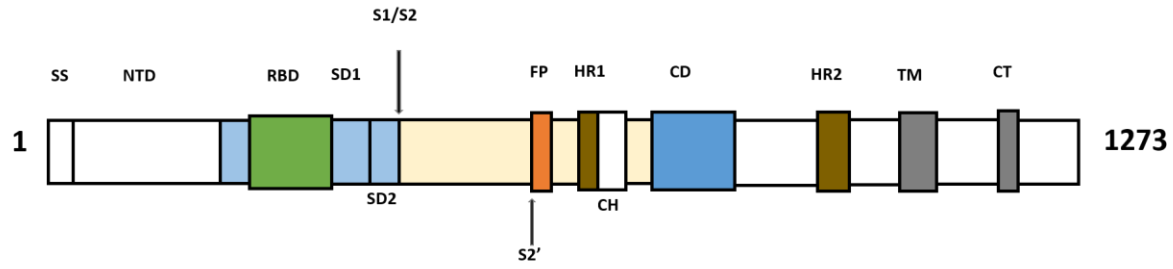

Figure 5.1 Schematic diagram of the SARS-CoV-2 spike protein

The domains within the SARS-CoV-2 spike protein are indicated in different colors. SS - signal sequence; NTD - N-terminal domain; RBD - receptor-binding domain (333-527) that contain the receptor binding motif (RBM) within residues 438-506; SD1 - subdomain 1; SD2 - subdomain 2; S1/S2 - the protease cleavage site; S2'- protease cleavage site; FP - fusion peptide; HR1 - heptad repeat 1; CH - central helix; CD - connector domain; HR2 - heptad repeat 2; TM - transmembrane domain; CT - cytoplasmic tail. The protease cleavage sites are indicated by black arrows. [The figure was adapted from (367,380)].

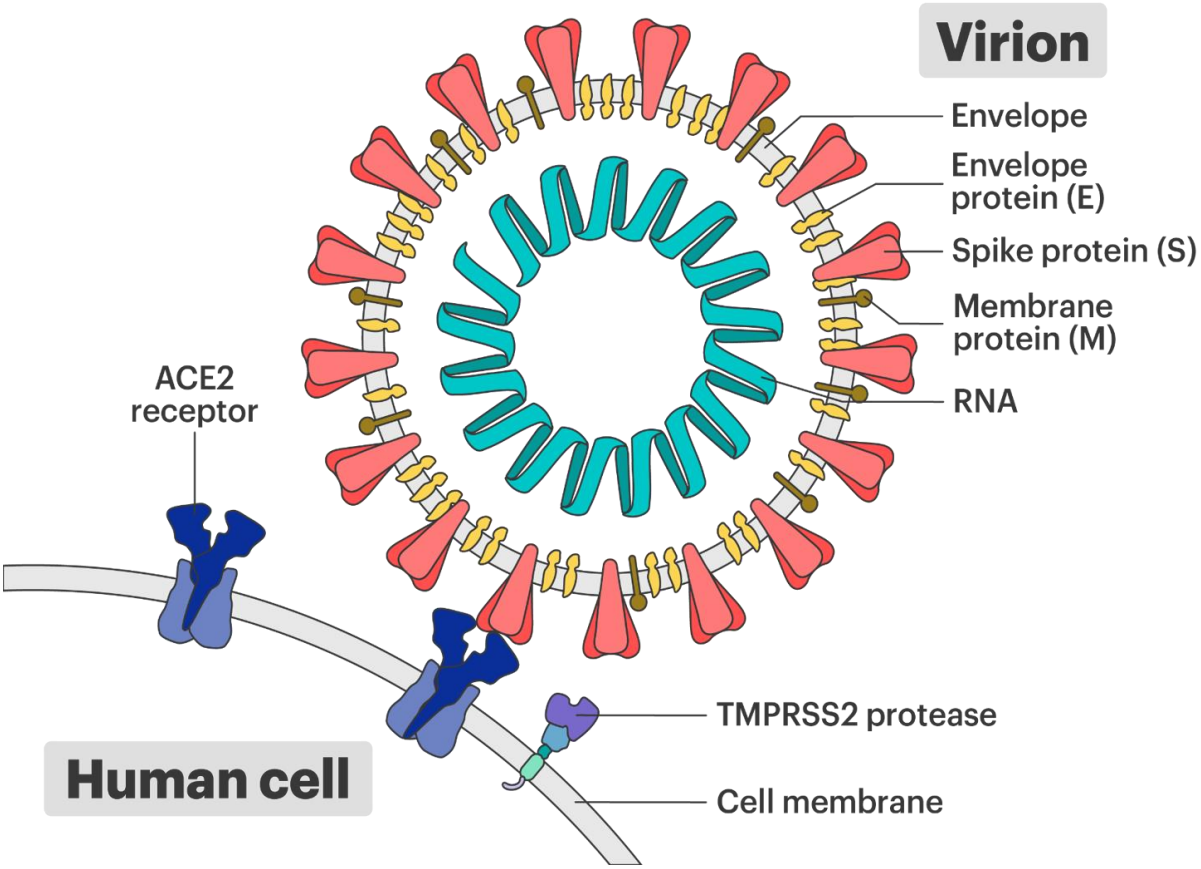

Figure 5.2 Interaction of SARS-CoV-2 spike protein with human ACE2

Image credit: Davian Ho for the Innovative Genomics Institute. (Creative commons license)

5.3.1 SARS-CoV-2 spike variants

New SARS-CoV-2 variants with altered antigenic properties and transmissibility have surfaced as the pandemic progressed. Some variants quickly became predominant over others, and some of these were classified as variants of concern based on the impact on public health. D614G substitution rapidly became dominant among the circulating SARS-CoV-2 strains. The D614G substitution reduces the shedding of S1 and increases the ability of RBD to remain in open conformation and to bind to ACE2 (379). Moreover, pseudoviruses bearing D164G grow to high

titers in cells, which might correlate with increased viral transmission observed in individuals infected with the virus carrying this mutation (381).

The ‘Alpha’ (UK/ B.1.1.7 variant) variant contained eight mutations in the S protein including N501Y, D614G, and P681H near the S1/S2 cleavage site, and appeared to be evade a few RBD and N-terminal domain targeting monoclonal antibodies against the SARS-CoV-2 S protein (382). However, convalescent plasma from patients infected with the parental SARS-CoV-2 were able to neutralize the Alpha variant (382,383) suggesting that the protective efficacy of the vaccines or sera were intact against this variant. The ‘Beta’ (B.1.351/ South African variant or 501Y.V2) variant emerged with eight mutations in the S protein, and three of these (K417N, E484K and N501Y) were within ACE2 binding region of the RBD (384). Some Beta variant isolates also had an additional substitution (A701V) near the S1/S2 cleavage site (382). Due to the number of mutations within the S gene, most importantly E484K, Beta variants were resistant against multiple monoclonal antibodies developed for SARS-CoV-2 that recognize the multiple regions of the SARS-CoV-2 S protein including the N terminal domain and RBM (382,385). Furthermore, Beta variants also showed poor neutralization by convalescent plasma and sera from vaccinated individuals (382). The subsequent ‘Gamma’ variant (P.1) contained 10 spike mutations along with K417N, E484K and N501Y (386) in the RBD and H655Y close to the S1/S2 cleavage site. Similar to Beta, the presence of E484K in the Gamma variant contributed to resistance against multiple RBD-directed neutralizing mAbs developed for SARS-CoV-2, convalescent plasma and sera from vaccinated individuals (387).

Studies on Alpha, Beta and Gamma variants highlight how a combination of three spike mutations, K417N/T, E484K, and N501Y could alter the neutralizing landscape of SARS-CoV-2 (385,388). E484K, K417N and N501Y in combination causes substantial changes in the conformation of RBD in the S protein, which could affect interactions with human ACE2. Specifically, E484K adjusts the conformation of the flexible loop region of RBD and further increases the interactions with ACE2 in combination with N501Y (389). This enhanced affinity of RBD containing E484K, K417N and N501Y to human ACE2 maybe the underlying cause of increased transmissibility of these variants (389). Importantly, variants with N501Y also displayed the ability to bind mouse and mink ACE2 which could potentially expand the SARS-CoV-2 host range (383,390). The neutralization resistance hierarchy of the variants at this point (Beta was the most resistant followed by Gamma and Alpha) was speculated to be dependent on the Y144del and 242–244del mutations in the N-terminal domain in addition to K417N/T, E484K, and N501Y mutations (383).

The subsequent ‘Delta’ variant (B.1.617.2) contained L452R and T478 K on the RBD and was associated with more severe disease in unvaccinated individuals than previous variants (391). Additionally, the P681R mutation in the Delta variant slightly increased the pathogenicity of the virus by enhancing fusogenicity (392). The delta variant showed poor neutralization by vaccine induced or convalescent sera from previous Beta or Gamma infections (393,394). The next ‘Omicron’ (B.1.1.529) variant carried up to 36 mutations within the spike protein, with multiple deletions and insertions in the S1-RBD/S2 domains (15 mutations in RBD including G339D, S371L, S373P, S375F, K417N, N440K, G446S, S477N, T478K, E484A, Q493R, G496S, Q498R, N501Y, and Y505H). The new variant quickly became dominant over the Delta variant and showed higher viral loads, increased rates of transmissibility, infectivity and re-infection (395–

397). Despite the efficacy in neutralization of the Delta variant, Omicron variant responded poorly to neutralizing sera from vaccinated individuals (398,399). However, primary immunization with two doses of COVID-19 vaccines appeared to prevent severe disease and provided sufficient protection against the omicron variant (400).

5.4 Susceptibility of other species to SARS-CoV-2 infection

Differences in the use of receptors and residues within the ACE2 receptors between animal species could change the susceptibility to SARS-CoV-2. An intense, multidisciplinary computational analysis of ACE2 sequences of different species within vertebrates proposed the potential broad host range of SARS-CoV-2 (401–403). However, whether these predicted animals could become infected, the epidemiological significance and their potential of becoming animal reservoirs require more in-depth surveillance, thorough investigations and experimental infections. Subsequently, SARS-CoV-2 infections have been reported in multiple animal species.

Early during the pandemic, multiple SARS-CoV-2 outbreaks were reported in mink farms in the Netherlands (404,405) and Denmark (406), where the infected animals often showed acute interstitial pneumonia. The possible source of infection was human contact and the virus was able to transmit between minks (405). Subsequent SARS-CoV-2 outbreaks in mink farms were also reported in multiple European countries and North America with incidences of human-to-mink and mink-to-human transmission (407–409). These outbreaks reveal that minks could serve as a potential animal reservoir of SARS-CoV-2. SARS-CoV-2 was also detected in feral cats and dogs that were near the infected mink farms (410). The viruses isolated from these infected cats clustered with the mink derived SARS-CoV-2 sequences, suggesting mink-to-cat transmission of

the virus (410). These infected cats also shed infectious virus and showed cat-to-cat transmission (411,412). Several other reports mentioned SARS-CoV-2 infection in domestic cats with possible human-cat and cat-cat transmissions (413,414). As mentioned above, dogs can also get infected with SARS-CoV-2, show seroconversion, and may also show signs of disease (411,412,415,416). Syrian hamsters can be naturally infected with SARS-CoV-2 and also transmit the virus to humans (417). Among domesticated animals, SARS-CoV-2 has shown no or low levels of replication in pigs, chicken and ducks (412,415). Infecting cattle with SARS-CoV-2 results in virus replication and seroconversion, however, the infected animals do not appear to transmit the virus to the uninfected and no reports exist about natural infection in cattle (418,419). Horses do not appear to support virus replication but can become seroconverted following close contact with humans infected with SARS-CoV-2 (418,420). No reports exist on natural infection of SARS-CoV-2 in camels. Overall, domesticated animals cannot be considered as highly susceptible hosts for SARS-CoV-2 that contribute to virus transmission.

White-tailed deer in North America shows possibility of becoming animal reservoirs of SARS-CoV-2. These animals were shown to be susceptible to SARS-CoV-2 (421) and the experimentally infected fawns showed efficient deer-to-deer transmission as well as spillover to humans (422). This observation raises a threat as white tailed deer that live close to humans could be established as an animal reservoir of SARS-CoV-2 (421,422). Red foxes (*Vulpes vulpes*) have also shown the presence of SARS-CoV-2 in oral and respiratory secretions (423). Interestingly, fruit bats showed transient infection of SARS-CoV-2 with clinical signs resembling subclinical infection in humans, and viral replication in the respiratory tract as well as transmission to direct contacts (415).

5.4.1 Animal models for SARS-CoV-2

Preclinical evaluation of antiviral agents and vaccines as well as studies on virus pathogenesis heavily rely on animal models. Different animal models have been established to study SARS-CoV-2 infection and disease progression. Mice show poor susceptibility as SARS-CoV-2 has low affinity to bind to mouse ACE2. To circumvent this issue, mouse-adapted SARS-CoV-2 has been engineered based on the interaction between SARS-CoV-2 spike protein and mouse ACE2 (390,424–426). However, this raised concerns on virus virulence and applicability of the results in humans. The other approach was generating transgenic mice expressing human ACE2 (427–432). C57BL/6 (B6) transgenic mice that express human ACE2 from the human cytokeratin 18 promoter (K18 hACE2) (430,432) shows features that correspond to severe COVID-19 upon SARS-CoV-2 infection. Still, whether these models accurately display the ACE2 distribution, tropism, pathogenesis of SARS-CoV-2 or age dependency and histopathological changes of severe COVID-19 related acute respiratory distress syndrome (ARDS) as observed in humans need to be investigated.

Ferrets also succumb to SARS-CoV-2 infection (412) similar to their susceptibility to experimental infection and transmission of SARS-CoV (433). Infection of 8 month old female ferrets with SARS-CoV-2 showed the presence of viral RNA in the respiratory tract in absence significant clinical signs (434). However, in 12- to 20- month old ferrets, SARS-CoV-2 infection resulted in virus replication, and shedding associated with fever, and acute bronchiolitis (435,436). These infected ferrets were also able to transmit the virus to other ferrets that were in direct contact (435). Overall, these studies suggest that SARS-CoV-2 infection in ferrets resembles the subclinical infection in humans with an efficient transmission pattern (436). Ferrets are established animal

models for multiple zoonotic pathogens. Therefore, these observations highlight their applicability to study vaccines or antivirals for SARS-CoV-2 (415). However, reproducibility of the infection and clinical signs in ferrets is questionable.

Similarly, infected golden (Syrian) hamsters show clinical signs that correlate with mild SARS-CoV-2 infections in humans and were also able to transmit the virus into naïve hamsters (437,438). However, intranasal infection of low doses of low-passage SARS-CoV-2 results in more severe signs of intranasal infection in hamsters compared to ferrets (436). Although mortality is rare, hamsters with intact immune systems show consistent development of severe respiratory infection following SARS-CoV-2 infection. This highlights their importance in the use as an animal model to study SARS-CoV-2 pathogenesis over the mouse model, where the mouse or the virus need to be altered (439). The relatively small size of hamsters, ease of handling and the cost effectiveness further contribute to this suggestion.

Rhesus macaques are non-human primates that are widely used as animal models. Infection of SARS-CoV-2 in rhesus macaques result in interstitial pneumonia and systemic viral dissemination predominantly in the respiratory and GI tracts (440). When the animals were re-infected, higher levels of neutralizing antibodies were detected with no signs of disease or viral dissemination, suggesting prior infection may protect from re-infection (440).

Overall, it is impossible to study disease pathology and transmission of SARS-CoV-2, and therapeutic approaches for COVID-19 using a single animal model due to the inherent differences among these animals. Therefore, a combination of data from different animal models is required

to fill the knowledge gaps on SARS-CoV-2. However, detailed animal studies provide valuable information especially for the development of vaccines and therapeutics.

Chapter 6 - Effects of spike mutations in SARS-CoV-2 variants of concern on human or animal ACE2-mediated virus entry and neutralization

6.1 Abstract

Severe acute respiratory syndrome coronavirus 2 (SARS-CoV-2) is a zoonotic agent capable of infecting humans and a wide range of animal species. Over the duration of the pandemic, mutations in the SARS-CoV-2 spike (S) protein have arisen, culminating in the spread of several variants of concern (VOCs) with various degrees of altered virulence, transmissibility, and neutralizing antibody escape. In this study, we used pseudoviruses that express specific SARS-CoV-2 S protein substitutions and cell lines that express angiotensin-converting enzyme 2 (ACE2) from nine different animal species to gain insights into the effects of VOC mutations on viral entry and antibody neutralization capability. All animal ACE2 receptors tested, except mink, support viral cell entry for pseudoviruses expressing the ancestral prototype S at levels comparable to human ACE2. Most single S substitutions did not significantly change virus entry, although 614G and 484K resulted in a decreased efficiency. Conversely, combinatorial VOC substitutions in the S protein were associated with increased entry of pseudoviruses. Neutralizing titers in sera from various animal species were significantly reduced against pseudoviruses expressing the S proteins of Beta, Delta, or Omicron VOCs compared to the parental S protein. Especially, substitutions in the S protein of the Omicron variant significantly reduced the neutralizing titers of the sera. This study reveals important insights into the host range of SARS-CoV-2 and the effect of recently

emergent S protein substitutions on viral entry, virus replication, and antibody-mediated viral neutralization.

This chapter is an excerpt from the published article (441), which can be accessed through the following links.

Citation - Kim, Y., Gaudreault, N. N., Meekins, D. A., Perera, K. D., Bold, D., Trujillo, J. D., Morozov, I., McDowell, C. D., Chang, K.-O., & Richt, J. A. (2022). Effects of Spike Mutations in SARS-CoV-2 Variants of Concern on Human or Animal ACE2-Mediated Virus Entry and Neutralization. Microbiology Spectrum, 10(3), e01789-21.
DOI: https://doi.org/10.1128/spectrum.01789-21

https://journals.asm.org/doi/10.1128/spectrum.01789-21

6.2 Introduction

Severe acute respiratory syndrome coronavirus 2 (SARS-CoV-2), the etiological agent of coronavirus disease 2019 (COVID-19), unexpectedly emerged in late 2019 and has spread throughout the world, infecting over 517 million people worldwide and causing over 6.2 million deaths as of May 2022-update (https://covid19.who.int/). The zoonotic origin and intermediate hosts of SARS-CoV-2 are still unclear, although bats are considered a likely source based on numerous SARS-CoV-2-related bat coronaviruses found in Southeast Asia (144,365,442). It is now increasingly apparent that SARS-CoV-2 has the capacity to infect several animal species besides humans, increasing concerns that domestic and wild animals may become secondary reservoirs of the virus (443–445). Outbreaks of SARS-CoV-2 in hundreds of mink farms in the European Union (405), where identification of human-to-mink and mink-to-human virus transmissions (406,446) as well as mink-associated variants led to the culling of over 20 million minks in Denmark, underscored the importance of identifying and assessing the risks associated with this pandemic for animal and human health (407–409,447). Other animal species, including cats, dogs, ferrets, hamsters, nonhuman primates, white-tailed deer, mice, cattle, pigs, tree shrews, rabbits, raccoon dogs, and fruit bats, have been investigated for their susceptibility to SARS-CoV-2 infection (448). Reports from natural and experimental infection studies determined a wide range of susceptibility of several domesticated (farm or companion) animals or wildlife to SARS-CoV-2 infection, including white-tailed deer (401–403,405,406,411,412,416,422,449,449–451).

SARS-CoV-2 is an enveloped, positive-sense RNA virus that belongs to the family *Coronaviridae*. RNA viruses are prone to high mutation rates, giving rise to new variants, although the mutation rate of coronaviruses is lower than that of many other RNA viruses due to proofreading activity of

their replicative complex (344,345). Some virus variants possess notable changes in virus transmissibility, virulence, or other characteristics that are important in host defense, such as immune evasion. Since the emergence of COVID-19, multiple variants of SARS-CoV-2 have been identified and have largely replaced the prototype SARS-CoV-2 strain (Wuhan-Hu-1) (452,453). Currently, the World Health Organization designated Alpha (lineage B.1.1.7), Beta (B.1.351, B.1.351.2, and B.1.351.3), Gamma (P.1, P.1.1, and P.1.2), Delta (B.1.617.2, AY.1, and AY.2), and Omicron (B.1.1.529) SARS-CoV-2 viruses as variants of concern (VOCs) (449,454), as they are associated with increased risks to global public health. These variants contain multiple amino acid substitutions in the spike (S) protein, some of which have received special attention as they span the receptor-binding domain (RBD) or the S1/S2 junction. Entry of SARS-CoV-2 into the target cells is mediated by the interaction of the S protein with its receptor angiotensin-converting enzyme 2 (ACE2) on the host cell membrane (365,368,455). The RBD in the S protein is located on residues 319 to 541 and interacts with 25 conserved residues on human ACE2 (hACE2) (368,456). Cleavage of the S1/S2 junction (residues 613 to 705) of SARS-CoV-2 S protein by cellular proteases triggers fusion and viral entry into host cells (377,457). Due to its involvement in receptor binding, most neutralizing antibodies are directed against the RBD (458). Mutations affecting the S protein, including the RBD, are of particular concern because they may enhance virus transmissibility and reduce neutralizing antibody binding and immune protection, thus compromising vaccine and therapeutic antibody efficacies (452). In addition, the interaction between the cellular receptor and virus, leading to virus entry into host cells, is one of the critical factors that determine host susceptibility to virus infection. With the recently emerged virus variants, it is also critical to understand the impact and significance of such mutations on virus neutralization, which has wide-reaching implications on vaccine efficacy; and on animal

susceptibility to SARS-CoV-2 in order to identify and manage risks of zoonotic/reverse zoonotic infections. Some of the key mutations found in SARS-CoV-2 VOCs have been studied using pseudotyped viruses or recombinant viruses carrying mutant SARS-CoV-2 S proteins (459); however, only limited information on the role of these mutations for a broad range of animal species, as well as humans, is available so far.

Small animal models, such as mice and Syrian Golden hamsters, are available to study various aspects of SARS-CoV-2 infection and pathogenesis (460). Parental (Wuhan-like) SARS-CoV-2 viruses can infect genetically engineered mice that express hACE2, although unmodified mice are only permissive to mouse-adapted SARS-CoV-2 (424,425), with the exception of SARS-CoV-2 variants containing the N501Y polymorphism in their S protein (461). Hamsters are highly permissive to SARS-CoV-2 infection, and efficient virus replication and moderate to severe lung pathology are observed following virus replication, usually accompanied by weight loss and other clinical signs during acute infection (438,462–464). Small animal models for COVID-19 have been used to study viral transmission, pathogenesis, and immunity as well as to evaluate vaccines and therapeutic drugs and are also suitable models for investigating virulence and infectivity of SARS-CoV-2 variants (222).

In this study, we investigated the characteristics of key mutations found in Alpha, Beta, Gamma, and Delta VOCs (single or combinations of 614G, 501Y, 484K, 452R, and 478K mutations). Using lentivirus-based pseudotyped virus assays, the effects of key substitutions on virus entry into human and various animal ACE2-expressing cells and on the neutralizing activities of antisera from humans, cats, and rabbits were determined. In addition, we generated key substitutions

(501Y, 484A, 417N, 446S, 440K, 477N, 478K, 493R, and 498R) found in the Omicron VOC and examined the effects of these substitutions on the neutralizing activities of the respective antisera.

The presented results provide important insights into the impact of S protein mutations found in emerging SARS-CoV-2 variants on cell entry in human and other animal species and on virus replication and virus neutralization.

6.3 Materials and Methods

6.3.1 Cells and plasmids.

HEK293, Crandell-Rees feline kidney (CRFK), and Calu-3 cells were purchased from American Type Culture Collection (ATCC; Manassas, VA). Vero E6 cells expressing human TMPRSS2 (Vero-TMPRSS2) were obtained from Creative Biogene (Shirley, NY) (465). Cells were maintained with either Dulbecco's modified Eagle medium (DMEM) or Eagle's minimal essential medium (MEM), both supplemented with 5% fetal bovine serum (FBS), 100 U/mL penicillin, and 100 μg/mL streptomycin. The codon-optimized cDNAs of the open reading frame (ORF) of the human or animal ACE2 gene with FLAG tag were synthesized by Integrated DNA Technologies (Coralville, IA) and cloned into pIRES-Neo3 (TaKaRa Bio, Mountain View, CA). For the ACE2 gene of white-tailed deer, because only a partial ORF is available, the full ORF was constructed with the human ACE2 gene. These plasmids were then designated pIRES-Neo-(species) ACE2-FLAG. The animal species from which ACE2 gene sequences (listed in Table S1 in the supplemental material) were derived are cat, dog, Arabian camel, European mink, horse, rabbit, cattle, Syrian golden hamster, and white-tailed deer. Pseudotyped viruses expressing SARS-CoV-

2 S protein were generated by synthesizing the S gene, which was truncated by 26 amino acids at the C terminus, fused with a hemagglutinin (HA) tag by Integrated DNA Technologies, and cloned into plasmid pAbVec1 (Addgene, Watertown, MA), and designated pAbVec-SARS2-S. The parental S gene sequence was the prototype SARS-CoV-2 S gene from Wuhan (GenBank ID YP_009724390.1). This clone was then used to generate single or multiple mutations in the RBD of the S gene with a site-directed mutagenesis kit (Agilent, Santa Clara, CA) using primers listed in Table S2 and designated pAbVec-SARS2-S (mutant). Single mutations in the RBD include N501Y (Alpha variant), E484K, K417N, T478K, and L452R, and multiple mutations include N501Y + E484K (Gamma variant), L452R + E484K (Delta variant), L478K + L452R (Delta variant), N501Y + E484K + K417N (Beta variant), D614G + N501Y + E484K + K417N (Beta variant), and D614G + N501Y + E484A + K417N + G446S + N440K + S477N + T478K + Q493R + Q498R (Omicron variant). Each mutation was confirmed by Sanger sequencing analysis.

6.3.2 Generation of CRFK cells stably expressing human or animal ACE2.

CRFK cells, plated the previous day, were transfected with pIRES-Neo-human (or cat, dog, cattle, horse, camel, hamster, rabbit, mink, or white-tailed deer) ACE2-FLAG. The transfected cells were then subsequently selected in the presence of 1 mg/mL G418. Expression of the ACE2 receptor of each animal species in the cells was confirmed by Western blotting using antibody against human ACE2 (Abcam, Waltham, MA). Parental CRFK cells served as a control (mock).

6.3.3 Generation of SARS-CoV-2 S pseudotyped viruses.

The second-generation lentiviral packaging plasmid psPAX2 (Addgene), a reporter plasmid pUCGFP-Luc (Addgene), and parental or mutant pAbVec-SARS2-S were transfected into

HEK293 cells to produce pseudotyped viruses. Briefly, cells plated in 6-well plates the previous day were transfected with three plasmids (1 μg each per well) using Lipofectamine 2000 (Thermo Fisher, Waltham, MA). Following overnight incubation, medium was replaced with fresh medium containing 5% FBS, and the cells were further incubated for 48 h. Supernatants were collected, and cell debris was removed by centrifugation at 400 × g for 10 min. Quantitation of pseudotyped viruses was performed using an HIV p24 assay kit (TaKaRa Bio) or ELISA for SARS-CoV-2 S (Sino Biological, Wayne, PA) before storing at –80°C.

6.3.4 Pseudotyped virus entry assays.

To study the entry efficiency of parental or mutant S in cells expressing human or animal ACE2, HEK293 cells or CRFK cells expressing human or animal ACE2 were infected with pseudotyped virus carrying parental or mutant S protein. Briefly, cells plated the previous day were infected with each pseudotyped virus at a multiplicity of infection (MOI) of approximately 1 based on the p24 ELISA for pseudotyped virus preparation. Cell lysates were prepared at 48 h after infection, and firefly luciferase activity was measured on a luminometer (GloMax 20/20, Promega, Madison, WI). Fold change over the parental pseudotyped viruses was calculated for each mutant pseudotyped virus.

6.3.5 Statistical analysis.

Statistical analysis was performed using GraphPad Prism software version 6 (San Diego, CA). A one-way analysis of variance (ANOVA) followed by a Tukey post hoc test on the log10-transformed firefly luminescent units or neutralization titers was used to compare the parental and mutant pseudotyped viruses. To identify significant differences between ACE2-expressing cell

cultures or hamsters infected with the different SARS-CoV-2 strains, virus titer data were first log10 transformed, and raw means and standard deviations were calculated. The data were then analyzed by two-way ANOVA, followed by a Tukey's multiple-comparison test; statistical differences are indicated with an asterisk (*) representing a P value of <0.05. Data are representative of at least two independent experiments.

6.4 Results

6.4.1 Entry of pseudotyped virus with SARS-CoV-2 S into HEK293T or Crandell-Rees feline kidney (CRFK) cells expressing human or animal ACE2.

Expression of ACE2 in human kidney-derived HEK293T or CRFK cells that were stably transfected with a plasmid encoding the ACE2 protein from humans and various animal species was confirmed by Western blotting (Fig. 6.1A). Entry of pseudotyped viruses, measured by firefly luciferase, was comparable between HEK293T and CRFK cells expressing the same ACE2 construct. However, CRFK cells yielded more robust and consistent results than HEK293T cells; therefore, CRFK cells were subsequently used for pseudotyped virus entry assays. The results of the virus entry assays are shown in Fig. 6.1B and C. Importantly, native CRFK cells that do not express exogenous ACE2, only inherent feline ACE2 (mock), yielded negligible virus entry (Fig. 6.1B), indicating that CRFK cells are suitable to determine the effects of exogenous heterologous ACE2 on viral entry. Expression of various animal ACE2 receptors in CRFK cells led to greatly enhanced entry of pseudotyped viruses expressing the parental SARS-CoV-2 S protein (Fig. 6.1B), except for mink ACE2, which did not show the marked increase in virus entry compared to the other animal ACE2s; however, mink ACE2 had a 31-fold increase over nontransfected cells.

Cellular entry of pseudotyped viruses in the presence of ACE2 receptors from various animal species ranged from an approximately 1,200-fold (horse/cat) to 3,000-fold (rabbit) increase in cellular entry compared to the mock control (no ACE2 transfection). Figure 6.1C shows a summary of the virus entry results using cells expressing different animal ACE2 receptors compared to cells expressing human ACE2. Virus entry levels for each ACE2 species were considered high, medium, or low when greater than 80%, 10 to 80%, or 1 to 10% of virus entry in ACE2-expressing cells (compared to hACE2-expressing cells) was observed, respectively, based on the criteria suggested by Damas et al. (403). High levels of virus entry were observed in cells expressing ACE2 from human, dog, cow, hamster, or rabbit (Fig. 6.1B and C), while medium levels of virus entry were seen in cells expressing ACE2 from cat, horse, camel, and white-tailed deer. Expression of mink ACE2 resulted in low virus entry. The overall trend of virus entry in cells expressing various animal ACE2 receptors was similar to the in silico predictions by Damas et al. (403) (Fig. 6.1C).

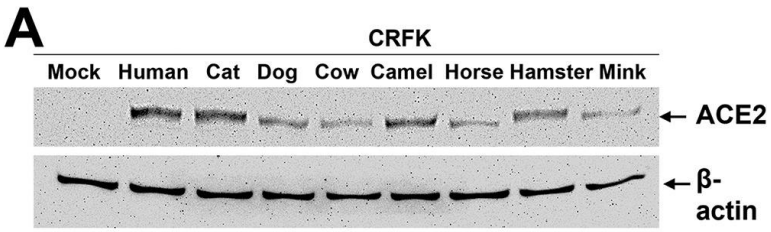

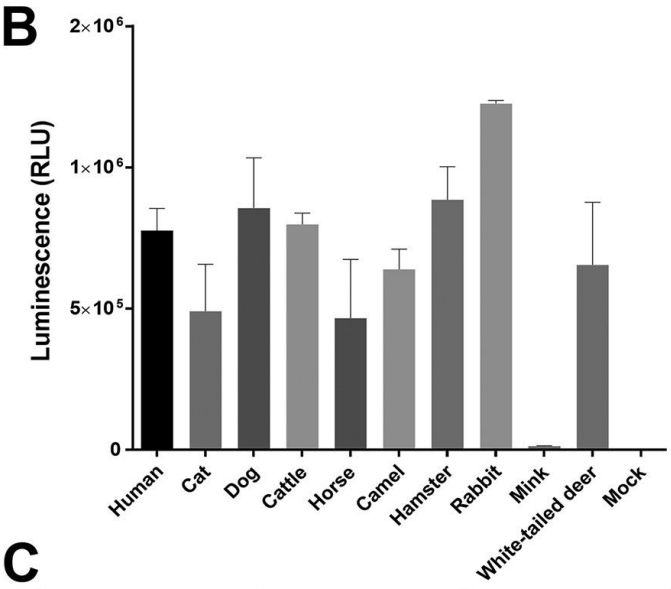

C

Origin of ACE2	Pseudotyped virus entry	In-silico Prediction*
Human	High#	High
Cat	Medium	Medium
Dog	High	Low
Cow	High	Medium
Horse	Medium	Low
Camel	Medium	Low
Hamster	High	Medium
Rabbit	High	Medium
Mink	Low	Very low
White-tailed deer	Medium	High

* Damas et al., PNAS 2020, #High: ≥ 80% of human, Medium: 10-80% of human, Low: 1-10% of human, Very low: < 1% of human

Figure 6.1 Effects of various ACE2 constructs on the entry of pseudotyped viruses carrying SARS-CoV-2 S into CRFK cells stably expressing ACE2 from various animal species.

(A) Western blot of CRFK cells stably expressing various ACE2 receptors or mock cells (no ACE2 transfection). Cell lysates were collected and probed using anti-ACE2 receptor or β-actin antibodies. (B) CRFK cells stably expressing various ACE2 receptors or mock cells (no ACE2

transfection) were infected with pseudotyped virus carrying the parental SARS-CoV-2 S protein. Following incubation of the cells with the pseudotyped virus for 48 h, cells were lysed, and luminescence units were measured. Each bar indicates the mean and the standard error of the means. (C) Summary of the results from the pseudotyped virus entry assay in B. Virus entry levels were considered high, medium, or low when greater than 80%, 10 to 80%, or 1 to 10% of virus entry in ACE2-expressing cells (compared to human ACE2 cells) was observed, respectively, based on the criteria suggested by Damas et al. (403). The asterisk (*) indicates in silico predictions by Damas et al. (403).

6.4.2 Entry of pseudotyped virus expressing SARS-CoV-2 parental or mutant S in human ACE2-expressing CRFK cells.

The pseudotyped virus preparations carrying single or multiple amino acid substitutions in S were quantitated and normalized by enzyme-linked immunosorbent assay (ELISA) p24 lentivirus antigen measurement or by SARS-CoV-2 S protein expression after transduction of the cells. Virus entry of each pseudotyped virus carrying single or multiple substitutions of 417N, 452R, 478K, 484K, 501Y, or 614G on the RBD of the S protein was compared to that of parental pseudotyped viruses (no substitution in S gene) in cells expressing human ACE2 or native CRFK cells (no human ACE2 expression). In CRFK cells expressing no exogenous ACEs (native feline ACE2-expressing CRFK cells), a significant decrease or increase in pseudotyped virus entry was observed with the 614G single mutation or the 614G-501Y-484K-417N quadruple mutation, respectively (Fig. 6.2A). However, the overall magnitude of pseudotyped virus entry in nontransfected CRFK cells was very low regardless of the presence or absence of S protein mutations, which confirms that nontransfected CRFK cells are poorly supportive of SARS-CoV-2 S-pseudotyped virus entry. However, expression of human ACE2 markedly enhanced viral entry

compared to native CRFK cells (Fig. 6.2B). In these cells, single substitutions of 501Y, 452R, or 478K did not lead to a statistically significant difference in virus entry compared to parental virus (Fig. 6.2B) except for 614G or 484K, which showed significantly reduced virus entry compared to the parental pseudotyped virus. Among the double substitutions (i.e., 614G-501Y, 501Y-484K, 452R-484K, or 452R-478K), only the 501Y-484K combination significantly increased pseudotyped virus entry compared to the parental pseudotyped virus. The addition of substitution 417N or 614G to the 501Y-484K combination, however, did not further increase the virus entry efficiency of pseudotyped virus compared to the 501Y-484K double substitution unless both 417N and 614G were combined with 501Y-484K in a quadruple combination (417N-484K-501Y-614G). Interestingly, when 501Y was combined with 614G (614G-501Y double substitution), an increase of virus entry was observed similar to the level of parental virus and the single 501Y virus. Virus entry capacity was further enhanced by the addition of 484K (614G-501Y-484K) or 484K-417N (614G-501Y-484K-417N). Similarly, the combination of 501Y and 484K led to significantly increased virus entry compared to the parental virus, suggesting that the 501Y substitution is important in negating the suppressive effects of the 484K and 614G single mutations (Fig. 6.2B). The reduced virus entry due to the 484K substitution was also restored to the level of the parental virus entry when combined with the 452R substitution (Fig. 6.2B). However, the 452R-478K double mutation did not lead to enhanced virus entry compared to the 452R or 478K single mutations.

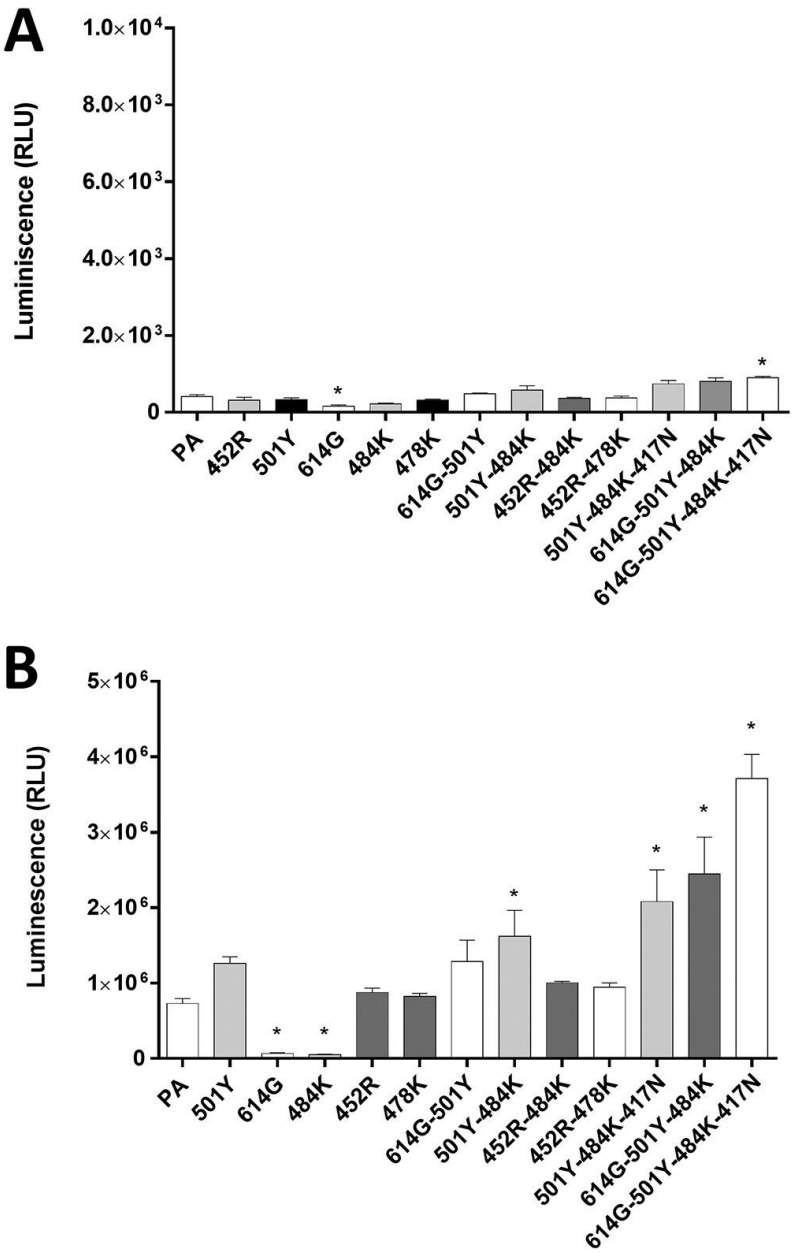

Figure 6.2 Entry of pseudotyped viruses carrying SARS-CoV-2 S with single or multiple substitutions on the RBD site into nontransfected CRFK or CRFK cells stably expressing human ACE2.

No human ACE2-expressing CRFK cells (A) or human ACE2-expressing CRFK cells (B) were infected with pseudotyped viruses with single or multiple RBD substitutions. Following incubation of the cells for 48 h, luminescence units were measured. Each bar indicates the mean and the

standard error of the means. PA indicates parental pseudotyped virus (no mutation in the S protein). One-way ANOVAs on the log10-transformed raw relative luminescence units were used to compare the parental (PA) group and other groups. Statistical differences between mutation and the parental virus groups are indicated with an asterisk (*, $P < 0.05$).

6.4.3 Entry of pseudotyped virus carrying SARS-CoV-2 parental or mutant S proteins in various ACE2-expressing CRFK cells.

In this experiment, we compared the entry of pseudotyped viruses with parental or mutant S into cells expressing ACE2 from various animal species, including humans. Overall, the trend of change in virus entry among various pseudotyped viruses was similar in all tested cells expressing various animal ACE2 receptors (Fig. 6.3). In general, the quadruple 614G-501Y-484K-417N substitution showed the highest fold increase compared to the parental S (no mutation), followed by the triple combination 614G-501Y-484K. The 501Y-484K and 501Y-484K-417N substitutions led to moderately increased virus entry compared to the parental S but without a statistically significant difference. The 614G single mutation led to a decrease in virus entry in cells expressing human and animal ACE2 (Fig. 6.2A and Fig. 6.3). Notably, even in mink ACE2-expressing cells, which support limited virus entry compared to other ACE2s, a similar trend was observed with pseudotyped viruses with single and multiple substitutions (Fig. 6.3). Interestingly, relatively little change was observed in virus entry among parental and mutant pseudotyped viruses in horse ACE2-expressing cells (Fig. 6.3). These results suggest that the effects of these mutations in the RBD region of the S protein for virus entry are shared among a wide range of animal ACE2 receptors.

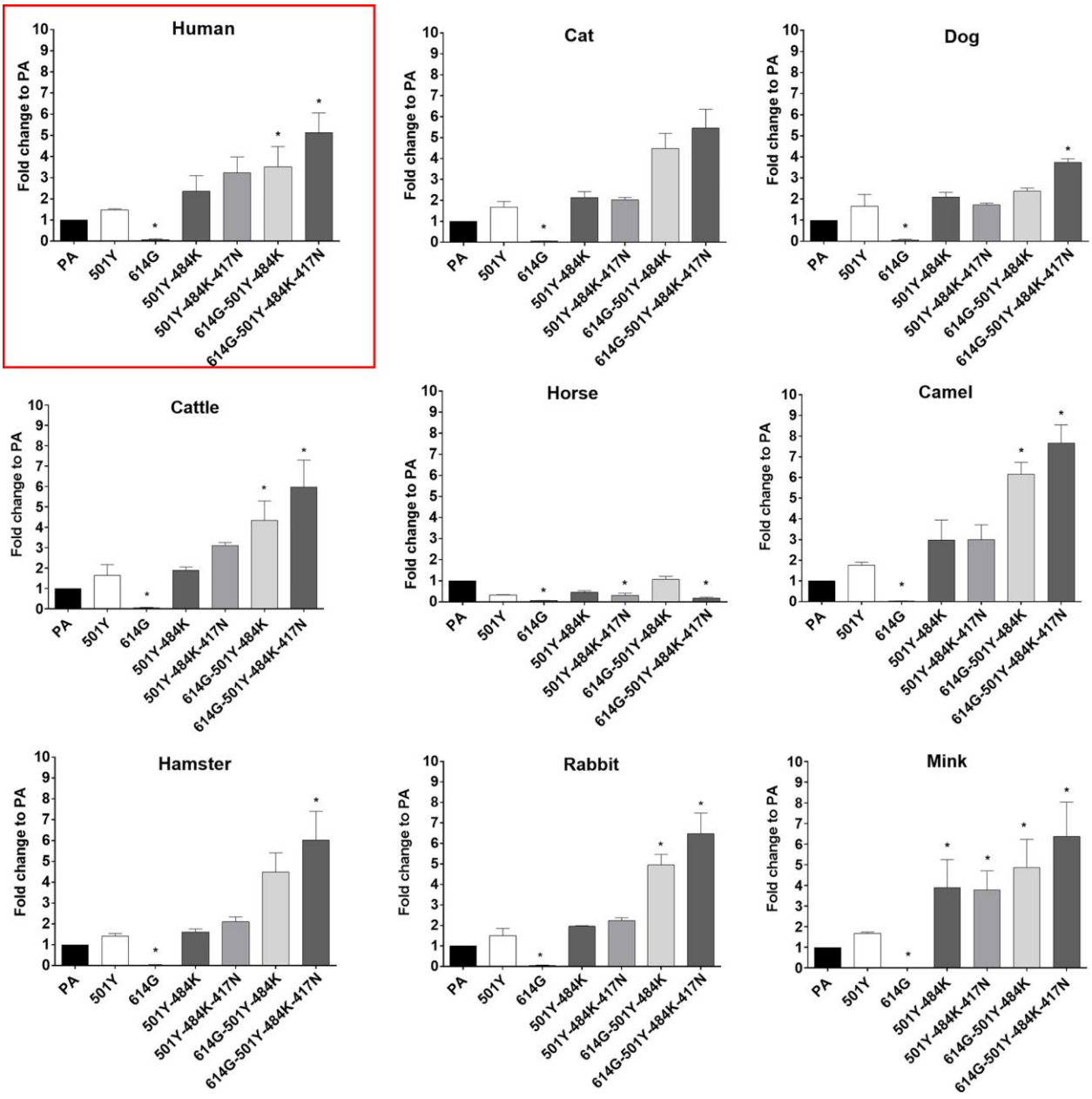

Figure 6.3 Entry of pseudotyped viruses carrying SARS-CoV-2 S with single or multiple mutations on the RBD site of S protein into CRFK cells expressing ACE2 of various species.

CRFK cells expressing ACE2 from different animal species were infected with pseudotyped viruses expressing single or multiple S protein substitutions. Following incubation of the cells for 48 h, cells were lysed, and relative luminescence units were measured. Each mutant pseudotyped

virus was compared with the parental pseudotyped virus (PA), and data are presented as the fold change to PA. One-way ANOVAs on the log10-transformed raw relative fluorescence units were used to compare the parental group and other groups. Statistical differences between mutation and the parental virus groups are indicated with an asterisk (*, $P < 0.05$). Red square: human data.

6.5 Discussion

Since the unexpected emergence of SARS-CoV-2 in human populations, extensive efforts have been directed toward both elucidating the risks associated with emerging virus variants and identifying susceptible animal species to better understand the zoonotic/reverse zoonotic implications of the pandemic. In our study, we used pseudotyped virus assays to elucidate the roles of ACE2 from various animal species, including humans, in viral entry, which is a central event determining host susceptibility to SARS-CoV-2 infection. Using the S protein from the ancestral prototype (parental) SARS-CoV-2 strain (Wuhan-Hu-1), we found that several animal ACE2 receptors can efficiently interact with SARS-CoV-2 S protein to allow virus entry into cells. The efficiencies of virus entry among animal ACE2 receptors tested are not remarkably different from that of human ACE2, except for mink ACE2, which was consistently associated with comparatively low virus entry efficacy. Many animal species have been reported to be susceptible to SARS-CoV-2 infection either in experimental studies or by natural infection, as evidenced by clinical disease, viral replication in the respiratory tract and other organs, viral shedding/transmission, or seroconversion; these include domestic and large captive cats, dogs, cattle, mink, ferrets, otters, fruit bats, nonhuman primates, New Zealand White rabbits, hamsters, deer mice, bushy-tailed woodrats, striped skunks, and white-tailed deer (419,466–469). Other animal species either have not been tested or showed no consistent evidence of active viral

infection. Among them, cats and dogs have been of particular interest due to their proximity to humans. These companion animals can be infected by SARS-CoV-2 in natural and experimental settings and usually remain asymptomatic, although some develop mild respiratory disease (411,470–472). Overall, our pseudotyped virus entry results are consistent with previous animal susceptibility studies with most of the animal ACE2 receptors (human, cat, dog, cattle, camel, hamster, rabbit, mink, and white-tailed deer) tested in this report for virus entry (419,466–469). Although there are currently no or few reports of natural or experimental infection in horses (418) and camels, there have been concerns that SARS-CoV-2 may infect these animals, based on predictions from structural in silico analyses or cell-to-cell fusion assays using pseudotyped virus (401–403). Our results regarding the horse and camel ACE2 receptors and pseudotyped viruses provide a further impetus to study viral susceptibility in these animal species; however, our structural modeling (Fig. 4 in this research article – not included in this chapter) coupled with previous experimental evidence (473) indicates that the horse ACE2 Y41H substitution may confer resistance to RBD binding of both parental and mutated S proteins. Recent reports showed no evidence of virus replication in a horse experimentally infected with SARS-CoV-2 (418), although this requires further confirmation. An experimental infection study of cattle revealed that SARS-CoV-2 infection in this species may occur but does not appear to be robust, which seems to support the results of pseudotyped virus assays conducted by us and others (402,474). Interestingly, mink ACE2 was predicted to have a weak interaction with S protein in a previous in silico analysis study (403); similarly, our pseudotyped virus entry assay showed that mink ACE2 allowed viral entry, although at a relatively lower level than that observed with ACE2 from other animals or humans. This is somewhat surprising because mink are highly susceptible to SARS-CoV-2 infection, leading to a significant number of outbreaks of COVID-19 in mink farms with high

morbidity/mortality (405,406). It is likely that an unknown disparity exists between virus entry mediated by pseudotyped viruses and native cell-virus interaction for mink. Structural models were generated to gain insight into the interaction between the S protein and selected animal ACE2 with a focus on the residues interacting with K417, E484, and N501 on the S protein (Fig. 4 in this research article – not included in this chapter). The respective ACE2 residues are mostly conserved with minor variations among human and animal ACE2s, which is in line with the pseudotyped virus assay results obtained in this study.

We also examined the effects of various mutations (417N, 452R, 478K, 484K, and 501Y) in the RBD, found in the Alpha (614G-501Y), Beta (614G-501Y-484K-417N), or Delta variants (452R-478K or 452R-484K), on virus entry in cells expressing human or animal ACE2 receptors using pseudotyped viruses. SARS-CoV-2 variants carrying 614G have replaced the prototype 614D virus and now are part of all major variants (475,476), most likely because 614G is associated with enhanced fitness in susceptible cells, including human airway cells (476,477). The 614G virus was also shown to enhance replication in the upper respiratory tract and transmission in infected hamsters (477,478), although this was not observed in hACE2 transgenic mice (477). In human ACE2-expressing 293T cells, pseudotyped viruses carrying 614G alone have been reported to either increase (476,479–482) or cause no change (459) in viral cell entry. In contrast to previous findings showing an increase in 614G cell entry in cells expressing human, cat, or dog ACE2 orthologs (476), pseudoviruses carrying the 614G mutation alone consistently showed decreased cell entry across all species in our assays. Structural studies have indicated that 614G does not result in a higher affinity toward ACE2 but instead results in allosteric changes conducive toward a more open conformation of the RBD in which it is better positioned to interact with the ACE2

receptor (476). The entry efficiency of the 484K single mutation alone has not yet been well studied. In our study using human ACE2-expressing cells, entry of the 614G or 484K mutant pseudotyped viruses was significantly decreased compared to the parental virus. In contrast, the 614G-501Y-484K (found in the Beta VOC) and 614G-501Y-484K-417N (found in Beta and Gamma VOCs) mutations in the S protein increased virus entry compared to the parental pseudotyped virus. In a previous report (474), pseudoviruses with these mutations did not change virus entry in cells expressing human and various animal ACE2 receptors, with the exception of murine ACE2-expressing cells (474). This observed difference in virus entry may be due to the different assay system, including cell types, variance of assays, or other factors.

In summary, our results obtained from a lentivirus-based pseudovirus system and hamster infection studies showed that a wide range of animal ACE2s support pseudotyped virus entry, and the key mutations found in the VOCs affect pseudotyped virus entry in cells expressing human or animal ACE2 as well as neutralizing activity of sera from humans, cats, and rabbits. The hamster infection study suggest a replicative advantage of the Beta variant over the parental and Alpha variant. The findings of this study highlight the importance of elucidating the roles of S mutations in detail and monitoring for evolving SARS-CoV-2 variants to assess their public health implications.

References

1. Le Pendu J, Abrantes J, Bertagnoli S, Guitton JS, Le Gall-Reculé G, Lopes AM, et al. Proposal for a unified classification system and nomenclature of lagoviruses. J Gen Virol [Internet]. 2017 Jul 1 [cited 2020 Aug 14];98(7):1658–66. Available from: https://www.microbiologyresearch.org/content/journal/jgv/10.1099/jgv.0.000840

2. Alexandrov M, Peshev R, Bozhkov S, Yanchev I, Doumanova L. Electron- and immunoelectron-microscopic investigation on the rabbit haemorrhagic disease virus. Comp Immunol Microbiol Infect Dis [Internet]. 1993 Jan 1 [cited 2020 Aug 18];16(1):21–7. Available from: http://www.sciencedirect.com/science/article/pii/014795719390057C

3. Liu SJ, Xue HP, Pu BQ, Qian NH. A new viral disease in rabbits. Anim Husb Vet Med Xumu Yu Shouyi [Internet]. 1984 [cited 2020 Aug 18];16(6):253–5. Available from: https://www.cabdirect.org/cabdirect/abstract/19852264426

4. Park JH, Kida H, Ueda K, Ochiai K, Goryo M, Itakura C. Etiology of rabbit haemorrhagic disease spontaneously occurring in Korea. Zentralblatt Vet Reihe B J Vet Med Ser B. 1991 Dec;38(10):749–54.

5. Smíd B, Valícek L, Stěpánek J, Jurák E, Rodák L. Experimental transmission and electron microscopic demonstration of the virus of haemorrhagic disease of rabbits in Czechoslovakia. Zentralblatt Vet Reihe B J Vet Med Ser B. 1989 May;36(3):237–40.

6. Zheng H, Zhao L, Sun F. [A new virus of rabbit. II. Study on morphological structure and some physicochemical properties of a strain of rabbit hemorrhagic disease virus]. Wei Sheng Wu Xue Bao. 1992 Jun;32(3):198–203.

7. Meyers G, Wirblich C, Thiel HJ. Genomic and subgenomic RNAs of rabbit hemorrhagic disease virus are both protein-linked and packaged into particles. Virology. 1991 Oct;184(2):677–86.

8. Ohlinger VF, Thiel HJ. Identification of the viral haemorrhagic disease virus of rabbits as a calicivirus. Rev Sci Tech Int Off Epizoot. 1991 Jun;10(2):311–23.

9. Parra F, Boga JA, Marin MS, Casais R. The amino terminal sequence of VP60 from rabbit hemorrhagic disease virus supports its putative subgenomic origin. Virus Res. 1993 Mar;27(3):219–28.

10. Boniotti B, Wirblich C, Sibilia M, Meyers G, Thiel HJ, Rossi C. Identification and characterization of a 3C-like protease from rabbit hemorrhagic disease virus, a calicivirus. J Virol. 1994 Oct;68(10):6487–95.

11. Gould AR, Kattenbelt JA, Lenghaus C, Morrissy C, Chamberlain T, Collins BJ, et al. The complete nucleotide sequence of rabbit haemorrhagic disease virus (Czech strain V351):

use of the polymerase chain reaction to detect replication in Australian vertebrates and analysis of viral population sequence variation. Virus Res [Internet]. 1997 Jan 1 [cited 2020 Aug 18];47(1):7–17. Available from: http://www.sciencedirect.com/science/article/pii/S0168170296013998

12. Wirblich C, Thiel HJ, Meyers G. Genetic map of the calicivirus rabbit hemorrhagic disease virus as deduced from in vitro translation studies. J Virol [Internet]. 1996 Nov;70(11):7974–83. Available from: https://www.ncbi.nlm.nih.gov/pmc/articles/PMC190870/

13. Le Gall G, Huguet S, Vende P, Vautherot JF, Rasschaert D. European brown hare syndrome virus: molecular cloning and sequencing of the genome. J Gen Virol. 1996 Aug;77 (Pt 8):1693–7.

14. Lopes AM, Gavier-Widén D, Le Gall-Reculé G, Esteves PJ, Abrantes J. Complete coding sequences of European brown hare syndrome virus (EBHSV) strains isolated in 1982 in Sweden. Arch Virol. 2013 Oct;158(10):2193–6.

15. Capucci L, Fusi P, Lavazza A, Pacciarini ML, Rossi C. Detection and preliminary characterization of a new rabbit calicivirus related to rabbit hemorrhagic disease virus but nonpathogenic. J Virol. 1996 Dec;70(12):8614–23.

16. Droillard C, Lemaitre E, Chatel M, Guitton JS, Marchandeau S, Eterradossi N, et al. First Complete Genome Sequence of a Hare Calicivirus Strain Isolated from Lepus europaeus. Microbiol Resour Announc. 2018 Dec;7(22).

17. Meyers G, Wirblich C, Thiel HJ. Rabbit hemorrhagic disease virus—molecular cloning and nucleotide sequencing of a calicivirus genome. Virology [Internet]. 1991 Oct 1 [cited 2020 Aug 11];184(2):664–76. Available from: http://www.sciencedirect.com/science/article/pii/004268229190436F

18. Oka T, Murakami K, Wakita T, Katayama K. Comparative site-directed mutagenesis in the catalytic amino acid triad in calicivirus proteases: In vitro calicivirus protease activity. Microbiol Immunol [Internet]. 2011 Feb [cited 2020 Nov 16];55(2):108–14. Available from: http://doi.wiley.com/10.1111/j.1348-0421.2010.00295.x

19. Martín Alonso JM, Casais R, Boga JA, Parra F. Processing of rabbit hemorrhagic disease virus polyprotein. J Virol. 1996 Feb;70(2):1261–5.

20. Thumfart JO, Meyers G. Rabbit hemorrhagic disease virus: identification of a cleavage site in the viral polyprotein that is not processed by the known calicivirus protease. Virology. 2002 Dec 20;304(2):352–63.

21. Men Y, Wang Y, Liu J, Tian J, Han X, Chen Y, et al. RHDV 3C protein antagonizes type I interferon signaling by cleaving interferon promoter stimulated 1 protein [Internet]. In Review; 2022 Jul [cited 2022 Aug 5]. Available from: https://www.researchsquare.com/article/rs-1832468/v1

22. Moss SR, Turner SL, Trout RC, White PJ, Hudson PJ, Desai A, et al. Molecular epidemiology of Rabbit haemorrhagic disease virus. J Gen Virol. 2002 Oct;83(Pt 10):2461–7.

23. Nam-Yong P, Chi-young C, Jin-ho K, Sung-man C, Yeon-ho C, Byung-tack J, et al. An Outbreak of Viral Haemorrhagic Pneumonia(Tentative Name) of Rabbits in Korea. J Korean Vet Med Assoc [Internet]. 1987 [cited 2020 Aug 18];23(9):603–10. Available from: https://www.koreascience.or.kr/article/JAKO198772605609206.page

24. Forrester NL, Abubakr MI, Abu Elzein EME, Al-Afaleq AI, Housawi FMT, Moss SR, et al. Phylogenetic analysis of rabbit haemorrhagic disease virus strains from the Arabian Peninsula: did RHDV emerge simultaneously in Europe and Asia? Virology. 2006 Jan 20;344(2):277–82.

25. Abu Elzein EM, al-Afaleq AI. Rabbit haemorrhagic disease in Saudi Arabia. Vet Rec. 1999 Apr 24;144(17):480–1.

26. Bouslama A, De Mia GM, Hammami S, Aouina T, Soussi H, Frescura T. Identification of the virus of rabbit haemorrhagic disease in Tunisia. Vet Rec. 1996 Feb 3;138(5):108–10.

27. Górski J, Mizak B, Chrobocińska M. Control of viral haemorrhagic disease of rabbits in Poland. Rev Sci Tech Int Off Epizoot [Internet]. 1994 Sep;13(3):881–91. Available from: https://pubmed.ncbi.nlm.nih.gov/7949360/

28. Gregg DA, House C, Meyer R, Berninger M. Viral haemorrhagic disease of rabbits in Mexico: epidemiology and viral characterization. Rev Sci Tech Int Off Epizoot. 1991 Jun;10(2):435–51.

29. Kölbl S, Settele J, Schönbauer M. [The first appearance of infectious hemorrhagic disease of rabbits in Austria]. Berl Munch Tierarztl Wochenschr. 1990 Aug 1;103(8):261–6.

30. Morisse JP (Centre N d'Etudes V et A, Le Gall G, Boilletot E. Hepatitis of viral origin in Leporidae: introduction and aetiological hypotheses [viral haemorrhagic disease of rabbits (VHD) and European brown hare syndrome (EBHS)]. Rev Sci Tech OIE Fr [Internet]. 1991 [cited 2020 Aug 18]; Available from: https://agris.fao.org/agris-search/search.do?recordID=FR9103933

31. Shien JH, Shieh HK, Lee LH. Characterization of rabbit hemorrhagic disease virus field isolates in Taiwan. J Virol Methods. 1998 Mar;71(1):27–33.

32. Kovaliski J. Monitoring the spread of rabbit hemorrhagic disease virus as a new biological agent for control of wild European rabbits in Australia. J Wildl Dis. 1998 Jul;34(3):421–8.

33. Mutze G, Cooke B, Alexander P. The initial impact of rabbit hemorrhagic disease on european rabbit populations in south australia. J Wildl Dis [Internet]. 1998 Apr 1 [cited 2020 Aug 18];34(2):221–7. Available from: https://www.jwildlifedis.org/doi/10.7589/0090-3558-34.2.221

34. Thompson J, Clark G. Rabbit calicivirus disease now established in New Zealand. Surveillance [Internet]. 1997 Jan 1;24(4):5–6. Available from: http://www.sciquest.org.nz/node/47034

35. Rabbit calicivirus infection confirmed in Iowa rabbitry [Internet]. American Veterinary Medical Association. [cited 2022 Nov 8]. Available from: https://www.avma.org/javma-news/2000-05-15/rabbit-calicivirus-infection-confirmed-iowa-rabbitry

36. Capucci L, Fallacara F, Grazioli S, Lavazza A, Pacciarini ML, Brocchi E. A further step in the evolution of rabbit hemorrhagic disease virus: the appearance of the first consistent antigenic variant. Virus Res. 1998 Nov;58(1–2):115–26.

37. Le Gall-Reculé G, Zwingelstein F, Laurent S, de Boisséson C, Portejoie Y, Rasschaert D. Phylogenetic analysis of rabbit haemorrhagic disease virus in France between 1993 and 2000, and the characterisation of RHDV antigenic variants. Arch Virol [Internet]. 2003 Jan 1 [cited 2020 Aug 18];148(1):65–81. Available from: https://doi.org/10.1007/s00705-002-0908-1

38. Oem JK, Lee KN, Roh IS, Lee KK, Kim SH, Kim HR, et al. Identification and characterization of rabbit hemorrhagic disease virus genetic variants isolated in Korea. J Vet Med Sci. 2009 Nov;71(11):1519–23.

39. Schirrmeier H, Reimann I, Köllner B, Granzow H. Pathogenic, antigenic and molecular properties of rabbit haemorrhagic disease virus (RHDV) isolated from vaccinated rabbits: detection and characterization of antigenic variants. Arch Virol. 1999;144(4):719–35.

40. Li Y, Yao X, Li Y, Xu F, Yang Z. Adaptive diversification between the classic rabbit hemorrhagic disease virus (RHDV) and the RHDVa isolates: A genome-wide perspective. Microb Pathog. 2017 Sep;110:527–32.

41. Abrantes J, Esteves PJ, van der Loo W. Evidence for recombination in the major capsid gene VP60 of the rabbit haemorrhagic disease virus (RHDV). Arch Virol. 2008;153(2):329–35.

42. Forrester NL, Moss SR, Turner SL, Schirrmeier H, Gould EA. Recombination in rabbit haemorrhagic disease virus: possible impact on evolution and epidemiology. Virology. 2008 Jul 5;376(2):390–6.

43. Lopes AM, Silvério D, Magalhães MJ, Areal H, Alves PC, Esteves PJ, et al. Characterization of old RHDV strains by complete genome sequencing identifies a novel genetic group. Sci Rep. 2017 19;7(1):13599.

44. Le Gall G, Arnauld C, Boilletot E, Morisse JP, Rasschaert D. Molecular epidemiology of rabbit haemorrhagic disease virus outbreaks in France during 1988 to 1995. J Gen Virol [Internet]. 1998 Jan;79 (Pt 1):11–6. Available from: https://www.microbiologyresearch.org/content/journal/jgv/10.1099/0022-1317-79-1-11

45. Nowotny N, Bascuñana CR, Ballagi-Pordány A, Gavier-Widén D, Uhlén M, Belák S. Phylogenetic analysis of rabbit haemorrhagic disease and European brown hare syndrome viruses by comparison of sequences from the capsid protein gene. Arch Virol. 1997;142(4):657–73.

46. Kesy A, Fitzner A, Niedbalski W, Paprocka G, Walkowiak B. A new variant of the viral haemorrhagic disease of rabbits virus. Rev Sci Tech Int Off Epizoot. 1996 Sep;15(3):1029–35.

47. White PJ, Trout RC, Moss SR, Desai A, Armesto M, Forrester NL, et al. Epidemiology of rabbit haemorrhagic disease virus in the United Kingdom: evidence for seasonal transmission by both virulent and avirulent modes of infection. Epidemiol Infect. 2004 Jun;132(3):555–67.

48. Drollette D. Wide use of rabbit virus is good news for native species. Science [Internet]. 1997 Jan 10;275(5297):154. Available from: https://science.sciencemag.org/content/275/5297/154

49. McColl KA, Merchant JC, Hardy J, Cooke BD, Robinson A, Westbury HA. Evidence for insect transmission of rabbit haemorrhagic disease virus. Epidemiol Infect. 2002 Dec;129(3):655–63.

50. Kimura T, Mitsui I, Okada Y, Furuya T, Ochiai K, Umemura T, et al. Distribution of rabbit haemorrhagic disease virus RNA in experimentally infected rabbits. J Comp Pathol. 2001 Apr;124(2–3):134–41.

51. Marcato PS, Benazzi C, Vecchi G, Galeotti M, Della Salda L, Sarli G, et al. Clinical and pathological features of viral haemorrhagic disease of rabbits and the European brown hare syndrome: -EN- -FR- -ES-. Rev Sci Tech OIE [Internet]. 1991 Jun 1 [cited 2020 Aug 18];10(2):371–92. Available from: https://doc.oie.int/dyn/portal/index.seam?page=alo&aloId=25329

52. Abrantes J, van der Loo W, Le Pendu J, Esteves PJ. Rabbit haemorrhagic disease (RHD) and rabbit haemorrhagic disease virus (RHDV): a review. Vet Res [Internet]. 2012 [cited 2020 Aug 11];43(1):12. Available from: http://www.veterinaryresearch.org/content/43/1/12

53. Campagnolo ER, Ernst MJ, Berninger ML, Gregg DA, Shumaker TJ, Boghossian AM. Outbreak of rabbit hemorrhagic disease in domestic lagomorphs. J Am Vet Med Assoc. 2003 Oct 15;223(8):1151–5, 1128.

54. Capucci L, Scicluna MT, Lavazza A. Diagnosis of viral haemorrhagic disease of rabbits and the European brown hare syndrome. Rev Sci Tech Int Off Epizoot. 1991 Jun;10(2):347–70.

55. Alves PC, Ferrand N, Hackländer K, editors. Lagomorph biology: evolution, ecology, and conservation. Berlin ; New York: Springer; 2008. 413 p.

56. Marchandeau S, Chantal J, Portejoie Y, Barraud S, Chaval Y. Impact of viral hemorrhagic disease on a wild population of European rabbits in France. J Wildl Dis. 1998 Jul;34(3):429–35.

57. Villafuerte R, Calvete C, Gortázar C, Moreno S. First epizootic of rabbit hemorrhagic disease in free living populations of Oryctolagus cuniculus at Doñana National Park, Spain. J Wildl Dis [Internet]. 1994 Apr;30(2):176–9. Available from: https://doi.org/10.7589/0090-3558-30.2.176

58. Ohlinger VF, Haas B, Meyers G, Weiland F, Thiel HJ. Identification and characterization of the virus causing rabbit hemorrhagic disease. J Virol. 1990 Jul;64(7):3331–6.

59. Parra F, Prieto M. Purification and characterization of a calicivirus as the causative agent of a lethal hemorrhagic disease in rabbits. J Virol [Internet]. 1990 Aug 1 [cited 2020 Aug 11];64(8):4013–5. Available from: https://jvi.asm.org/content/64/8/4013

60. Ueda K, Park JH, Ochiai K, Itakura C. Disseminated intravascular coagulation (DIC) in rabbit haemorrhagic disease. Jpn J Vet Res [Internet]. 1992 Dec;40(4):133–41. Available from: https://pubmed.ncbi.nlm.nih.gov/1338394/

61. Hall RN, Peacock DE, Kovaliski J, Mahar JE, Mourant R, Piper M, et al. Detection of RHDV2 in European brown hares (Lepus europaeus) in Australia. Vet Rec. 2017 Feb 4;180(5):121.

62. Strive T, Elsworth P, Liu J, Wright JD, Kovaliski J, Capucci L. The non-pathogenic Australian rabbit calicivirus RCV-A1 provides temporal and partial cross protection to lethal Rabbit Haemorrhagic Disease Virus infection which is not dependent on antibody titres. Vet Res [Internet]. 2013 [cited 2020 Aug 18];44(1):51. Available from: https://www.ncbi.nlm.nih.gov/pmc/articles/PMC3733936/

63. Frölich K, Klima F, Dedek J. Antibodies against rabbit hemorrhagic disease virus in free-ranging red foxes from Germany. J Wildl Dis. 1998 Jul;34(3):436–42.

64. Leighton FA, Artois M, Capucci L, Gavier-Widén D, Morisse JP. Antibody response to rabbit viral hemorrhagic disease virus in red foxes (Vulpes vulpes) consuming livers of infected rabbits (Oryctolagus cuniculus). J Wildl Dis. 1995 Oct;31(4):541–4.

65. Parkes JP, Heyward RP, Henning J, Motha MXJ. Antibody responses to rabbit haemorrhagic disease virus in predators, scavengers, and hares in New Zealand during epidemics in sympatric rabbit populations. N Z Vet J. 2004 Apr;52(2):85–9.

66. Merchán T, Rocha G, Alda F, Silva E, Thompson G, de Trucios SH, et al. Detection of rabbit haemorrhagic disease virus (RHDV) in nonspecific vertebrate hosts sympatric to the European wild rabbit (Oryctolagus cuniculus). Infect Genet Evol [Internet]. 2011 Aug 1 [cited 2020 Aug 18];11(6):1469–74. Available from: http://www.sciencedirect.com/science/article/pii/S1567134811001389

67. Buddle BM, de Lisle GW, McColl K, Collins BJ, Morrissy C, Westbury HA. Response of the North Island brown kiwi, Apteryx australis mantelli and the lesser short-tailed bat, Mystacina tuberculata to a measured dose of rabbit haemorrhagic disease virus. N Z Vet J. 1997 Jun;45(3):109–13.

68. Shien JH, Lee LH. Susceptibility of piglets to rabbit hemorrhagic disease virus following experimental infection. Can J Vet Res Rev Can Rech Veterinaire. 2000 Apr;64(2):134–7.

69. Carman JA, Garner MG, Catton MG, Thomas S, Westbury HA, Cannon RM, et al. Viral haemorrhagic disease of rabbits and human health. Epidemiol Infect. 1998 Oct;121(2):409–18.

70. Tunon MJ, Sanchez-Campos S, Garcia-Ferreras J, Alvarez M, Jorquera F, Gonzalez-Gallego J. Rabbit hemorrhagic viral disease: Characterization of a new animal model of fulminant liver failure. J Lab Clin Med [Internet]. 2003 Apr 1 [cited 2020 Aug 19];141(4):272–8. Available from: http://www.sciencedirect.com/science/article/pii/S0022214302930374

71. Le Gall-Reculé G, Zwingelstein F, Boucher S, Le Normand B, Plassiart G, Portejoie Y, et al. Detection of a new variant of rabbit haemorrhagic disease virus in France. Vet Rec. 2011 Feb 5;168(5):137–8.

72. Abrantes J, Lopes AM, Dalton KP, Melo P, Correia JJ, Ramada M, et al. New variant of rabbit hemorrhagic disease virus, Portugal, 2012-2013. Emerg Infect Dis. 2013 Nov;19(11):1900–2.

73. Baily JL, Dagleish MP, Graham M, Maley M, Rocchi MS. RHDV variant 2 presence detected in Scotland. Vet Rec. 2014 Apr 19;174(16):411.

74. Dalton KP, Nicieza I, Abrantes J, Esteves PJ, Parra F. Spread of new variant RHDV in domestic rabbits on the Iberian Peninsula. Vet Microbiol. 2014 Feb 21;169(1–2):67–73.

75. Hall RN, Mahar JE, Haboury S, Stevens V, Holmes EC, Strive T. Emerging Rabbit Hemorrhagic Disease Virus 2 (RHDVb), Australia. Emerg Infect Dis. 2015 Dec;21(12):2276–8.

76. Le Gall-Reculé G, Lavazza A, Marchandeau S, Bertagnoli S, Zwingelstein F, Cavadini P, et al. Emergence of a new lagovirus related to Rabbit Haemorrhagic Disease Virus. Vet Res. 2013 Sep 8;44:81.

77. Westcott DG, Frossard JP, Everest D, Dastjerdi A, Duff JP, Steinbach F, et al. Incursion of RHDV2-like variant in Great Britain. Vet Rec. 2014 Mar 29;174(13):333.

78. Abrantes J, Droillard C, Lopes AM, Lemaitre E, Lucas P, Blanchard Y, et al. Recombination at the emergence of the pathogenic rabbit haemorrhagic disease virus Lagovirus europaeus/GI.2. Sci Rep. 2020 Sep 2;10(1):14502.

79. Lopes AM, Dalton KP, Magalhães MJ, Parra F, Esteves PJ, Holmes EC, et al. Full genomic analysis of new variant rabbit hemorrhagic disease virus revealed multiple recombination events. J Gen Virol. 2015 Jun;96(Pt 6):1309–19.

80. Silvério D, Lopes AM, Melo-Ferreira J, Magalhães MJ, Monterroso P, Serronha A, et al. Insights into the evolution of the new variant rabbit haemorrhagic disease virus (GI.2) and the identification of novel recombinant strains. Transbound Emerg Dis. 2018 Aug;65(4):983–92.

81. Mahar JE, Jenckel M, Huang N, Smertina E, Holmes EC, Strive T, et al. Frequent intergenotypic recombination between the non-structural and structural genes is a major driver of epidemiological fitness in caliciviruses. Virus Evol. 2021;7(2):veab080.

82. Lankton JS, Knowles S, Keller S, Shearn-Bochsler VI, Ip HS. Pathology of Lagovirus europaeus GI.2/RHDV2/b (Rabbit Hemorrhagic Disease Virus 2) in Native North American Lagomorphs. J Wildl Dis. 2021 May 7;

83. Williams LBA, Edmonds SE, Kerr SR, Broughton-Neiswanger LE, Snekvik KR. Clinical and pathologic findings in an outbreak in rabbits of natural infection by rabbit hemorrhagic disease virus 2 in the northwestern United States. J Vet Diagn Investig Off Publ Am Assoc Vet Lab Diagn Inc. 2021 Jun 7;10406387211022466.

84. Dalton KP, Nicieza I, Balseiro A, Muguerza MA, Rosell JM, Casais R, et al. Variant rabbit hemorrhagic disease virus in young rabbits, Spain. Emerg Infect Dis. 2012 Dec;18(12):2009–12.

85. Neimanis A, Larsson Pettersson U, Huang N, Gavier-Widén D, Strive T. Elucidation of the pathology and tissue distribution of Lagovirus europaeus GI.2/RHDV2 (rabbit haemorrhagic disease virus 2) in young and adult rabbits (Oryctolagus cuniculus). Vet Res. 2018 05;49(1):46.

86. Calvete C, Mendoza M, Alcaraz A, Sarto MP, Jiménez-de-Bagüéss MP, Calvo AJ, et al. Rabbit haemorrhagic disease: Cross-protection and comparative pathogenicity of GI.2/RHDV2/b and GI.1b/RHDV lagoviruses in a challenge trial. Vet Microbiol. 2018 Jun;219:87–95.

87. Neave MJ, Hall RN, Huang N, McColl KA, Kerr P, Hoehn M, et al. Robust Innate Immunity of Young Rabbits Mediates Resistance to Rabbit Hemorrhagic Disease Caused by Lagovirus Europaeus GI.1 But Not GI.2. Viruses. 2018 19;10(9).

88. Taggart PL, Hall RN, Cox TE, Kovaliski J, McLeod SR, Strive T. Changes in virus transmission dynamics following the emergence of RHDV2 shed light on its competitive advantage over previously circulating variants. Transbound Emerg Dis. 2021 Mar 16;

89. Calvete C, Sarto MP, Iguacel L, Calvo JH. Infectivity of rabbit haemorrhagic disease virus excreted in rabbit faecal pellets. Vet Microbiol. 2021 Jun;257:109079.

90. Peacock D, Kovaliski J, Sinclair R, Mutze G, Iannella A, Capucci L. RHDV2 overcoming RHDV immunity in wild rabbits (Oryctolagus cuniculus) in Australia. Vet Rec. 2017 18;180(11):280.

91. Buehler M, Jesse ST, Kueck H, Lange B, Koenig P, Jo WK, et al. Lagovirus europeus GI.2 (rabbit hemorrhagic disease virus 2) infection in captive mountain hares (Lepus timidus) in Germany. BMC Vet Res. 2020 May 27;16(1):166.

92. Camarda A, Pugliese N, Cavadini P, Circella E, Capucci L, Caroli A, et al. Detection of the new emerging rabbit haemorrhagic disease type 2 virus (RHDV2) in Sicily from rabbit (Oryctolagus cuniculus) and Italian hare (Lepus corsicanus). Res Vet Sci. 2014 Dec;97(3):642–5.

93. Le Gall-Reculé G, Lemaitre E, Bertagnoli S, Hubert C, Top S, Decors A, et al. Large-scale lagovirus disease outbreaks in European brown hares (Lepus europaeus) in France caused by RHDV2 strains spatially shared with rabbits (Oryctolagus cuniculus). Vet Res. 2017 28;48(1):70.

94. Puggioni G, Cavadini P, Maestrale C, Scivoli R, Botti G, Ligios C, et al. The new French 2010 Rabbit Hemorrhagic Disease Virus causes an RHD-like disease in the Sardinian Cape hare (Lepus capensis mediterraneus). Vet Res. 2013 Oct 7;44:96.

95. Calvete C, Mendoza M, Sarto MP, Bagüés MPJ de, Luján L, Molín J, et al. Detection of Rabbit Hemorrhagic Disease Virus GI.2/RHDV2/b in the Mediterranean Pine Vole (Microtus duodecimcostatus) and White-Toothed Shrew (Crocidura russula). J Wildl Dis. 2019;55(2):467–72.

96. Bao S, An K, Liu C, Xing X, Fu X, Xue H, et al. Rabbit Hemorrhagic Disease Virus Isolated from Diseased Alpine Musk Deer (Moschus sifanicus). Viruses. 2020 Aug 17;12(8):E897.

97. Abade Dos Santos FA, Pinto A, Burgoyne T, Dalton KP, Carvalho CL, Ramilo DW, et al. Spillover events of rabbit haemorrhagic disease virus 2 (recombinant GI.4P-GI.2) from Lagomorpha to Eurasian badger. Transbound Emerg Dis. 2021 Mar 8;

98. Ambagala A, Schwantje H, Laurendeau S, Snyman H, Joseph T, Pickering B, et al. Incursions of rabbit haemorrhagic disease virus 2 in Canada-Clinical, molecular and epidemiological investigation. Transbound Emerg Dis. 2021 Apr 29;

99. Rabbit Hemorrhagic Disease Found in Ohio | Ohio Department of Agriculture [Internet]. [cited 2022 Nov 8]. Available from: https://agri.ohio.gov/home/news-and-events/all-news/RHD2

100. WSVMA | Deadly Rabbit Disease Confirmed on Orcas Island [Internet]. [cited 2022 Nov 8]. Available from: https://wsvma.org/2019/07/19/deadly-rabbit-disease-confirmed-on-orcas-island/

101. Chasey D, Lucas M, Westcott D, Williams M. European brown hare syndrome in the U.K.; a calicivirus related to but distinct from that of viral haemorrhagic disease in rabbits. Arch Virol [Internet]. 1992 Sep 1 [cited 2020 Aug 18];124(3):363–70. Available from: https://doi.org/10.1007/BF01309816

102. Gavier-Widén D, Mörner T. Descriptive epizootiological study of european brown hare syndrome in sweden. J Wildl Dis [Internet]. 1993 Jan 1 [cited 2020 Aug 18];29(1):15–20. Available from: https://www.jwildlifedis.org/doi/abs/10.7589/0090-3558-29.1.15

103. Wirblich C, Meyers G, Ohlinger VF, Capucci L, Eskens U, Haas B, et al. European brown hare syndrome virus: relationship to rabbit hemorrhagic disease virus and other caliciviruses. J Virol [Internet]. 1994 Aug [cited 2020 Aug 14];68(8):5164–73. Available from: https://www.ncbi.nlm.nih.gov/pmc/articles/PMC236460/

104. Zanni ML, Benassi MC, Scicluna MT, Lavazza A, Capucci L. Clinical evolution and diagnosis of an outbreak of European brown hare syndrome in hares reared in captivity. Rev Sci Tech Int Off Epizoot. 1993 Sep;12(3):931–40.

105. Fuchs A, Weissenböck H. Comparative histopathological study of rabbit haemorrhagic disease (RHD) and European brown hare syndrome (EBHS). J Comp Pathol [Internet]. 1992 Jul 1 [cited 2020 Aug 18];107(1):103–13. Available from: http://www.sciencedirect.com/science/article/pii/0021997592901009

106. Frölich K, Haerer G, Bacciarini L, Janovsky M, Rudolph M, Giacometti M. European Brown Hare Syndrome in Free-ranging European Brown and Mountain Hares from Switzerland. J Wildl Dis [Internet]. 2001 Oct 1 [cited 2022 Sep 6];37(4):803–7. Available from: https://doi.org/10.7589/0090-3558-37.4.803

107. Syrjälä P, Nylund M, Heinikainen S. EUROPEAN BROWN HARE SYNDROME IN FREE-LIVING MOUNTAIN HARES (LEPUS TIMIDUS) AND EUROPEAN BROWN HARES (LEPUS EUROPAEUS) IN FINLAND 1990–2002. J Wildl Dis [Internet]. 2005 Jan 1 [cited 2022 Sep 6];41(1):42–7. Available from: https://doi.org/10.7589/0090-3558-41.1.42

108. Lavazza A, Cavadini P, Barbieri I, Tizzani P, Pinheiro A, Abrantes J, et al. Field and experimental data indicate that the eastern cottontail (Sylvilagus floridanus) is susceptible to infection with European brown hare syndrome (EBHS) virus and not with rabbit haemorrhagic disease (RHD) virus. Vet Res [Internet]. 2015 Feb 24 [cited 2022 Sep 6];46(1):13. Available from: https://doi.org/10.1186/s13567-015-0149-4

109. Rodák L, Smíd B, Valícek L, Veselý T, Stěpánek J, Hampl J, et al. Enzyme-linked immunosorbent assay of antibodies to rabbit haemorrhagic disease virus and determination of its major structural proteins. J Gen Virol. 1990 May;71 (Pt 5):1075–80.

110. Bergin IL, Wise AG, Bolin SR, Mullaney TP, Kiupel M, Maes RK. Novel calicivirus identified in rabbits, Michigan, USA. Emerg Infect Dis. 2009 Dec;15(12):1955–62.

111. Strive T, Wright JD, Robinson AJ. Identification and partial characterisation of a new Lagovirus in Australian wild rabbits. Virology. 2009 Feb 5;384(1):97–105.

112. Cavadini P, Molinari S, Merzoni F, Vismarra A, Posautz A, Alzaga Gil V, et al. Widespread occurrence of the non-pathogenic hare calicivirus (HaCV Lagovirus GII.2) in captive-reared and free-living wild hares in Europe. Transbound Emerg Dis [Internet]. 2021 [cited 2022 Aug 3];68(2):509–18. Available from: https://onlinelibrary.wiley.com/doi/abs/10.1111/tbed.13706

113. Mahar JE, Hall RN, Shi M, Mourant R, Huang N, Strive T, et al. The discovery of three new hare lagoviruses reveals unexplored viral diversity in this genus. Virus Evol [Internet]. 2019 Apr 9 [cited 2020 Aug 18];5(1). Available from: https://www.ncbi.nlm.nih.gov/pmc/articles/PMC6456799/

114. Florida Department of Agriculture and Consumer Services. 2022. Rabbit hemorrhagic disease update. Florida Department of Agriculture and Consumer Services, Tallahassee, FL. :5. Available from: https://www.fdacs.gov/content/download/98220/file/rabbit-hemorrhagic-disease-update-3172022.pdf.

115. König M, Thiel HJ, Meyers G. Detection of viral proteins after infection of cultured hepatocytes with rabbit hemorrhagic disease virus. J Virol. 1998 May;72(5):4492–7.

116. Netzler NE, Enosi Tuipulotu D, Eltahla AA, Lun JH, Ferla S, Brancale A, et al. Broad-spectrum non-nucleoside inhibitors for caliciviruses. Antiviral Res [Internet]. 2017 Oct 1 [cited 2022 Oct 31];146:65–75. Available from: https://www.sciencedirect.com/science/article/pii/S0166354217303431

117. Ferla S, Netzler NE, Ferla S, Veronese S, Tuipulotu DE, Guccione S, et al. In silico screening for human norovirus antivirals reveals a novel non-nucleoside inhibitor of the viral polymerase. Sci Rep [Internet]. 2018 Mar 7 [cited 2022 Oct 31];8(1):4129. Available from: https://www.nature.com/articles/s41598-018-22303-y

118. Du H, Zhang S, He M, Ming K, Wang J, Yuan W, et al. Evaluation of the Therapeutic Effect of a Flavonoid Prescription against Rabbit Hemorrhagic Disease In Vivo. BioMed Res Int [Internet]. 2019 Apr 4 [cited 2022 Aug 5];2019:e5201790. Available from: https://www.hindawi.com/journals/bmri/2019/5201790/

119. Perera KD, Johnson D, Lovell S, Groutas WC, Chang KO, Kim Y. Potent Protease Inhibitors of Highly Pathogenic Lagoviruses: Rabbit Hemorrhagic Disease Virus and European Brown Hare Syndrome Virus. Microbiol Spectr. 2022 Jun 29;e0014222.

120. de Vries AAF, Horzinek MC, Rottier PJM, de Groot RJ. The Genome Organization of the Nidovirales: Similarities and Differences between Arteri-, Toro-, and Coronaviruses. Semin Virol [Internet]. 1997;8(1):33–47. Available from: https://www.sciencedirect.com/science/article/pii/S1044577397901049

121. Sawicki SG, Sawicki DL. Coronavirus transcription: subgenomic mouse hepatitis virus replicative intermediates function in RNA synthesis. J Virol [Internet]. 1990;64(3):1050–6. Available from: http://jvi.asm.org/content/64/3/1050.abstract

122. Sawicki SG, Sawicki DL. Coronaviruses use discontinuous extension for synthesis of subgenome-length negative strands. Adv Exp Med Biol [Internet]. 1995;380:499. Available from: http://www.ncbi.nlm.nih.gov/pubmed/8830530

123. Jackwood MW, Hall D, Handel A. Molecular evolution and emergence of avian gammacoronaviruses. Infect Genet Evol J Mol Epidemiol Evol Genet Infect Dis [Internet]. 2012;12(6):1305. Available from: http://www.ncbi.nlm.nih.gov/pubmed/22609285

124. Patrick CYW, Susanna KPL, Carol SFL, Candy CYL, Alan KLT, John HNL, et al. Discovery of Seven Novel Mammalian and Avian Coronaviruses in the Genus Deltacoronavirus Supports Bat Coronaviruses as the Gene Source of Alphacoronavirus and Betacoronavirus and Avian Coronaviruses as the Gene Source of Gammacoronavirus and Deltacoronavirus. J Virol [Internet]. 2012;86(7):3995–4008. Available from: http://jvi.asm.org/content/86/7/3995.abstract

125. Wang L, Byrum B, Zhang Y. Detection and genetic characterization of deltacoronavirus in pigs, Ohio, USA, 2014. Emerg Infect Dis [Internet]. 2014;20(7):1227. Available from: http://www.ncbi.nlm.nih.gov/pubmed/24964136

126. Lednicky JA, Tagliamonte MS, White SK, Elbadry MA, Alam MdM, Stephenson CJ, et al. Emergence of porcine delta-coronavirus pathogenic infections among children in Haiti through independent zoonoses and convergent evolution. medRxiv [Internet]. 2021 Mar 25 [cited 2022 Oct 31];2021.03.19.21253391. Available from: https://www.ncbi.nlm.nih.gov/pmc/articles/PMC8010738/

127. Virus Taxonomy: The Classification and Nomenclature of Viruses The Online (10th) Report of the ICTV [Internet]. [cited 2018 May 5]. Available from: https://talk.ictvonline.org/ictv-reports/ictv_online_report/

128. Gorbalenya AE, Enjuanes L, Ziebuhr J, Snijder EJ. Nidovirales: Evolving the largest RNA virus genome. Virus Res [Internet]. 2006;117(1):17–37. Available from: http://www.sciencedirect.com/science/article/pii/S0168170206000360

129. Montserrat B, Gert TO, Willem B, Frank GAF, Arie V, Peter JMR, et al. Cryo-Electron Tomography of Mouse Hepatitis Virus: Insights into the Structure of the Coronavirion. Proc Natl Acad Sci U S A [Internet]. 2009;106(2):582–7. Available from: http://www.jstor.org/stable/40254823

130. Tyrrell DA, Alexander DJ, Almeida JD, Cunningham CH, Easterday BC, Garwes DJ, et al. Coronaviridae: second report. Intervirology [Internet]. 1978;10(6):321–8. Available from: http://www.ncbi.nlm.nih.gov/pubmed/213397

131. Lai MMC. Coronavirus: Organization, replication and expression of genome. Annu Rev Microbiol [Internet]. 1990;44(1):303–33. Available from: http://www.ncbi.nlm.nih.gov/pubmed/2252386

132. Brierley I, Jenner AJ. Mutational analysis of the “slippery-sequence” component of a coronavirus ribosomal frameshifting signal. J Mol Biol [Internet]. 1992;227(2):463–79. Available from: http://www.ncbi.nlm.nih.gov/pubmed/1404364

133. Dye C, Siddell SG. Genomic RNA sequence of Feline coronavirus strain FIPV WSU-79/1146. J Gen Virol [Internet]. 2005;86(8):2249–53. Available from: http://vir.sgmjournals.org/cgi/content/abstract/86/8/2249

134. Kocherhans R, Bridgen A, Ackermann M, Tobler K. Completion of the Porcine Epidemic Diarrhoea Coronavirus (PEDV) Genome Sequence. Virus Genes [Internet]. 2001;23(2):137–44. Available from: http://www.ncbi.nlm.nih.gov/pubmed/11724265

135. Fehr AR, Perlman S. Coronaviruses: an overview of their replication and pathogenesis. Methods Mol Biol Clifton NJ [Internet]. 2015;1282:1. Available from: http://www.ncbi.nlm.nih.gov/pubmed/25720466

136. Delmas B, Laude H. Assembly of coronavirus spike protein into trimers and its role in epitope expression. J Virol [Internet]. 1990;64(11):5367–75. Available from: http://jvi.asm.org/content/64/11/5367.abstract

137. Krishna N, Akihiko M, Junko M, Shinji M. Characterization of the Coronavirus M Protein and Nucleocapsid Interaction in Infected Cells. J Virol [Internet]. 2000;74(17):8127–34. Available from: http://jvi.asm.org/content/74/17/8127.abstract

138. Nelson GW, Stohlman SA, Tahara SM. High affinity interaction between nucleocapsid protein and leader/intergenic sequence of mouse hepatitis virus RNA. J Gen Virol [Internet]. 2000;81(1):181–8. Available from: http://vir.sgmjournals.org/cgi/content/abstract/81/1/181

139. Wilson L, McKinlay C, Gage P, Ewart G. SARS coronavirus E protein forms cation-selective ion channels. Virology [Internet]. 2004;330(1):322–31. Available from: http://www.sciencedirect.com/science/article/pii/S0042682204006440

140. Guan B, Bao L, Qin C, Kuba K, Liu D, Penninger JM, et al. A crucial role of angiotensin converting enzyme 2 (ACE2) in SARS coronavirus-induced lung injury. Nat Med [Internet]. 2005;11(8):875–9. Available from: http://dx.doi.org/10.1038/nm1267

141. Heike H, Krzysztof P, Lia van der H, Martina G, Ben B, Stefan P, et al. Human Coronavirus NL63 Employs the Severe Acute Respiratory Syndrome Coronavirus Receptor for Cellular Entry. Proc Natl Acad Sci U S A [Internet]. 2005;102(22):7988–93. Available from: https://www.jstor.org/stable/3375706

142. Walls AC, Park YJ, Tortorici MA, Wall A, McGuire AT, Veesler D. Structure, Function, and Antigenicity of the SARS-CoV-2 Spike Glycoprotein. Cell [Internet]. 2020 Apr 16

[cited 2022 Aug 9];181(2):281-292.e6. Available from: https://www.sciencedirect.com/science/article/pii/S0092867420302622

143. Wang Q, Zhang Y, Wu L, Niu S, Song C, Zhang Z, et al. Structural and Functional Basis of SARS-CoV-2 Entry by Using Human ACE2. Cell [Internet]. 2020 May 14 [cited 2022 Aug 10];181(4):894-904.e9. Available from: https://www.sciencedirect.com/science/article/pii/S009286742030338X

144. Zhou P, Yang XL, Wang XG, Hu B, Zhang L, Zhang W, et al. A pneumonia outbreak associated with a new coronavirus of probable bat origin. Nature [Internet]. 2020 Mar [cited 2022 Aug 10];579(7798):270–3. Available from: https://www.nature.com/articles/s41586-020-2012-7

145. Raj VS, Huihui M, Saskia LS, Dick HWD, Marcel AM, Ronald D, et al. Dipeptidyl peptidase 4 is a functional receptor for the emerging human coronavirus-EMC. Nature [Internet]. 2013;495(7440):251. Available from: http://www.ncbi.nlm.nih.gov/pubmed/23486063

146. Benbacer L, Kut E, Besnardeau L, Laude H, Delmas B. Interspecies aminopeptidase-N chimeras reveal species-specific receptor recognition by canine coronavirus, feline infectious peritonitis virus, and transmissible gastroenteritis virus. J Virol [Internet]. 1997;71(1):734–7. Available from: http://jvi.asm.org/content/71/1/734.abstract

147. Delmas B, L'Haridon R, Laude H, Norén, Gelfi J, Sjöström H, et al. Aminopeptidase N is a major receptor for the enteropathogenic coronavirus TGEV. Nature [Internet]. 1992;357(6377):417–20. Available from: http://dx.doi.org/10.1038/357417a0

148. Holmes KV, Shapiro LH, Cardellichio CB, Williams RK, Ashmun RA, Yeager CL, et al. Human aminopeptidase N is a receptor for human coronavirus 229E. Nature [Internet]. 1992;357(6377):420–2. Available from: http://www.ncbi.nlm.nih.gov/pubmed/1350662

149. Berend Jan B, Ruurd van der Z, Cornelis AM de H, Peter JMR. The Coronavirus Spike Protein Is a Class I Virus Fusion Protein: Structural and Functional Characterization of the Fusion Core Complex. J Virol [Internet]. 2003;77(16):8801–11. Available from: http://jvi.asm.org/content/77/16/8801.abstract

150. Abraham S, Kienzle TE, Lapps W, Brian DA. Deduced sequence of the bovine coronavirus spike protein and identification of the internal proteolytic cleavage site. Virology [Internet]. 1990;176(1):296–301. Available from: http://www.sciencedirect.com/science/article/pii/004268229090257R

151. Madu IG, Roth SL, Belouzard S, Whittaker GR. Characterization of a highly conserved domain within the severe acute respiratory syndrome coronavirus spike protein S2 domain with characteristics of a viral fusion peptide. J Virol [Internet]. 2009 Aug;83(15):7411–21. Available from: https://www.ncbi.nlm.nih.gov/pubmed/19439480

152. Sandrine B, Victor CC, Gary RW, Peter P. Activation of the SARS Coronavirus Spike Protein via Sequential Proteolytic Cleavage at Two Distinct Sites. Proc Natl Acad Sci U S A [Internet]. 2009;106(14):5871–6. Available from: http://www.jstor.org/stable/40454883

153. Ziebuhr J, Snijder EJ, Gorbalenya AE. Virus-encoded proteinases and proteolytic processing in the Nidovirales. J Gen Virol [Internet]. 2000;81(4):853–79. Available from: http://www.ncbi.nlm.nih.gov/pubmed/10725411

154. Erik P, Jerome WG, Tamotsu Y, Noboru M, Mark RD. Coronavirus Replication Complex Formation Utilizes Components of Cellular Autophagy. J Biol Chem [Internet]. 2004;279(11):10136–41. Available from: http://www.jbc.org/content/279/11/10136.abstract

155. Knoops K, Kikkert M, van den Worm SHE, Zevenhoven-Dobbe JC, van der Meer Y, Koster AJ, et al. SARS-Coronavirus Replication Is Supported by a Reticulovesicular Network of Modified Endoplasmic Reticulum. PLoS Biol [Internet]. 2008;6(9):e226. Available from: http://www.ncbi.nlm.nih.gov/pubmed/18798692

156. Sawicki S. Coronavirus Genome Replication. In: Viral Genome Replication. Boston, MA: Springer US; 2009. p. 25–39.

157. Sawicki SG, Sawicki DL, Siddell SG. A contemporary view of coronavirus transcription. J Virol [Internet]. 2007 Jan;81(1):20–9. Available from: https://www.ncbi.nlm.nih.gov/pubmed/16928755

158. Stertz S, Reichelt M, Spiegel M, Kuri T, Martínez-Sobrido L, García-Sastre A, et al. The intracellular sites of early replication and budding of SARS-coronavirus. Virology [Internet]. 2007;361(2):304–15. Available from: http://www.sciencedirect.com/science/article/pii/S0042682206008762

159. Jacomine KL, Maria E, Peter JMR, Gareth G. Characterization of the Budding Compartment of Mouse Hepatitis Virus: Evidence That Transport from the RER to the Golgi Complex Requires Only One Vesicular Transport Step. J Cell Biol [Internet]. 1994;124(1/2):55–70. Available from: http://www.jstor.org/stable/1616211

160. Anand K, Palm GJ, Siddell SG, Hilgenfeld R, Mesters JR, Ziebuhr J. Structure of coronavirus main proteinase reveals combination of a chymotrypsin fold with an extra α-helical domain. EMBO J [Internet]. 2002;21(13):3213–24. Available from: http://dx.doi.org/10.1093/emboj/cdf327

161. Haitao Y, Maojun Y, Yi D, Yiwei L, Zhiyong L, Zhe Z, et al. The Crystal Structures of Severe Acute Respiratory Syndrome Virus Main Protease and Its Complex with an Inhibitor. Proc Natl Acad Sci U S A [Internet]. 2003;100(23):13190–5. Available from: http://www.jstor.org/stable/3148115

162. Hegyi A, Friebe A, Gorbalenya AE, Ziebuhr J. Mutational analysis of the active centre of coronavirus 3C-like proteases. J Gen Virol [Internet]. 2002;83(3):581–93. Available from: http://vir.sgmjournals.org/cgi/content/abstract/83/3/581

163. Kanchan A, John Z, Parvesh W, Jeroen RM, Rolf H. Coronavirus Main Proteinase (3CLpro) Structure: Basis for Design of Anti-SARS Drugs. Science [Internet]. 2003;300(5626):1763–7. Available from: http://www.sciencemag.org/content/300/5626/1763.abstract

164. Wang F, Chen C, Liu X, Yang K, Xu X, Yang H. Crystal Structure of Feline Infectious Peritonitis Virus Main Protease in Complex with Synergetic Dual Inhibitors. J Virol [Internet]. 2016;90(4):1910–7. Available from: http://www.ncbi.nlm.nih.gov/pubmed/26656689

165. Tan J, Verschueren KHG, Anand K, Shen J, Yang M, Xu Y, et al. pH-dependent conformational flexibility of the SARS-CoV main proteinase (M(pro)) dimer: molecular dynamics simulations and multiple X-ray structure analyses. J Mol Biol [Internet]. 2005;354(1):25–40. Available from: http://www.ncbi.nlm.nih.gov/pubmed/16242152

166. Chou CY, Chang HC, Hsu WC, Lin TZ, Lin CH, Chang GG. Quaternary Structure of the Severe Acute Respiratory Syndrome (SARS) Coronavirus Main Protease. Biochemistry [Internet]. 2004;43(47):14958–70. Available from: http://www.ncbi.nlm.nih.gov/pubmed/15554703

167. Hsu MF, Kuo CJ, Chang KT, Chang HC, Chou CC, Ko TP, et al. Mechanism of the maturation process of SARS-CoV 3CL protease. J Biol Chem [Internet]. 2005 Sep 2;280(35):31257–66. Available from: https://www.ncbi.nlm.nih.gov/pubmed/15788388

168. Wang F, Chen C, Tan W, Yang K, Yang H. Structure of Main Protease from Human Coronavirus NL63: Insights for Wide Spectrum Anti-Coronavirus Drug Design. Sci Rep [Internet]. 2016;6:22677. Available from: http://www.ncbi.nlm.nih.gov/pubmed/26948040

169. Hegyi A, Ziebuhr J. Conservation of substrate specificities among coronavirus main proteases. J Gen Virol [Internet]. 2002;83(3):595–9. Available from: http://vir.sgmjournals.org/cgi/content/abstract/83/3/595

170. St. John SE, Therkelsen MD, Nyalapatla PR, Osswald HL, Ghosh AK, Mesecar AD. X-ray structure and inhibition of the feline infectious peritonitis virus 3C-like protease: Structural implications for drug design. Bioorg Med Chem Lett [Internet]. 2015;25(22):5072–7. Available from: http://www.sciencedirect.com/science/article/pii/S0960894X15301311

171. Perera KDI. 3C-like protease inhibitors against coronaviruses. :94.

172. Arnold APMH, Ingrid S, Marian CH, Peter JMR, Raoul J de G. Feline Coronavirus Type II Strains 79-1683 and 79-1146 Originate from a Double Recombination between Feline Coronavirus Type I and Canine Coronavirus. Note [Internet]. 1998;72(5):4508–14. Available from: http://jvi.asm.org/content/72/5/4508.abstract

173. Fiscus SA, Teramoto YA. Antigenic comparison of feline coronavirus isolates: evidence for markedly different peplomer glycoproteins. J Virol [Internet]. 1987;61(8):2607–13. Available from: http://jvi.asm.org/content/61/8/2607.abstract

174. Yutaka T, Nobutaka M, Keita N, Ryusei K, Hiroshi S, Takehisa S, et al. Emergence of Pathogenic Coronaviruses in Cats by Homologous Recombination between Feline and Canine Coronaviruses. PLoS One [Internet]. 2014;9(9):e106534. Available from: http://www.ncbi.nlm.nih.gov/pubmed/25180686

175. Benetka V, Kübber-Heiss A, Kolodziejek J, Nowotny N, Hofmann-Parisot M, Möstl K. Prevalence of feline coronavirus types I and II in cats with histopathologically verified feline infectious peritonitis. Vet Microbiol [Internet]. 2004;99(1):31–42. Available from: https://www.sciencedirect.com/science/article/pii/S0378113503003821

176. Dong-Jun A, Hye-Young J, WooSeog J, Jee-Yong P, Myoung-Heon L, Bong-Kyun P. Prevalence of Korean cats with natural feline coronavirus infections. Virol J [Internet]. 2011;8(1):455. Available from: http://www.ncbi.nlm.nih.gov/pubmed/21951835

177. Duarte A, Veiga I, Tavares L. Genetic diversity and phylogenetic analysis of Feline Coronavirus sequences from Portugal. Vet Microbiol [Internet]. 2009;138(1):163–8. Available from: https://www.sciencedirect.com/science/article/pii/S0378113509001138

178. Maya K, Marina LM, Michael H, Enikoe G, Amy P, Niels CP, et al. Feline Coronavirus Serotypes 1 and 2: Seroprevalence and Association with Disease in Switzerland. Clin Diagn Lab Immunol [Internet]. 2005;12(10):1209–15. Available from: http://cvi.asm.org/content/12/10/1209.abstract

179. Dye C, Temperton N, Siddell SG. Type I feline coronavirus spike glycoprotein fails to recognize aminopeptidase N as a functional receptor on feline cell lines. J Gen Virol [Internet]. 2007;88(6):1753–60. Available from: http://vir.sgmjournals.org/cgi/content/abstract/88/6/1753

180. Tresnan DB, Levis R, Holmes KV. Feline aminopeptidase N serves as a receptor for feline, canine, porcine, and human coronaviruses in serogroup I. J Virol [Internet]. 1996;70(12):8669–74. Available from: http://jvi.asm.org/content/70/12/8669.abstract

181. Andrew DR, David GO, Gary RW. Feline Lectin Activity Is Critical for the Cellular Entry of Feline Infectious Peritonitis Virus. J Virol [Internet]. 2010;84(15):7917–21. Available from: http://jvi.asm.org/content/84/15/7917.abstract

182. Andrew DR, Gary RW. Utilization of DC-SIGN for Entry of Feline Coronaviruses into Host Cells. J Virol [Internet]. 2008;82(23):11992–6. Available from: http://jvi.asm.org/content/82/23/11992.abstract

183. Desmarets LMB, Theuns S, Olyslaegers DAJ, Dedeurwaerder A, Vermeulen BL, Roukaerts IDM, et al. Establishment of feline intestinal epithelial cell cultures for the propagation and study of feline enteric coronaviruses. Vet Res [Internet]. 2013;44(1):71. Available from: http://www.ncbi.nlm.nih.gov/pubmed/23964891

184. Herrewegh AAPM, Mähler M, Hedrich HJ, Haagmans BL, Egberink HF, Horzinek MC, et al. Persistence and Evolution of Feline Coronavirus in a Closed Cat-Breeding Colony.

Virology [Internet]. 1997;234(2):349–63. Available from: https://www.sciencedirect.com/science/article/pii/S0042682297986633

185. Kipar A, Meli ML, Baptiste KE, Bowker LJ, Lutz H. Sites of feline coronavirus persistence in healthy cats. J Gen Virol [Internet]. 2010;91(7):1698–707. Available from: http://www.ncbi.nlm.nih.gov/pubmed/20237226

186. Kipar A, Kremendahl J, Addie DD, Leukert W, Grant CK, Reinacher M. Fatal enteritis associated with coronavirus infection in cats. J Comp Pathol [Internet]. 1998;119(1):1–14. Available from: https://www.sciencedirect.com/science/article/pii/S0021997598800674

187. Pedersen NC, Boyle JF, Floyd K, Fudge A, Barker J. An enteric coronavirus infection of cats and its relationship to feline infectious peritonitis. Am J Vet Res [Internet]. 1981;42(3):368. Available from: http://www.ncbi.nlm.nih.gov/pubmed/6267960

188. Pedersen NC, Allen CE, Lyons LA. Pathogenesis of feline enteric coronavirus infection. J Feline Med Surg [Internet]. 2008;10(6):529–41. Available from: http://www.sciencedirect.com/science/article/pii/S1098612X08000764

189. Foley JE, Poland A, Carlson J, Pedersen NC. Patterns of feline coronavirus infection and fecal shedding from cats in multiple-cat environments. J Am Vet Med Assoc [Internet]. 1997;210(9):1307. Available from: http://www.ncbi.nlm.nih.gov/pubmed/9143535

190. Addie DD, Schaap IAT, Nicolson L, Jarrett O. Persistence and transmission of natural type I feline coronavirus infection. J Gen Virol [Internet]. 2003;84(10):2735–44. Available from: http://vir.sgmjournals.org/cgi/content/abstract/84/10/2735

191. Kipar A, Meli ML. Feline Infectious Peritonitis. Vet Pathol [Internet]. 2014;51(2):505–26. Available from: http://journals.sagepub.com/doi/full/10.1177/0300985814522077

192. Addie DD, Toth S, Murray GD, Jarrett O. Risk of feline infectious peritonitis in cats naturally infected with feline coronavirus. Am J Vet Res [Internet]. 1995;56(4):429–34. Available from: http://www.ncbi.nlm.nih.gov/pubmed/7785816

193. Addie DD, Jarrett O. Use of a reverse-transcriptase polymerase chain reaction for monitoring the shedding of feline coronavirus by healthy cats. Vet Rec [Internet]. 2001;148(21):649–53. Available from: http://www.ncbi.nlm.nih.gov/pubmed/11400984

194. Pedersen NC. A review of feline infectious peritonitis virus infection: 1963–2008. J Feline Med Surg [Internet]. 2009;11(4):225–58. Available from: http://www.sciencedirect.com/science/article/pii/S1098612X09000175

195. Pedersen NC, Liu H, Scarlett J, Leutenegger CM, Golovko L, Kennedy H, et al. Feline infectious peritonitis: Role of the feline coronavirus 3c gene in intestinal tropism and pathogenicity based upon isolates from resident and adopted shelter cats. Virus Res [Internet]. 2012;165(1):17. Available from: http://www.sciencedirect.com/science/article/pii/S0168170211005156

196. Pedersen NC, Liu H, Durden M, Lyons LA. Natural resistance to experimental feline infectious peritonitis virus infection is decreased rather than increased by positive genetic selection. Vet Immunol Immunopathol [Internet]. 2016;171:17–20. Available from: http://www.ncbi.nlm.nih.gov/pubmed/26964713

197. Pesteanu-Somogyi LD, Radzai C, Pressler BM. Prevalence of feline infectious peritonitis in specific cat breeds. J Feline Med Surg [Internet]. 2006;8(1):1–5. Available from: https://www.sciencedirect.com/science/article/pii/S1098612X0500080X

198. Foley JE, Pedersen NC. The inheritance of susceptibility to feline infectious peritonitis in purebred catteries. Feline Pract [Internet]. 1996;24(1):14–22. Available from: https://www.cabdirect.org/cabdirect/abstract/19962208577

199. Golovko L, Lyons LA, Liu H, Sorensen A, Wehnert S, Pedersen NC. Genetic susceptibility to feline infectious peritonitis in Birman cats. Virus Res [Internet]. 2013 Jul;175(1):58–63. Available from: https://www.ncbi.nlm.nih.gov/pubmed/23619280

200. Addie D, Belak S, Boucraut-Baralon C, Egberink H, Frymus T, Gruffydd-Jones T, et al. Feline infectious peritonitis. ABCD guidelines on prevention and management. J Feline Med Surg [Internet]. 2009 Jul;11(7):594–604. Available from: https://www.ncbi.nlm.nih.gov/pubmed/19481039

201. Rohrbach BW, Legendre AM, Baldwin CA, Lein DH, Reed WM, Wilson RB. Epidemiology of feline infectious peritonitis among cats examined at veterinary medical teaching hospitals. J Am Vet Med Assoc [Internet]. 2001;218(7):1111–5. Available from: http://www.ncbi.nlm.nih.gov/pubmed/11318361

202. Pedersen NC. Virologic and immunologic aspects of feline infectious peritonitis virus infection. Adv Exp Med Biol [Internet]. 1987;218:529. Available from: http://www.ncbi.nlm.nih.gov/pubmed/2829567

203. Stoddart CA, Scott FW. Intrinsic resistance of feline peritoneal macrophages to coronavirus infection correlates with in vivo virulence. J Virol [Internet]. 1989;63(1):436–40. Available from: http://jvi.asm.org/content/63/1/436.abstract

204. Pedersen NC. An update on feline infectious peritonitis: virology and immunopathogenesis. Vet J Lond Engl 1997 [Internet]. 2014;201(2):123–32. Available from: http://www.ncbi.nlm.nih.gov/pubmed/24837550

205. Corapi WV, Olsen CW, Scott FW. Monoclonal antibody analysis of neutralization and antibody-dependent enhancement of feline infectious peritonitis virus. J Virol [Internet]. 1992;66(11):6695–705. Available from: http://jvi.asm.org/content/66/11/6695.abstract

206. Hohdatsu T, Yamada M, Tominaga R, Makino K, Kida K, Koyama H. Antibody-Dependent Enhancement of Feline Infectious Peritonitis Virus Infection in Feline Alveolar Macrophages and Human Monocyte Cell Line U937 by Serum of Cats Experimentally or Naturally Infected with Feline Coronavirus. J Vet Med Sci [Internet]. 1998;60(1):49–55. Available from: https://jlc.jst.go.jp/DN/JALC/00084528247?from=SUMMON

207. Olsen CW, Corapi WV, Ngichabe CK, Baines JD, Scott FW. Monoclonal antibodies to the spike protein of feline infectious peritonitis virus mediate antibody-dependent enhancement of infection of feline macrophages. J Virol [Internet]. 1992;66(2):956–65. Available from: http://jvi.asm.org/content/66/2/956.abstract

208. Takano T, Katada Y, Moritoh S, Ogasawara M, Satoh K, Satoh R, et al. Analysis of the mechanism of antibody-dependent enhancement of feline infectious peritonitis virus infection: aminopeptidase N is not important and a process of acidification of the endosome is necessary. J Gen Virol [Internet]. 2008 Apr;89(Pt 4):1025–9. Available from: https://www.ncbi.nlm.nih.gov/pubmed/18343845

209. Takano T, Kawakami C, Yamada S, Satoh R, Hohdatsu T. Antibody-Dependent Enhancement Occurs Upon Re-Infection with the Identical Serotype Virus in Feline Infectious Peritonitis Virus Infection. J Vet Med Sci [Internet]. 2008;70(12):1315–21. Available from: https://jlc.jst.go.jp/DN/JALC/00323523200?from=SUMMON

210. Diaz JV, Poma R. Diagnosis and clinical signs of feline infectious peritonitis in the central nervous system. Can Vet J Rev Vét Can [Internet]. 2009;50(10):1091. Available from: http://www.ncbi.nlm.nih.gov/pubmed/20046611

211. Hartmann K. Feline infectious peritonitis. Vet Clin North Am Small Anim Pract [Internet]. 2005;35(1):39–79. Available from: http://www.ncbi.nlm.nih.gov/pubmed/15627627

212. Kipar A, May H, Menger S, Weber M, Leukert W, Reinacher M. Morphologic Features and Development of Granulomatous Vasculitis in Feline Infectious Peritonitis. Vet Pathol [Internet]. 2005;42(3):321–30. Available from: http://journals.sagepub.com/doi/full/10.1354/vp.42-3-321

213. Pedersen NC. An update on feline infectious peritonitis: diagnostics and therapeutics. Vet J Lond Engl 1997 [Internet]. 2014;201(2):133–41. Available from: http://www.ncbi.nlm.nih.gov/pubmed/24857253

214. Brown MA, Troyer JL, Pecon-Slattery J, Roelke ME, O'Brien SJ. Genetics and Pathogenesis of Feline Infectious Peritonitis Virus. Emerg Infect Dis [Internet]. 2009;15(9):1445. Available from: http://www.ncbi.nlm.nih.gov/pubmed/19788813

215. Barker EN, Tasker S, Gruffydd-Jones TJ, Tuplin CK, Burton K, Porter E, et al. Phylogenetic Analysis of Feline Coronavirus Strains in an Epizootic Outbreak of Feline Infectious Peritonitis. J Vet Intern Med [Internet]. 2013;27(3):445–50. Available from: http://onlinelibrary.wiley.com/doi/10.1111/jvim.12058/abstract

216. Chang HW, Egberink HF, Rottier PJM. Sequence analysis of feline coronaviruses and the circulating virulent/avirulent theory. Emerg Infect Dis [Internet]. 2011;17(4):744. Available from: http://www.ncbi.nlm.nih.gov/pubmed/21470478

217. Poland AM, Vennema H, Foley JE, Pedersen NC. Two related strains of feline infectious peritonitis virus isolated from immunocompromised cats infected with a feline enteric

coronavirus. J Clin Microbiol [Internet]. 1996;34(12):3180–4. Available from: http://jcm.asm.org/content/34/12/3180.abstract

218. Vennema H, Poland A, Foley J, Pedersen NC. Feline Infectious Peritonitis Viruses Arise by Mutation from Endemic Feline Enteric Coronaviruses. Virology [Internet]. 1998;243(1):150–7. Available from: http://www.sciencedirect.com/science/article/pii/S0042682298990456

219. Dedeurwaerder A, Desmarets LM, Olyslaegers DAJ, Vermeulen BL, Dewerchin HL, Nauwynck HJ. The role of accessory proteins in the replication of feline infectious peritonitis virus in peripheral blood monocytes. Vet Microbiol [Internet]. 2013;162(2–4):447–55. Available from: http://www.ncbi.nlm.nih.gov/pubmed/23182908

220. Herrewegh AAPM, Vennema H, Horzinek MC, Rottier PJM, de Groot RJ. The Molecular Genetics of Feline Coronaviruses: Comparative Sequence Analysis of the ORF7a/7b Transcription Unit of Different Biotypes. Virology [Internet]. 1995;212(2):622–31. Available from: https://www.sciencedirect.com/science/article/pii/S0042682285715206

221. Fehr D, Holznagel E, Bolla S, Hauser B, Herrewegh AAPM, Horzinek MC, et al. Placebo-controlled evaluation of a modified life virus vaccine against feline infectious peritonitis: safety and efficacy under field conditions. Vaccine [Internet]. 1997;15(10):1101–9. Available from: https://www.sciencedirect.com/science/article/pii/S0264410X97000066

222. Abdelnabi R, Foo CS, De Jonghe S, Maes P, Weynand B, Neyts J. Molnupiravir Inhibits Replication of the Emerging SARS-CoV-2 Variants of Concern in a Hamster Infection Model. J Infect Dis [Internet]. 2021 Sep 1 [cited 2022 Sep 21];224(5):749–53. Available from: https://doi.org/10.1093/infdis/jiab361

223. Agostini ML, Andres EL, Sims AC, Graham RL, Sheahan TP, Lu X, et al. Coronavirus Susceptibility to the Antiviral Remdesivir (GS-5734) Is Mediated by the Viral Polymerase and the Proofreading Exoribonuclease. MBio. 2018/03/08 ed. 2018 Mar 6;9(2).

224. Agostini ML, Pruijssers AJ, Chappell JD, Gribble J, Lu X, Andres EL, et al. Small-Molecule Antiviral β-d-N4-Hydroxycytidine Inhibits a Proofreading-Intact Coronavirus with a High Genetic Barrier to Resistance. J Virol [Internet]. 2019 Nov 26 [cited 2022 Sep 21];93(24):e01348-19. Available from: https://journals.asm.org/doi/full/10.1128/JVI.01348-19

225. Barlough JE, Shacklett BL. Antiviral studies of feline infectious peritonitis virus in vitro. Vet Rec [Internet]. 1994;135(8):177–9. Available from: http://www.ncbi.nlm.nih.gov/pubmed/7992474

226. Cox RM, Wolf JD, Plemper RK. Therapeutically administered ribonucleoside analogue MK-4482/EIDD-2801 blocks SARS-CoV-2 transmission in ferrets. Nat Microbiol [Internet]. 2021 Jan [cited 2022 Sep 21];6(1):11–8. Available from: https://www.nature.com/articles/s41564-020-00835-2.

227. Jayk Bernal A, Gomes da Silva MM, Musungaie DB, Kovalchuk E, Gonzalez A, Delos Reyes V, et al. Molnupiravir for Oral Treatment of Covid-19 in Nonhospitalized Patients. N Engl J Med [Internet]. 2022 Feb 10 [cited 2022 Sep 21];386(6):509–20. Available from: https://doi.org/10.1056/NEJMoa2116044

228. Sheahan TP, Sims AC, Zhou S, Graham RL, Pruijssers AJ, Agostini ML, et al. An orally bioavailable broad-spectrum antiviral inhibits SARS-CoV-2 in human airway epithelial cell cultures and multiple coronaviruses in mice. Sci Transl Med [Internet]. 2020 Apr 29 [cited 2022 Sep 21];12(541):eabb5883. Available from: https://www.science.org/doi/full/10.1126/scitranslmed.abb5883

229. Weiss RC, Cox NR, Martinez ML. Evaluation of free or liposome-encapsulated ribavirin for antiviral therapy of experimentally induced feline infectious peritonitis. Res Vet Sci [Internet]. 1993;55(2):162–72. Available from: https://www.sciencedirect.com/science/article/pii/003452889390076R

230. McDonagh P, Sheehy PA, Norris JM. In vitro inhibition of feline coronavirus replication by small interfering RNAs. Vet Microbiol [Internet]. 2011;150(3):220–9. Available from: https://www.sciencedirect.com/science/article/pii/S0378113511000423

231. McDonagh P, Sheehy PA, Norris JM. Combination siRNA therapy against feline coronavirus can delay the emergence of antiviral resistance in vitro. Vet Microbiol [Internet]. 2015;176(1–2):10–8. Available from: http://www.ncbi.nlm.nih.gov/pubmed/25596968

232. Davide C, Jincun Z, Mattia P, Luca S, Sudhakar A, Craig F, et al. Prophylactic and postexposure efficacy of a potent human monoclonal antibody against MERS coronavirus. Proc Natl Acad Sci [Internet]. 2015;112(33):10473. Available from: http://www.pnas.org/content/112/33/10473.abstract

233. Du L, Yang Y, Zhou Y, Lu L, Li F, Jiang S. MERS-CoV spike protein: a key target for antivirals. Expert Opin Ther Targets. 2017;21(2):131–43.

234. Hsieh LE, Lin CN, Lin DS, Lin CT, Su BL, Jan TR, et al. Synergistic antiviral effect of Galanthus nivalis agglutinin and nelfinavir against feline coronavirus. Antiviral Res [Internet]. 2010;88(1):25–30. Available from: https://www.sciencedirect.com/science/article/pii/S0166354210006431

235. Jing G, Guangwen L, Jianxun Q, Yan L, Ying W, Yao D, et al. Structure of the Fusion Core and Inhibition of Fusion by a Heptad Repeat Peptide Derived from the S Protein of Middle East Respiratory Syndrome Coronavirus. J Virol [Internet]. 2013;87(24):13134. Available from: http://jvi.asm.org/content/87/24/13134.abstract

236. Kazuya S, Miyuki K, Shutoku M. Middle East Respiratory Syndrome Coronavirus Infection Mediated by the Transmembrane Serine Protease TMPRSS2. J Virol [Internet]. 2013;87(23):12552–61. Available from: http://jvi.asm.org/content/87/23/12552.abstract

237. Liu W, Zhu HM, Niu GJ, Shi EZ, Chen J, Sun B, et al. Synthesis, modification and docking studies of 5-sulfonyl isatin derivatives as SARS-CoV 3C-like protease inhibitors. Bioorg Med Chem [Internet]. 2014;22(1):292–302. Available from: http://www.ncbi.nlm.nih.gov/pubmed/24316352

238. Liwei J, Nianshuang W, Teng Z, Xuanling S, Kwok-Man Vincent P, Yongkang W, et al. Potent neutralization of MERS-CoV by human neutralizing monoclonal antibodies to the viral spike glycoprotein. Sci Transl Med [Internet]. 2014;6(234):234ra59. Available from: http://www.ncbi.nlm.nih.gov/pubmed/24778414

239. Tianlei Y, Lanying D, Tina WJ, Ponraj P, Candy CYL, Lu L, et al. Exceptionally potent neutralization of Middle East respiratory syndrome coronavirus by human monoclonal antibodies. J Virol [Internet]. 2014;88(14):7796–805. Available from: http://www.ncbi.nlm.nih.gov/pubmed/24789777

240. Zhou Y, Vedantham P, Lu K, Agudelo J, Carrion R Jr, Nunneley JW, et al. Protease inhibitors targeting coronavirus and filovirus entry. Antiviral Res [Internet]. 2015;116:76–84. Available from: http://www.ncbi.nlm.nih.gov/pubmed/25666761

241. Abigail LS, Christine BC, Deborah FW, Mark S de S, Stephen WB, Kathryn VH. Monoclonal Antibody to the Receptor for Murine Coronavirus MHV-A59 Inhibits Viral Replication in vivo. J Infect Dis [Internet]. 1991;163(4):879–82. Available from: https://www.jstor.org/stable/30132438

242. Báez-Santos YM, St John SE, Mesecar AD. The SARS-coronavirus papain-like protease: structure, function and inhibition by designed antiviral compounds. Antiviral Res [Internet]. 2015;115:21–38. Available from: http://www.ncbi.nlm.nih.gov/pubmed/25554382

243. Jozlyn RC, Yahira MB santos, Robert CM, Amornrat O, Susan CB, Andrew DM. X-ray Structure and Enzymatic Activity Profile of a Core Papain-like Protease of MERS Coronavirus with utility for structure-based drug design. Sci Rep Nat Publ Group [Internet]. 2017;7:40292. Available from: https://search.proquest.com/docview/1899430529

244. Kiira R, Scott P, Jun T, Katrina S, Melissa C, Surendranath B, et al. A Noncovalent Class of Papain-Like Protease/Deubiquitinase Inhibitors Blocks SARS Virus Replication. Proc Natl Acad Sci U S A [Internet]. 2008;105(42):16119–24. Available from: https://www.jstor.org/stable/25465055

245. Lee H, Lei H, Santarsiero BD, Gatuz JL, Cao S, Rice AJ, et al. Inhibitor recognition specificity of MERS-CoV papain-like protease may differ from that of SARS-CoV. ACS Chem Biol [Internet]. 2015;10(6):1456. Available from: http://www.ncbi.nlm.nih.gov/pubmed/25746232

246. Chia-Nan C, Coney PCL, Kuo-Kuei H, Wei-Cheng C, Hsin-Pang H, Po-Huang L, et al. Inhibition of SARS-CoV 3C-like Protease Activity by Theaflavin-3,3'-digallate (TF3). Evid Based Complement Alternat Med [Internet]. 2005;2(2):209–15. Available from: http://dx.doi.org/10.1093/ecam/neh081

247. Lin CW, Tsai CH, Tsai FJ, Lai CC, Wan L, Ho TY, et al. Anti-SARS coronavirus 3C-like protease effects of Isatis indigotica root and plant-derived phenolic compounds. Antiviral Res [Internet]. 2005;68(1):36–42. Available from: https://www.sciencedirect.com/science/article/pii/S0166354205001257

248. Wen CC, Kuo YH, Jan JT, Liang PH, Wang SY, Liu HG, et al. Specific Plant Terpenoids and Lignoids Possess Potent Antiviral Activities against Severe Acute Respiratory Syndrome Coronavirus. J Med Chem [Internet]. 2007;50(17):4087–95. Available from: http://www.ncbi.nlm.nih.gov/pubmed/17663539

249. Berry M, Fielding BC, Gamieldien J. Potential Broad Spectrum Inhibitors of the Coronavirus 3CLpro: A Virtual Screening and Structure-Based Drug Design Study. Viruses [Internet]. 2015;7(12):6642–60. Available from: http://www.ncbi.nlm.nih.gov/pubmed/26694449

250. Hsu JTA, Kuo CJ, Hsieh HP, Wang YC, Huang KK, Huang PF, et al. Evaluation of metal-conjugated compounds as inhibitors of 3CL protease of SARS-CoV. FEBS Lett [Internet]. 2004;574(1):116–20. Available from: https://www.sciencedirect.com/science/article/pii/S0014579304010087

251. Jacobs J, Grum-Tokars V, Zhou Y, Turlington M, Saldanha SA, Chase P, et al. Discovery, synthesis, and structure-based optimization of a series of N-(tert-butyl)-2-(N-arylamido)-2-(pyridin-3-yl) acetamides (ML188) as potent noncovalent small molecule inhibitors of the severe acute respiratory syndrome coronavirus (SARS-CoV) 3CL protease. J Med Chem [Internet]. 2013;56(2):534. Available from: http://www.ncbi.nlm.nih.gov/pubmed/23231439

252. Lee CC, Kuo CJ, Hsu MF, Liang PH, Fang JM, Shie JJ, et al. Structural basis of mercury- and zinc-conjugated complexes as SARS-CoV 3C-like protease inhibitors. FEBS Lett [Internet]. 2007;581(28):5454–8. Available from: https://www.sciencedirect.com/science/article/pii/S0014579307011167

253. Ramajayam R, Tan KP, Liu HG, Liang PH. Synthesis, docking studies, and evaluation of pyrimidines as inhibitors of SARS-CoV 3CL protease. Bioorg Med Chem Lett [Internet]. 2010;20(12):3569–72. Available from: https://www.sciencedirect.com/science/article/pii/S0960894X10005962

254. Jain RP, Pettersson HI, Zhang J, Aull KD, Fortin PD, Huitema C, et al. Synthesis and evaluation of keto-glutamine analogues as potent inhibitors of severe acute respiratory syndrome 3CLpro. J Med Chem [Internet]. 2004;47(25):6113–6. Available from: http://www.ncbi.nlm.nih.gov/pubmed/15566280

255. Bacha U, Barrila J, Velazquez-Campoy A, Leavitt SA, Freire E. Identification of novel inhibitors of the SARS coronavirus main protease 3CLpro. Biochemistry [Internet]. 2004;43(17):4906–12. Available from: http://www.ncbi.nlm.nih.gov/pubmed/15109248

256. Blanchard JE, Elowe NH, Huitema C, Fortin PD, Cechetto JD, Eltis LD, et al. High-Throughput Screening Identifies Inhibitors of the SARS Coronavirus Main Proteinase.

Chem Biol [Internet]. 2004;11(10):1445–53. Available from: https://www.sciencedirect.com/science/article/pii/S1074552104002443

257. Chen SF, Chen TSS, Chen LR, Wang YC, Lin YW, Chou SY, et al. Synthesis and evaluation of isatin derivatives as effective SARS coronavirus 3CL protease inhibitors. Bioorg Med Chem Lett [Internet]. 2005;15(12):3058–62. Available from: https://www.sciencedirect.com/science/article/pii/S0960894X05004889

258. Kao RY, Tsui WHW, Lee TSW, Tanner JA, Watt RM, Huang JD, et al. Identification of Novel Small-Molecule Inhibitors of Severe Acute Respiratory Syndrome-Associated Coronavirus by Chemical Genetics. Chem Biol [Internet]. 2004;11(9):1293–9. Available from: https://www.sciencedirect.com/science/article/pii/S1074552104002273

259. Shao YM, Yang WB, Yang AS, Kuo TH, Tsai KC, Lin CH, et al. Design, synthesis, and evaluation of trifluoromethyl ketones as inhibitors of SARS-CoV 3CL protease. Bioorg Med Chem [Internet]. 2008;16(8):4652–60. Available from: https://www.sciencedirect.com/science/article/pii/S0968089608001612

260. Shimamoto Y, Hattori Y, Kobayashi K, Teruya K, Sanjoh A, Nakagawa A, et al. Fused-ring structure of decahydroisoquinolin as a novel scaffold for SARS 3CL protease inhibitors. Bioorg Med Chem [Internet]. 2015;23(4):876–90. Available from: http://www.ncbi.nlm.nih.gov/pubmed/25614110

261. Zhou L, Liu Y, Zhang W, Wei P, Huang C, Pei J, et al. Isatin compounds as noncovalent SARS coronavirus 3C-like protease inhibitors. J Med Chem [Internet]. 2006;49(12):3440–3. Available from: http://www.ncbi.nlm.nih.gov/pubmed/16759084

262. Chuck CP, Ke ZH, Chen C, Wan DCC, Chow HF, Wong KB. Profiling of substrate-specificity and rational design of broad-spectrum peptidomimetic inhibitors for main proteases of coronaviruses. Hong Kong Med J Xianggang Yi Xue Za Zhi Hong Kong Acad Med [Internet]. 2014;20 Suppl 4:22. Available from: http://www.ncbi.nlm.nih.gov/pubmed/25224114

263. Galasiti Kankanamalage AC, Kim Y, Damalanka VC, Rathnayake AD, Fehr AR, Mehzabeen N, et al. Structure-guided design of potent and permeable inhibitors of MERS coronavirus 3CL protease that utilize a piperidine moiety as a novel design element. Eur J Med Chem [Internet]. 2018 Apr 25;150:334–46. Available from: https://www.ncbi.nlm.nih.gov/pubmed/29544147

264. Ghosh AK, Xi K, Ratia K, Santarsiero BD, Fu W, Harcourt BH, et al. Design and Synthesis of Peptidomimetic Severe Acute Respiratory Syndrome Chymotrypsin-like Protease Inhibitors. J Med Chem [Internet]. 2005;48(22):6767–71. Available from: http://www.ncbi.nlm.nih.gov/pubmed/16250632

265. Ghosh AK, Xi K, Grum-Tokars V, Xu X, Ratia K, Fu W, et al. Structure-based design, synthesis, and biological evaluation of peptidomimetic SARS-CoV 3CLpro inhibitors. Bioorg Med Chem Lett [Internet]. 2007;17(21):5876–80. Available from: https://www.sciencedirect.com/science/article/pii/S0960894X07009341

266. Han-Zhong Z, Hong Z, William K, Ben T, Jindrich C, Martin M, et al. Design and synthesis of dipeptidyl glutaminyl fluoromethyl ketones as potent severe acute respiratory syndrome coronovirus (SARS-CoV) inhibitors. J Med Chem [Internet]. 2006;49(3):1198–201. Available from: http://www.ncbi.nlm.nih.gov/pubmed/16451084

267. Kumar V, Shin JS, Shie JJ, Ku KB, Kim C, Go YY, et al. Identification and evaluation of potent Middle East respiratory syndrome coronavirus (MERS-CoV) 3CLPro inhibitors. Antiviral Res. 2017;141:101–6.

268. Prior A, Kim Y, Weerasekara S, Moroze M, Alliston K, Uy R, et al. Design, synthesis, and bioevaluation of viral 3C and 3C-like protease inhibitors. Bioorg Med Chem Lett [Internet]. 2013;23(23):6317–20. Available from: http://www.ncbi.nlm.nih.gov/pubmed/24125888

269. Yang S, Chen SJ, Hsu MF, Wu JD, Tseng CTK, Liu YF, et al. Synthesis, crystal structure, structure-activity relationships, and antiviral activity of a potent SARS coronavirus 3CL protease inhibitor. J Med Chem [Internet]. 2006;49(16):4971–80. Available from: http://www.ncbi.nlm.nih.gov/pubmed/16884309

270. Zhenming L, Changkang H, Keqiang F, Ping W. Virtual Screening of Novel Noncovalent Inhibitors for SARS-CoV 3C-like Proteinase. J Chem Inf Model [Internet]. 2005;45(1):10–7. Available from: http://www.ncbi.nlm.nih.gov/pubmed/15667124

271. Anand K, Yang H, Bartlam M, Hilgenfeld R. Coronavirus main proteinase: target for antiviral drug therapy. In: Coronaviruses with Special Emphasis on First Insights Concerning SARS. Basel: Birkhäuser Basel; 2005. p. 173–99. (Birkhäuser Advances in Infectious Diseases BAID).

272. Wei P, Fan K, Chen H, Ma L, Huang C, Tan L, et al. The N-terminal octapeptide acts as a dimerization inhibitor of SARS coronavirus 3C-like proteinase. Biochem Biophys Res Commun [Internet]. 2006;339(3):865–72. Available from: http://www.sciencedirect.com/science/article/pii/S0006291X05026331

273. Kim Y, Scott L, Kok-Chuan T, Sivakoteswara Rao M, Kevin RA, Kevin PB, et al. Broad-Spectrum Antivirals against 3C or 3C-Like Proteases of Picornaviruses, Noroviruses, and Coronaviruses. J Virol [Internet]. 2012;86(21):11754. Available from: http://jvi.asm.org/content/86/21/11754.abstract

274. Kim Y, Mandadapu SR, Groutas WC, Chang KO. Potent inhibition of feline coronaviruses with peptidyl compounds targeting coronavirus 3C-like protease. Antiviral Res [Internet]. 2013;97(2):161–8. Available from: http://www.ncbi.nlm.nih.gov/pubmed/23219425

275. Kim Y, Shivanna V, Narayanan S, Prior AM, Weerasekara S, Hua DH, et al. Broad-Spectrum Inhibitors against 3C-Like Proteases of Feline Coronaviruses and Feline Caliciviruses. J Virol [Internet]. 2015;89(9):4942–50. Available from: http://www.ncbi.nlm.nih.gov/pubmed/25694593

276. Mandadapu SR, Weerawarna PM, Gunnam MR, Alliston KR, Lushington GH, Kim Y, et al. Potent inhibition of norovirus 3CL protease by peptidyl α-ketoamides and α-

ketoheterocycles. Bioorg Med Chem Lett [Internet]. 2012;22(14):4820–6. Available from: http://www.ncbi.nlm.nih.gov/pubmed/22698498

277. Mandadapu SR, Gunnam MR, Tiew KC, Uy RAZ, Prior AM, Alliston KR, et al. Inhibition of norovirus 3CL protease by bisulfite adducts of transition state inhibitors. Bioorg Med Chem Lett [Internet]. 2013;23(1):62–5. Available from: http://www.ncbi.nlm.nih.gov/pubmed/23218713

278. Perera KD, Galasiti Kankanamalage AC, Rathnayake AD, Honeyfield A, Groutas W, Chang KO, et al. Protease inhibitors broadly effective against feline, ferret and mink coronaviruses. Antiviral Res. 2018 Dec;160:79–86.

279. Kim Y, Hongwei L, Anushka CGK, Sahani W, Duy HH, William CG, et al. Reversal of the Progression of Fatal Coronavirus Infection in Cats by a Broad-Spectrum Coronavirus Protease Inhibitor. PLoS Pathog [Internet]. 2016;12(3):e1005531. Available from: http://www.ncbi.nlm.nih.gov/pubmed/27027316

280. Pedersen NC, Kim Y, Liu H, Anushka CGK, Eckstrand C, William CG, et al. Efficacy of a 3C-like protease inhibitor in treating various forms of acquired feline infectious peritonitis. J Feline Med Surg [Internet]. 2017;1098612X17729626. Available from: https://doi.org/10.1177/1098612X17729626

281. Dampalla CS, Rathnayake AD, Perera KD, Jesri ARM, Nguyen HN, Miller MJ, et al. Structure-Guided Design of Potent Inhibitors of SARS-CoV-2 3CL Protease: Structural, Biochemical, and Cell-Based Studies. J Med Chem [Internet]. 2021 Dec 23 [cited 2022 Feb 22];64(24):17846–65. Available from: https://pubs.acs.org/doi/10.1021/acs.jmedchem.1c01037

282. Dampalla CS, Zheng J, Perera KD, Wong LYR, Meyerholz DK, Nguyen HN, et al. Postinfection treatment with a protease inhibitor increases survival of mice with a fatal SARS-CoV-2 infection. Proc Natl Acad Sci [Internet]. 2021 Jul 20 [cited 2022 Sep 21];118(29):e2101555118. Available from: https://www.pnas.org/doi/10.1073/pnas.2101555118

283. Fu L, Ye F, Feng Y, Yu F, Wang Q, Wu Y, et al. Both Boceprevir and GC376 efficaciously inhibit SARS-CoV-2 by targeting its main protease. Nat Commun [Internet]. 2020 Sep 4 [cited 2022 Sep 21];11:4417. Available from: https://www.ncbi.nlm.nih.gov/pmc/articles/PMC7474075/

284. Ma C, Sacco MD, Hurst B, Townsend JA, Hu Y, Szeto T, et al. Boceprevir, GC-376, and calpain inhibitors II, XII inhibit SARS-CoV-2 viral replication by targeting the viral main protease. bioRxiv [Internet]. 2020 Jan 6 [cited 2022 Sep 21];2020.04.20.051581. Available from: https://www.ncbi.nlm.nih.gov/pmc/articles/PMC7263507/

285. Rathnayake AD, Zheng J, Kim Y, Perera KD, Mackin S, Meyerholz DK, et al. 3C-like protease inhibitors block coronavirus replication in vitro and improve survival in MERS-CoV–infected mice. Sci Transl Med [Internet]. 2020 Aug 19 [cited 2022 Sep

21];12(557):eabc5332. Available from: https://www.science.org/doi/10.1126/scitranslmed.abc5332

286. Vuong W, Khan MB, Fischer C, Arutyunova E, Lamer T, Shields J, et al. Feline coronavirus drug inhibits the main protease of SARS-CoV-2 and blocks virus replication. Nat Commun [Internet]. 2020 Aug 27 [cited 2022 Sep 21];11:4282. Available from: https://www.ncbi.nlm.nih.gov/pmc/articles/PMC7453019/

287. Owen DR, Allerton CMN, Anderson AS, Aschenbrenner L, Avery M, Berritt S, et al. An oral SARS-CoV-2 Mpro inhibitor clinical candidate for the treatment of COVID-19. Science [Internet]. 2021 Dec 24 [cited 2022 Sep 21];374(6575):1586–93. Available from: https://www.science.org/doi/full/10.1126/science.abl4784

288. Zhu J, Zhang H, Lin Q, Lyu J, Lu L, Chen H, et al. Progress on SARS-CoV-2 3CLpro Inhibitors: Inspiration from SARS-CoV 3CLpro Peptidomimetics and Small-Molecule Anti-Inflammatory Compounds. Drug Des Devel Ther [Internet]. 2022 Apr 8 [cited 2022 Sep 21];16:1067–82. Available from: https://www.ncbi.nlm.nih.gov/pmc/articles/PMC9015912/

289. Andino R, Domingo E. Viral quasispecies. Virology [Internet]. 2015;479:46–51. Available from: https://www.clinicalkey.es/playcontent/1-s2.0-S0042682215001580

290. Halfon P, Locarnini S. Hepatitis C virus resistance to protease inhibitors. J Hepatol [Internet]. 2011;55(1):192–206. Available from: https://www.clinicalkey.es/playcontent/1-s2.0-S0168827811000791

291. Irwin KK, Renzette N, Kowalik TF, Jensen JD. Antiviral drug resistance as an adaptive process. Virus Evol. 2016;1.

292. Kimberlin DW, Whitley RJ. Antiviral resistance: Mechanisms, clinical significance, and future implications. J Antimicrob Chemother [Internet]. 1996;37(3):403–21. Available from: http://www.ncbi.nlm.nih.gov/pubmed/9182098

293. Luber AD. Genetic Barriers to Resistance and Impact on Clinical Response. J Int AIDS Soc [Internet]. 2005;7(1):69. Available from: https://onlinelibrary.wiley.com/doi/abs/10.1186/1758-2652-7-3-69

294. Megan HP, Egor PT, Robert AK, Rodney SR, Ross M, Evguenia SS, et al. Contribution of a mutational bias in hepatitis C virus replication to the genetic barrier in the development of drug resistance. Proc Natl Acad Sci U S A [Internet]. 2011;108(51):20509–13. Available from: http://www.jstor.org/stable/23077276

295. Menéndez-Arias L. Molecular basis of human immunodeficiency virus type 1 drug resistance: overview and recent developments. Antiviral Res [Internet]. 2013;98(1):93–120. Available from: http://www.ncbi.nlm.nih.gov/pubmed/23403210

296. Bartlett JA, DeMasi R, Quinn J, Moxham C, Rousseau F. Overview of the effectiveness of triple combination therapy in antiretroviral-naive HIV-1 infected adults. AIDS [Internet]. 2001;15(11):1369–77. Available from: http://www.ncbi.nlm.nih.gov/pubmed/11504958

297. Strasfeld L, Chou S. Antiviral Drug Resistance: Mechanisms and Clinical Implications. Infect Dis Clin North Am [Internet]. 2010;24(2):413–37. Available from: http://www.sciencedirect.com/science/article/pii/S0891552010000024

298. Minskaia E, Hertzig T, Gorbalenya AE, Campanacci V, Cambillau C, Canard B, et al. Discovery of an RNA virus 3'->5' exoribonuclease that is critically involved in coronavirus RNA synthesis. Proc Natl Acad Sci U S A. 2006 Mar 28;103(13):5108–13.

299. Sanjuán R, Nebot MR, Chirico N, Mansky LM, Belshaw R. Viral Mutation Rates. J Virol [Internet]. 2010 Oct [cited 2022 Nov 8];84(19):9733–48. Available from: https://journals.asm.org/doi/10.1128/JVI.00694-10

300. Ullrich S, Ekanayake KB, Otting G, Nitsche C. Main protease mutants of SARS-CoV-2 variants remain susceptible to nirmatrelvir. Bioorg Med Chem Lett [Internet]. 2022 Apr 15 [cited 2022 Sep 16];62:128629. Available from: https://www.sciencedirect.com/science/article/pii/S0960894X22001056

301. Greasley SE, Noell S, Plotnikova O, Ferre RA, Liu W, Bolanos B, et al. Structural basis for Nirmatrelvir in vitro efficacy against SARS-CoV-2 variants [Internet]. bioRxiv; 2022 [cited 2022 Sep 16]. p. 2022.01.17.476556. Available from: https://www.biorxiv.org/content/10.1101/2022.01.17.476556v2

302. Li P, Wang Y, Lavrijsen M, Lamers MM, de Vries AC, Rottier RJ, et al. SARS-CoV-2 Omicron variant is highly sensitive to molnupiravir, nirmatrelvir, and the combination. Cell Res [Internet]. 2022 Mar [cited 2022 Sep 16];32(3):322–4. Available from: https://www.nature.com/articles/s41422-022-00618-w

303. Rai DK, Yurgelonis I, McMonagle P, Rothan HA, Hao L, Gribenko A, et al. Nirmatrelvir, an orally active Mpro inhibitor, is a potent inhibitor of SARS-CoV-2 Variants of Concern [Internet]. bioRxiv; 2022 [cited 2022 Sep 16]. p. 2022.01.17.476644. Available from: https://www.biorxiv.org/content/10.1101/2022.01.17.476644v1

304. Vangeel L, Chiu W, De Jonghe S, Maes P, Slechten B, Raymenants J, et al. Remdesivir, Molnupiravir and Nirmatrelvir remain active against SARS-CoV-2 Omicron and other variants of concern. Antiviral Res [Internet]. 2022 Feb 1 [cited 2022 Sep 16];198:105252. Available from: https://www.sciencedirect.com/science/article/pii/S0166354222000201

305. Heilmann E, Costacurta F, Moghadasi SA, Ye C, Pavan M, Bassani D, et al. SARS-CoV-2 3CLpro mutations selected in a VSV-based system confer resistance to nirmatrelvir, ensitrelvir, and GC376. Sci Transl Med [Internet]. 2022 Oct 4 [cited 2022 Nov 1];0(0):eabq7360. Available from: https://www.science.org/doi/10.1126/scitranslmed.abq7360

306. Iketani S, Mohri H, Culbertson B, Hong SJ, Duan Y, Luck MI, et al. Multiple pathways for SARS-CoV-2 resistance to nirmatrelvir [Internet]. bioRxiv; 2022 [cited 2022 Nov 1]. p. 2022.08.07.499047. Available from: https://www.biorxiv.org/content/10.1101/2022.08.07.499047v2

307. Zhou Y, Gammeltoft KA, Ryberg LA, Pham LV, Fahnøe U, Binderup A, et al. Nirmatrelvir Resistant SARS-CoV-2 Variants with High Fitness in Vitro [Internet]. bioRxiv; 2022 [cited 2022 Nov 1]. p. 2022.06.06.494921. Available from: https://www.biorxiv.org/content/10.1101/2022.06.06.494921v1

308. Deng X, StJohn SE, Osswald HL, O'Brien A, Banach BS, Sleeman K, et al. Coronaviruses Resistant to a 3C-Like Protease Inhibitor Are Attenuated for Replication and Pathogenesis, Revealing a Low Genetic Barrier but High Fitness Cost of Resistance. J Virol [Internet]. 2014;88(20):11886–98. Available from: http://www.ncbi.nlm.nih.gov/pubmed/25100843

309. Perera KD, Rathnayake AD, Liu H, Pedersen NC, Groutas WC, Chang KO, et al. Characterization of amino acid substitutions in feline coronavirus 3C-like protease from a cat with feline infectious peritonitis treated with a protease inhibitor. Vet Microbiol [Internet]. 2019 Oct 1 [cited 2022 Sep 21];237:108398. Available from: https://www.sciencedirect.com/science/article/pii/S0378113519308259

310. Jiao Z, Yan Y, Chen Y, Wang G, Wang X, Li L, et al. Adaptive Mutation in the Main Protease Cleavage Site of Feline Coronavirus Renders the Virus More Resistant to Main Protease Inhibitors. J Virol [Internet]. 2022 Aug 24 [cited 2022 Aug 31];0(0):e00907-22. Available from: https://journals.asm.org/doi/10.1128/jvi.00907-22

311. Juranka PF, Zastawny RL, Ling V. P-glycoprotein: multidrug-resistance and a superfamily of membrane-associated transport proteins. FASEB J [Internet]. 1989 [cited 2022 Aug 24];3(14):2583–92. Available from: https://onlinelibrary.wiley.com/doi/abs/10.1096/fasebj.3.14.2574119

312. van Veen HW, Konings WN. The ABC family of multidrug transporters in microorganisms. Biochim Biophys Acta BBA - Bioenerg [Internet]. 1998 Jun 10 [cited 2022 Aug 26];1365(1):31–6. Available from: https://www.sciencedirect.com/science/article/pii/S0005272898000395

313. Cascorbi I. P-glycoprotein: Tissue Distribution, Substrates, and Functional Consequences of Genetic Variations. In: Fromm MF, Kim RB, editors. Drug Transporters [Internet]. Berlin, Heidelberg: Springer; 2011 [cited 2022 Aug 24]. p. 261–83. (Handbook of Experimental Pharmacology). Available from: https://doi.org/10.1007/978-3-642-14541-4_6

314. Heyden SVD, Chiers K, Ducatelle R. Tissue Distribution of P-Glycoprotein in Cats. Anat Histol Embryol [Internet]. 2009 [cited 2021 Jun 16];38(6):455–60. Available from: https://onlinelibrary.wiley.com/doi/abs/10.1111/j.1439-0264.2009.00972.x

315. Dey S, Ramachandra M, Pastan I, Gottesman MM, Ambudkar SV. Evidence for two nonidentical drug-interaction sites in the human P-glycoprotein. Proc Natl Acad Sci U S A. 1997 Sep 30;94(20):10594–9.

316. Garrigos M, Mir LM, Orlowski S. Competitive and Non-Competitive Inhibition of the Multidrug-Resistance-Associated P-glycoprotein ATPase. Eur J Biochem [Internet]. 1997 [cited 2022 Aug 29];244(2):664–73. Available from: https://onlinelibrary.wiley.com/doi/abs/10.1111/j.1432-1033.1997.00664.x

317. Bin W, Masaki U, Masayuki O, Takashi K, Cheng-long H, Naohisa H, et al. Age-Related Changes in P-Glycoprotein Expression in Senescence- Accelerated Mouse. Curr Aging Sci [Internet]. 2009 Nov 30 [cited 2021 Jun 16];2(3):187–92. Available from: https://www.eurekaselect.com/95332/article

318. Schinkel AH, Mayer U, Wagenaar E, Mol CAAM, van Deemter L, Smit JJM, et al. Normal viability and altered pharmacokinetics in mice lacking mdr1-type (drug-transporting) P-glycoproteins. Proc Natl Acad Sci [Internet]. 1997 Apr 15 [cited 2022 Aug 24];94(8):4028–33. Available from: https://www.pnas.org/doi/abs/10.1073/pnas.94.8.4028

319. Panwala CM, Jones JC, Viney JL. A Novel Model of Inflammatory Bowel Disease: Mice Deficient for the Multiple Drug Resistance Gene, mdr1a, Spontaneously Develop Colitis. J Immunol [Internet]. 1998 Nov 15 [cited 2022 Aug 24];161(10):5733–44. Available from: https://www.jimmunol.org/content/161/10/5733

320. Mealey KL, Bentjen SA, Gay JM, Cantor GH. Ivermectin sensitivity in collies is associated with a deletion mutation of the mdr1 gene. Pharmacogenet Genomics [Internet]. 2001 Nov [cited 2022 Aug 24];11(8):727–33. Available from: https://journals.lww.com/jpharmacogenetics/Abstract/2001/11000/Ivermectin_sensitivity_in_collies_is_associated.12.aspx

321. Van der Heyden S, Chiers K, Vercauteren G, Daminet S, Wegge B, Paepe D, et al. Expression of Multidrug Resistance-Associated P-Glycoprotein in Feline Tumours. J Comp Pathol [Internet]. 2011 Feb 1 [cited 2021 Jun 16];144(2):164–9. Available from: https://www.sciencedirect.com/science/article/pii/S0021997510001234

322. Hifumi T, Miyoshi N, Kawaguchi H, Nomura K, Yasuda N. Immunohistochemical Detection of Proteins Associated with Multidrug Resistance to Anti-Cancer Drugs in Canine and Feline Primary Pulmonary Carcinoma. J Vet Med Sci. 2010;72(5):665–8.

323. Okai Y, Nakamura N, Matsushiro H, Kato H, Setoguchi A, Yazawa M, et al. Molecular analysis of multidrug resistance in feline lymphoma cells. Am J Vet Res [Internet]. 2000 Sep 1 [cited 2022 Aug 24];61(9):1122–7. Available from: https://avmajournals.avma.org/view/journals/ajvr/61/9/ajvr.2000.61.1122.xml

324. Brenn SH, Couto SS, Craft DM, Leung C, Bergman PJ. Evaluation of P-glycoprotein expression in feline lymphoma and correlation with clinical outcome. Vet Comp Oncol [Internet]. 2008 [cited 2022 Aug 24];6(3):201–11. Available from: https://onlinelibrary.wiley.com/doi/abs/10.1111/j.1476-5829.2008.00161.x

325. Cheng AL, Su IJ, Chen YC, Lee TC, Wang CH. Expression of P-glycoprotein and glutathione-S-transferase in recurrent lymphomas: the possible role of Epstein-Barr virus, immunophenotypes, and other predisposing factors. J Clin Oncol [Internet]. 1993 Jan [cited 2022 Aug 29];11(1):109–15. Available from: https://ascopubs.org/doi/abs/10.1200/JCO.1993.11.1.109

326. Antonelli G, Turriziani O, Cianfriglia M, Riva E, Dong G, Fattorossi A, et al. Resistance of HIV-1 to AZT might also involve the cellular expression of multidrug resistance P-glycoprotein. AIDS Res Hum Retroviruses. 1992 Oct;8(10):1839–44.

327. Andreana A, Aggarwal S, Gollapudi S, Wien D, Tsuruo T, Gupta S. Abnormal Expression of a 170-Kilodalton P-Glycoprotein Encoded by MDR1 Gene, a Metabolically Active Efflux Pump, in CD4+ and CD8+ T Cells from Patients with Human Immunodeficiency Virus Type 1 Infection. AIDS Res Hum Retroviruses [Internet]. 1996 Oct 10 [cited 2022 Aug 30];12(15):1457–62. Available from: https://www.liebertpub.com/doi/abs/10.1089/aid.1996.12.1457

328. Gollapudi S, Gupta S. Human immunodeficiency virus I-induced expression of P-glycoprotein. Biochem Biophys Res Commun [Internet]. 1990 Sep 28 [cited 2021 Jun 22];171(3):1002–7. Available from: https://www.sciencedirect.com/science/article/pii/0006291X9090783J

329. Ashraf T, Ronaldson PT, Persidsky Y, Bendayan R. Regulation of P-glycoprotein by human immunodeficiency virus-1 in primary cultures of human fetal astrocytes. J Neurosci Res. 2011 Nov;89(11):1773–82.

330. Lee CGL, Ramachandra M, Jeang KT, Martin MA, Pastan I, Gottesman MM. Effect of ABC transporters on HIV-1 infection: inhibition of virus production by the MDR1 transporter. FASEB J [Internet]. 2000 [cited 2021 Jun 22];14(3):516–22. Available from: https://faseb.onlinelibrary.wiley.com/doi/abs/10.1096/fasebj.14.3.516

331. Speck RR, Yu XF, Hildreth J, Flexner C. Differential effects of p-glycoprotein and multidrug resistance protein-1 on productive human immunodeficiency virus infection. J Infect Dis. 2002 Aug 1;186(3):332–40.

332. Cory TJ, He H, Winchester LC, Kumar S, Fletcher CV. Alterations in P-Glycoprotein Expression and Function Between Macrophage Subsets. Pharm Res [Internet]. 2016 Nov 1 [cited 2022 Aug 31];33(11):2713–21. Available from: https://doi.org/10.1007/s11095-016-1998-x

333. Choo EF, Leake B, Wandel C, Imamura H, Wood AJ, Wilkinson GR, et al. Pharmacological inhibition of P-glycoprotein transport enhances the distribution of HIV-1 protease inhibitors into brain and testes. Drug Metab Dispos Biol Fate Chem. 2000 Jun;28(6):655–60.

334. Martinec O, Huliciak M, Staud F, Cecka F, Vokral I, Cerveny L. Anti-HIV and Anti-Hepatitis C Virus Drugs Inhibit P-Glycoprotein Efflux Activity in Caco-2 Cells and Precision-Cut Rat and Human Intestinal Slices. Antimicrob Agents Chemother [Internet].

2019 Oct 22 [cited 2022 Aug 5];63(11):e00910-19. Available from: https://journals.asm.org/doi/10.1128/AAC.00910-19

335. van der Sandt IC, Vos CM, Nabulsi L, Blom-Roosemalen MC, Voorwinden HH, de Boer AG, et al. Assessment of active transport of HIV protease inhibitors in various cell lines and the in vitro blood--brain barrier. AIDS Lond Engl. 2001 Mar 9;15(4):483–91.

336. Zhang JC, Xie F, Yu XH, Deng ZY, Wang Y, Liang P, et al. Expression levels of P-glycoprotein in peripheral blood CD8+ T lymphocytes from HIV-1-infected patients on antiretroviral therapy. Int J Mol Med [Internet]. 2014 Feb 1 [cited 2021 Jun 22];33(2):431–40. Available from: https://www.spandidos-publications.com/10.3892/ijmm.2013.1584

337. Sankatsing SUC, Beijnen JH, Schinkel AH, Lange JMA, Prins JM. P Glycoprotein in Human Immunodeficiency Virus Type 1 Infection and Therapy. Antimicrob Agents Chemother [Internet]. 2004 Apr [cited 2022 Aug 5];48(4):1073–81. Available from: https://www.ncbi.nlm.nih.gov/pmc/articles/PMC375313/

338. Beusekom CD van, Lange R, Schrickx JA. A functional model for feline P-glycoprotein. J Vet Pharmacol Ther [Internet]. 2016 [cited 2021 May 17];39(1):95–7. Available from: https://onlinelibrary.wiley.com/doi/abs/10.1111/jvp.12248

339. Millward MJ, Cantwell BM, Munro NC, Robinson A, Corris PA, Harris AL. Oral verapamil with chemotherapy for advanced non-small cell lung cancer: a randomised study. Br J Cancer [Internet]. 1993 May [cited 2022 Aug 29];67(5):1031–5. Available from: https://www.ncbi.nlm.nih.gov/pmc/articles/PMC1968472/

340. Zakeri-Milani P, Valizadeh H. Intestinal transporters: enhanced absorption through P-glycoprotein-related drug interactions. Expert Opin Drug Metab Toxicol [Internet]. 2014 Jun 1 [cited 2022 Aug 26];10(6):859–71. Available from: https://doi.org/10.1517/17425255.2014.905543

341. Mayer U, Wagenaar E, Dorobek B, Beijnen JH, Borst P, Schinkel AH. Full blockade of intestinal P-glycoprotein and extensive inhibition of blood-brain barrier P-glycoprotein by oral treatment of mice with PSC833. J Clin Invest. 1997 Nov 15;100(10):2430–6.

342. Takenaga T, Zhang Z, Muramoto Y, Fehling SK, Hirabayashi A, Takamatsu Y, et al. CP100356 Hydrochloride, a P-Glycoprotein Inhibitor, Inhibits Lassa Virus Entry: Implication of a Candidate Pan-Mammarenavirus Entry Inhibitor. Viruses. 2021 Sep 3;13(9):1763.

343. Belpomme D, Gauthier S, Pujade-Lauraine E, Facchini T, Goudier MJ, Krakowski I, et al. Verapamil increases the survival of patients with anthracycline-resistant metastatic breast carcinoma. Ann Oncol Off J Eur Soc Med Oncol. 2000 Nov;11(11):1471–6.

344. Dolan PT, Whitfield ZJ, Andino R. Mechanisms and Concepts in RNA Virus Population Dynamics and Evolution. Annu Rev Virol [Internet]. 2018 [cited 2022 Sep 30];5(1):69–92. Available from: https://doi.org/10.1146/annurev-virology-101416-041718

345. Robson F, Khan KS, Le TK, Paris C, Demirbag S, Barfuss P, et al. Coronavirus RNA Proofreading: Molecular Basis and Therapeutic Targeting. Mol Cell [Internet]. 2020 Sep 3 [cited 2022 Sep 30];79(5):710–27. Available from: https://www.sciencedirect.com/science/article/pii/S1097276520305189

346. REED LJ, MUENCH H. A SIMPLE METHOD OF ESTIMATING FIFTY PER CENT ENDPOINTS12. Am J Epidemiol [Internet]. 1938 May 1 [cited 2022 Oct 3];27(3):493–7. Available from: https://doi.org/10.1093/oxfordjournals.aje.a118408

347. Madeira F, Pearce M, Tivey ARN, Basutkar P, Lee J, Edbali O, et al. Search and sequence analysis tools services from EMBL-EBI in 2022. Nucleic Acids Res [Internet]. 2022 Apr 1 [cited 2022 Oct 3];gkac240. Available from: https://europepmc.org/articles/PMC9252731

348. Waterhouse A, Bertoni M, Bienert S, Studer G, Tauriello G, Gumienny R, et al. SWISS-MODEL: homology modelling of protein structures and complexes. Nucleic Acids Res. 2018 Jul 2;46(W1):W296–303.

349. Chang KO, Takahashi D, Prakash O, Kim Y. Characterization and inhibition of norovirus proteases of genogroups I and II using a fluorescence resonance energy transfer assay. Virology [Internet]. 2012 Feb 20 [cited 2022 Oct 3];423(2):125–33. Available from: https://www.sciencedirect.com/science/article/pii/S0042682211005599

350. Lamb YN. Nirmatrelvir Plus Ritonavir: First Approval. Drugs [Internet]. 2022 Apr 1 [cited 2022 Oct 3];82(5):585–91. Available from: https://doi.org/10.1007/s40265-022-01692-5

351. Cattaneo D, Cossu MV, Rizzardini G. Pharmacokinetic drug evaluation of ritonavir (versus cobicistat) as adjunctive therapy in the treatment of HIV. Expert Opin Drug Metab Toxicol [Internet]. 2019 Nov 2 [cited 2022 Oct 5];15(11):927–35. Available from: https://doi.org/10.1080/17425255.2019.1685495

352. Marzolini C, Kuritzkes DR, Marra F, Boyle A, Gibbons S, Flexner C, et al. Prescribing Nirmatrelvir–Ritonavir: How to Recognize and Manage Drug–Drug Interactions. Ann Intern Med [Internet]. 2022 Mar 1 [cited 2022 Oct 5];M22-0281. Available from: https://www.ncbi.nlm.nih.gov/pmc/articles/PMC8890619/

353. Ayaz M, Subhan F, Sadiq A, Ullah F, Ahmed J, Sewell RDE. Cellular efflux transporters and the potential role of natural products in combating efflux mediated drug resistance. Front Biosci Landmark Ed. 2017 Jan 1;22(4):732–56.

354. Robey RW, Pluchino KM, Hall MD, Fojo AT, Bates SE, Gottesman MM. Revisiting the role of efflux pumps in multidrug-resistant cancer. Nat Rev Cancer [Internet]. 2018 Jul [cited 2022 Oct 6];18(7):452–64. Available from: https://www.ncbi.nlm.nih.gov/pmc/articles/PMC6622180/

355. Zhu N, Zhang D, Wang W, Li X, Yang B, Song J, et al. A Novel Coronavirus from Patients with Pneumonia in China, 2019. N Engl J Med [Internet]. 2020 Feb 20 [cited 2022 Aug 9];382(8):727–33. Available from: https://www.ncbi.nlm.nih.gov/pmc/articles/PMC7092803/

356. Huang C, Wang Y, Li X, Ren L, Zhao J, Hu Y, et al. Clinical features of patients infected with 2019 novel coronavirus in Wuhan, China. The Lancet [Internet]. 2020 Feb 15 [cited 2022 Aug 9];395(10223):497–506. Available from: https://www.sciencedirect.com/science/article/pii/S0140673620301835

357. Chan JFW, Yuan S, Kok KH, To KKW, Chu H, Yang J, et al. A familial cluster of pneumonia associated with the 2019 novel coronavirus indicating person-to-person transmission: a study of a family cluster. Lancet Lond Engl [Internet]. 2020 [cited 2022 Aug 9];395(10223):514–23. Available from: https://www.ncbi.nlm.nih.gov/pmc/articles/PMC7159286/

358. WHO Coronavirus (COVID-19) Dashboard [Internet]. [cited 2022 Aug 8]. Available from: https://covid19.who.int

359. Gorbalenya AE, Baker SC, Baric RS, de Groot RJ, Drosten C, Gulyaeva AA, et al. The species Severe acute respiratory syndrome-related coronavirus: classifying 2019-nCoV and naming it SARS-CoV-2. Nat Microbiol [Internet]. 2020 Apr [cited 2022 Aug 9];5(4):536–44. Available from: https://www.nature.com/articles/s41564-020-0695-z

360. Bhatt PR, Scaiola A, Loughran G, Leibundgut M, Kratzel A, Meurs R, et al. Structural basis of ribosomal frameshifting during translation of the SARS-CoV-2 RNA genome. Science [Internet]. 2021 Jun 18 [cited 2022 Aug 9];372(6548):1306–13. Available from: https://www.science.org/doi/full/10.1126/science.abf3546

361. Chiara M, D'Erchia AM, Gissi C, Manzari C, Parisi A, Resta N, et al. Next generation sequencing of SARS-CoV-2 genomes: challenges, applications and opportunities. Brief Bioinform [Internet]. 2021 Mar 1 [cited 2022 Aug 9];22(2):616–30. Available from: https://doi.org/10.1093/bib/bbaa297

362. Jungreis I, Sealfon R, Kellis M. SARS-CoV-2 gene content and COVID-19 mutation impact by comparing 44 Sarbecovirus genomes. Nat Commun [Internet]. 2021 May 11 [cited 2022 Aug 9];12(1):2642. Available from: https://www.nature.com/articles/s41467-021-22905-7

363. Lu R, Zhao X, Li J, Niu P, Yang B, Wu H, et al. Genomic characterisation and epidemiology of 2019 novel coronavirus: implications for virus origins and receptor binding. Lancet Lond Engl [Internet]. 2020 [cited 2022 Aug 9];395(10224):565–74. Available from: https://www.ncbi.nlm.nih.gov/pmc/articles/PMC7159086/

364. Tan W, Zhao X, Ma X, Wang W, Niu P, Xu W, et al. A Novel Coronavirus Genome Identified in a Cluster of Pneumonia Cases — Wuhan, China 2019−2020. China CDC Wkly [Internet]. 2020 Jan 1 [cited 2022 Aug 9];2(4):61–2. Available from: https://weekly.chinacdc.cn/en/article/doi/10.46234/ccdcw2020.017

365. Zhou H, Chen X, Hu T, Li J, Song H, Liu Y, et al. A Novel Bat Coronavirus Closely Related to SARS-CoV-2 Contains Natural Insertions at the S1/S2 Cleavage Site of the Spike Protein. Curr Biol [Internet]. 2020 Jun 8 [cited 2022 Sep 16];30(11):2196-2203.e3. Available from: https://www.sciencedirect.com/science/article/pii/S096098222030662X

366. Bosch BJ, van der Zee R, de Haan CAM, Rottier PJM. The Coronavirus Spike Protein Is a Class I Virus Fusion Protein: Structural and Functional Characterization of the Fusion Core Complex. J Virol [Internet]. 2003 Aug 15 [cited 2022 Aug 9];77(16):8801–11. Available from: https://journals.asm.org/doi/full/10.1128/JVI.77.16.8801-8811.2003

367. Lan J, Ge J, Yu J, Shan S, Zhou H, Fan S, et al. Structure of the SARS-CoV-2 spike receptor-binding domain bound to the ACE2 receptor. Nature [Internet]. 2020 May [cited 2022 Aug 10];581(7807):215–20. Available from: https://www.nature.com/articles/s41586-020-2180-5

368. Shang J, Wan Y, Luo C, Ye G, Geng Q, Auerbach A, et al. Cell entry mechanisms of SARS-CoV-2. Proc Natl Acad Sci [Internet]. 2020 May 26 [cited 2022 Sep 16];117(21):11727–34. Available from: https://www.pnas.org/doi/full/10.1073/pnas.2003138117

369. Cantuti-Castelvetri L, Ojha R, Pedro LD, Djannatian M, Franz J, Kuivanen S, et al. Neuropilin-1 facilitates SARS-CoV-2 cell entry and infectivity. Science [Internet]. 2020 Nov 13 [cited 2022 Aug 12];370(6518):856–60. Available from: https://www.science.org/doi/full/10.1126/science.abd2985

370. Daly JL, Simonetti B, Klein K, Chen KE, Williamson MK, Antón-Plágaro C, et al. Neuropilin-1 is a host factor for SARS-CoV-2 infection. Science [Internet]. 2020 Nov 13 [cited 2022 Aug 15];370(6518):861–5. Available from: https://www.science.org/doi/full/10.1126/science.abd3072

371. Wang S, Qiu Z, Hou Y, Deng X, Xu W, Zheng T, et al. AXL is a candidate receptor for SARS-CoV-2 that promotes infection of pulmonary and bronchial epithelial cells. Cell Res [Internet]. 2021 Feb [cited 2022 Aug 12];31(2):126–40. Available from: https://www.nature.com/articles/s41422-020-00460-y

372. Wu C, Zheng M, Yang Y, Gu X, Yang K, Li M, et al. Furin: A Potential Therapeutic Target for COVID-19. iScience [Internet]. 2020 Oct 23 [cited 2022 Aug 10];23(10):101642. Available from: https://www.sciencedirect.com/science/article/pii/S2589004220308348

373. Peacock TP, Goldhill DH, Zhou J, Baillon L, Frise R, Swann OC, et al. The furin cleavage site of SARS-CoV-2 spike protein is a key determinant for transmission due to enhanced replication in airway cells [Internet]. bioRxiv; 2020 [cited 2022 Aug 11]. p. 2020.09.30.318311. Available from: https://www.biorxiv.org/content/10.1101/2020.09.30.318311v1

374. Zhu Y, Feng F, Hu G, Wang Y, Yu Y, Zhu Y, et al. A genome-wide CRISPR screen identifies host factors that regulate SARS-CoV-2 entry. Nat Commun [Internet]. 2021 Feb 11 [cited 2022 Aug 11];12(1):961. Available from: https://www.nature.com/articles/s41467-021-21213-4

375. Jackson CB, Farzan M, Chen B, Choe H. Mechanisms of SARS-CoV-2 entry into cells. Nat Rev Mol Cell Biol [Internet]. 2022 Jan [cited 2022 Aug 10];23(1):3–20. Available from: https://www.nature.com/articles/s41580-021-00418-x

376. Hoffmann M, Kleine-Weber H, Pöhlmann S. A Multibasic Cleavage Site in the Spike Protein of SARS-CoV-2 Is Essential for Infection of Human Lung Cells. Mol Cell. 2020 May 21;78(4):779-784.e5.

377. Ou X, Liu Y, Lei X, Li P, Mi D, Ren L, et al. Characterization of spike glycoprotein of SARS-CoV-2 on virus entry and its immune cross-reactivity with SARS-CoV. Nat Commun. 2020 Mar 27;11(1):1620.

378. Yu S, Zheng X, Zhou B, Li J, Chen M, Deng R, et al. SARS-CoV-2 spike engagement of ACE2 primes S2′ site cleavage and fusion initiation. Proc Natl Acad Sci [Internet]. 2022 Jan 4 [cited 2022 Nov 1];119(1):e2111199119. Available from: https://www.pnas.org/doi/abs/10.1073/pnas.2111199119

379. Benton DJ, Wrobel AG, Xu P, Roustan C, Martin SR, Rosenthal PB, et al. Receptor binding and priming of the spike protein of SARS-CoV-2 for membrane fusion. Nature [Internet]. 2020 Dec [cited 2022 Aug 10];588(7837):327–30. Available from: https://www.nature.com/articles/s41586-020-2772-0

380. Wang MY, Zhao R, Gao LJ, Gao XF, Wang DP, Cao JM. SARS-CoV-2: Structure, Biology, and Structure-Based Therapeutics Development. Front Cell Infect Microbiol [Internet]. 2020 [cited 2022 Oct 3];10. Available from: https://www.frontiersin.org/articles/10.3389/fcimb.2020.587269

381. Korber B, Fischer WM, Gnanakaran S, Yoon H, Theiler J, Abfalterer W, et al. Tracking Changes in SARS-CoV-2 Spike: Evidence that D614G Increases Infectivity of the COVID-19 Virus. Cell [Internet]. 2020 Aug 20 [cited 2022 Aug 12];182(4):812-827.e19. Available from: https://www.sciencedirect.com/science/article/pii/S0092867420308205

382. Wang P, Nair MS, Liu L, Iketani S, Luo Y, Guo Y, et al. Antibody resistance of SARS-CoV-2 variants B.1.351 and B.1.1.7. Nature [Internet]. 2021 May [cited 2022 Aug 11];593(7857):130–5. Available from: https://www.nature.com/articles/s41586-021-03398-2

383. Wang R, Zhang Q, Ge J, Ren W, Zhang R, Lan J, et al. Analysis of SARS-CoV-2 variant mutations reveals neutralization escape mechanisms and the ability to use ACE2 receptors from additional species. Immunity [Internet]. 2021 Jul 13 [cited 2022 Aug 12];54(7):1611-1621.e5. Available from: https://www.sciencedirect.com/science/article/pii/S1074761321002478

384. Tegally H, Wilkinson E, Giovanetti M, Iranzadeh A, Fonseca V, Giandhari J, et al. Detection of a SARS-CoV-2 variant of concern in South Africa. Nature [Internet]. 2021 Apr [cited 2022 Aug 11];592(7854):438–43. Available from: https://www.nature.com/articles/s41586-021-03402-9

385. Liu Z, VanBlargan LA, Bloyet LM, Rothlauf PW, Chen RE, Stumpf S, et al. Identification of SARS-CoV-2 spike mutations that attenuate monoclonal and serum antibody neutralization. Cell Host Microbe [Internet]. 2021 Mar 10 [cited 2022 Aug 12];29(3):477-

488.e4. Available from: https://www.sciencedirect.com/science/article/pii/S1931312821000445

386. Faria N. Genomic characterisation of an emergent SARS-CoV-2 lineage in Manaus: preliminary findings - SARS-CoV-2 coronavirus / nCoV-2019 Genomic Epidemiology [Internet]. Virological. 2021 [cited 2022 Aug 11]. Available from: https://virological.org/t/genomic-characterisation-of-an-emergent-sars-cov-2-lineage-in-manaus-preliminary-findings/586

387. Wang P, Casner RG, Nair MS, Wang M, Yu J, Cerutti G, et al. Increased resistance of SARS-CoV-2 variant P.1 to antibody neutralization. Cell Host Microbe [Internet]. 2021 May 12 [cited 2022 Aug 11];29(5):747-751.e4. Available from: https://www.sciencedirect.com/science/article/pii/S1931312821001839

388. Garcia-Beltran WF, Lam EC, Denis KS, Nitido AD, Garcia ZH, Hauser BM, et al. Multiple SARS-CoV-2 variants escape neutralization by vaccine-induced humoral immunity [Internet]. medRxiv; 2021 [cited 2022 Aug 11]. p. 2021.02.14.21251704. Available from: https://www.medrxiv.org/content/10.1101/2021.02.14.21251704v2

389. Nelson G, Buzko O, Spilman P, Niazi K, Rabizadeh S, Soon-Shiong P. Molecular dynamic simulation reveals E484K mutation enhances spike RBD-ACE2 affinity and the combination of E484K, K417N and N501Y mutations (501Y.V2 variant) induces conformational change greater than N501Y mutant alone, potentially resulting in an escape mutant [Internet]. Biophysics; 2021 Jan [cited 2022 Aug 12]. Available from: http://biorxiv.org/lookup/doi/10.1101/2021.01.13.426558

390. Gu H, Chen Q, Yang G, He L, Fan H, Deng YQ, et al. Adaptation of SARS-CoV-2 in BALB/c mice for testing vaccine efficacy. Science [Internet]. 2020 Sep 25 [cited 2022 Aug 12];369(6511):1603–7. Available from: https://www.science.org/doi/full/10.1126/science.abc4730

391. Lauring AS, Tenforde MW, Chappell JD, Gaglani M, Ginde AA, McNeal T, et al. Clinical severity of, and effectiveness of mRNA vaccines against, covid-19 from omicron, delta, and alpha SARS-CoV-2 variants in the United States: prospective observational study. BMJ [Internet]. 2022 Mar 9 [cited 2022 Sep 16];376:e069761. Available from: https://www.bmj.com/content/376/bmj-2021-069761

392. Saito A, Irie T, Suzuki R, Maemura T, Nasser H, Uriu K, et al. Enhanced fusogenicity and pathogenicity of SARS-CoV-2 Delta P681R mutation. Nature [Internet]. 2022 Feb [cited 2022 Aug 12];602(7896):300–6. Available from: https://www.nature.com/articles/s41586-021-04266-9

393. Hoffmann M, Hofmann-Winkler H, Krüger N, Kempf A, Nehlmeier I, Graichen L, et al. SARS-CoV-2 variant B.1.617 is resistant to bamlanivimab and evades antibodies induced by infection and vaccination. Cell Rep [Internet]. 2021 Jul 20 [cited 2022 Sep 16];36(3):109415. Available from: https://www.sciencedirect.com/science/article/pii/S2211124721008287

394. Liu C, Ginn HM, Dejnirattisai W, Supasa P, Wang B, Tuekprakhon A, et al. Reduced neutralization of SARS-CoV-2 B.1.617 by vaccine and convalescent serum. Cell [Internet]. 2021 Aug 5 [cited 2022 Sep 16];184(16):4220-4236.e13. Available from: https://www.sciencedirect.com/science/article/pii/S0092867421007558

395. Papanikolaou V, Chrysovergis A, Ragos V, Tsiambas E, Katsinis S, Manoli A, et al. From delta to Omicron: S1-RBD/S2 mutation/deletion equilibrium in SARS-CoV-2 defined variants. Gene [Internet]. 2022 Mar 10 [cited 2022 Sep 16];814:146134. Available from: https://www.sciencedirect.com/science/article/pii/S0378111921007290

396. Pulliam JRC, Schalkwyk C van, Govender N, Gottberg A von, Cohen C, Groome MJ, et al. Increased risk of SARS-CoV-2 reinfection associated with emergence of Omicron in South Africa [Internet]. medRxiv; 2022 [cited 2022 Sep 16]. p. 2021.11.11.21266068. Available from: https://www.medrxiv.org/content/10.1101/2021.11.11.21266068v3

397. Riediker M, Briceno-Ayala L, Ichihara G, Albani D, Poffet D, Tsai DH, et al. Higher viral load and infectivity increase risk of aerosol transmission for Delta and Omicron variants of SARS-CoV-2. Swiss Med Wkly [Internet]. 2022 Jan 6 [cited 2022 Sep 16];(1). Available from: https://smw.ch/article/doi/smw.2022.w30133

398. Pérez-Then E, Lucas C, Monteiro VS, Miric M, Brache V, Cochon L, et al. Neutralizing antibodies against the SARS-CoV-2 Delta and Omicron variants following heterologous CoronaVac plus BNT162b2 booster vaccination. Nat Med [Internet]. 2022 Mar [cited 2022 Sep 16];28(3):481–5. Available from: https://www.nature.com/articles/s41591-022-01705-6

399. Ren Z, Sun R, Cui G, Wang H, Zhang D, Li J, et al. Effects of Inactivated Vaccination on Humoral Immune Responses in Patients Infected With Delta or Omicron Variants. J Infect Dis [Internet]. 2022 Jul 5 [cited 2022 Sep 16];jiac274. Available from: https://doi.org/10.1093/infdis/jiac274

400. Andrews N, Stowe J, Kirsebom F, Toffa S, Rickeard T, Gallagher E, et al. Covid-19 Vaccine Effectiveness against the Omicron (B.1.1.529) Variant. N Engl J Med [Internet]. 2022 Apr 21 [cited 2022 Sep 16];386(16):1532–46. Available from: https://www.nejm.org/doi/10.1056/NEJMoa2119451

401. Alexander MR, Schoeder CT, Brown JA, Smart CD, Moth C, Wikswo JP, et al. Predicting susceptibility to SARS-CoV-2 infection based on structural differences in ACE2 across species. FASEB J [Internet]. 2020 [cited 2022 Sep 16];34(12):15946–60. Available from: https://onlinelibrary.wiley.com/doi/abs/10.1096/fj.202001808R

402. Conceicao C, Thakur N, Human S, Kelly JT, Logan L, Bialy D, et al. The SARS-CoV-2 Spike protein has a broad tropism for mammalian ACE2 proteins. PLOS Biol [Internet]. 2020 Dec 21 [cited 2022 Sep 16];18(12):e3001016. Available from: https://journals.plos.org/plosbiology/article?id=10.1371/journal.pbio.3001016

403. Damas J, Hughes GM, Keough KC, Painter CA, Persky NS, Corbo M, et al. Broad host range of SARS-CoV-2 predicted by comparative and structural analysis of ACE2 in

vertebrates. Proc Natl Acad Sci [Internet]. 2020 Sep 8;117(36):22311. Available from: http://www.pnas.org/content/117/36/22311.abstract

404. Molenaar RJ, Vreman S, Hakze-van der Honing RW, Zwart R, de Rond J, Weesendorp E, et al. Clinical and Pathological Findings in SARS-CoV-2 Disease Outbreaks in Farmed Mink (Neovison vison). Vet Pathol [Internet]. 2020 Sep 1 [cited 2022 Aug 15];57(5):653–7. Available from: https://doi.org/10.1177/0300985820943535

405. Oreshkova N, Molenaar RJ, Vreman S, Harders F, Munnink BBO, Honing RWH van der, et al. SARS-CoV-2 infection in farmed minks, the Netherlands, April and May 2020. Eurosurveillance [Internet]. 2020 Jun 11 [cited 2022 Sep 16];25(23):2001005. Available from: https://www.eurosurveillance.org/content/10.2807/1560-7917.ES.2020.25.23.2001005

406. Hammer AS, Quaade ML, Rasmussen TB, Fonager J, Rasmussen M, Mundbjerg K, et al. SARS-CoV-2 Transmission between Mink (Neovison vison) and Humans, Denmark. Emerg Infect Dis [Internet]. 2021 Feb [cited 2022 Sep 16];27(2):547–51. Available from: https://www.ncbi.nlm.nih.gov/pmc/articles/PMC7853580/

407. Fenollar F, Mediannikov O, Maurin M, Devaux C, Colson P, Levasseur A, et al. Mink, SARS-CoV-2, and the Human-Animal Interface. Front Microbiol [Internet]. 2021 [cited 2022 Sep 16];12. Available from: https://www.frontiersin.org/articles/10.3389/fmicb.2021.663815

408. Pomorska-Mól M, Włodarek J, Gogulski M, Rybska M. Review: SARS-CoV-2 infection in farmed minks – an overview of current knowledge on occurrence, disease and epidemiology. Animal [Internet]. 2021 Jul 1 [cited 2022 Sep 16];15(7):100272. Available from: https://www.sciencedirect.com/science/article/pii/S1751731121001142

409. Wang L, Didelot X, Bi Y, Gao GF. Assessing the extent of community spread caused by mink-derived SARS-CoV-2 variants. The Innovation [Internet]. 2021 Aug 28 [cited 2022 Sep 16];2(3):100128. Available from: https://www.sciencedirect.com/science/article/pii/S2666675821000539

410. van Aart AE, Velkers FC, Fischer EAJ, Broens EM, Egberink H, Zhao S, et al. SARS-CoV-2 infection in cats and dogs in infected mink farms. Transbound Emerg Dis [Internet]. [cited 2022 Sep 16];n/a(n/a). Available from: https://onlinelibrary.wiley.com/doi/abs/10.1111/tbed.14173

411. Bosco-Lauth AM, Hartwig AE, Porter SM, Gordy PW, Nehring M, Byas AD, et al. Experimental infection of domestic dogs and cats with SARS-CoV-2: Pathogenesis, transmission, and response to reexposure in cats. Proc Natl Acad Sci [Internet]. 2020 Oct 20 [cited 2022 Sep 16];117(42):26382–8. Available from: https://www.pnas.org/doi/abs/10.1073/pnas.2013102117

412. Shi J, Wen Z, Zhong G, Yang H, Wang C, Huang B, et al. Susceptibility of ferrets, cats, dogs, and other domesticated animals to SARS–coronavirus 2. Science [Internet]. 2020

May 29 [cited 2022 Aug 15];368(6494):1016–20. Available from: https://www.science.org/doi/full/10.1126/science.abb7015

413. Barrs VR, Peiris M, Tam KWS, Law PYT, Brackman CJ, To EMW, et al. SARS-CoV-2 in Quarantined Domestic Cats from COVID-19 Households or Close Contacts, Hong Kong, China. Emerg Infect Dis [Internet]. 2020 Dec [cited 2022 Sep 26];26(12):3071–4. Available from: https://www.ncbi.nlm.nih.gov/pmc/articles/PMC7706951/

414. Halfmann PJ, Hatta M, Chiba S, Maemura T, Fan S, Takeda M, et al. Transmission of SARS-CoV-2 in Domestic Cats. N Engl J Med [Internet]. 2020 Aug 6 [cited 2022 Sep 26];383(6):592–4. Available from: https://doi.org/10.1056/NEJMc2013400

415. Schlottau K, Rissmann M, Graaf A, Schön J, Sehl J, Wylezich C, et al. SARS-CoV-2 in fruit bats, ferrets, pigs, and chickens: an experimental transmission study. Lancet Microbe [Internet]. 2020 Sep 1 [cited 2022 Aug 15];1(5):e218–25. Available from: https://www.sciencedirect.com/science/article/pii/S2666524720300896

416. Sit THC, Brackman CJ, Ip SM, Tam KWS, Law PYT, To EMW, et al. Infection of dogs with SARS-CoV-2. Nature [Internet]. 2020 Oct [cited 2022 Sep 16];586(7831):776–8. Available from: https://www.nature.com/articles/s41586-020-2334-5

417. Yen HL, Sit THC, Brackman CJ, Chuk SSY, Gu H, Tam KWS, et al. Transmission of SARS-CoV-2 delta variant (AY.127) from pet hamsters to humans, leading to onward human-to-human transmission: a case study. The Lancet [Internet]. 2022 Mar 12 [cited 2022 Nov 1];399(10329):1070–8. Available from: https://www.sciencedirect.com/science/article/pii/S0140673622003269

418. Bosco-Lauth AM, Walker A, Guilbert L, Porter S, Hartwig A, McVicker E, et al. Susceptibility of livestock to SARS-CoV-2 infection. Emerg Microbes Infect [Internet]. 2021 Jan 1 [cited 2022 Sep 30];10(1):2199–201. Available from: https://doi.org/10.1080/22221751.2021.2003724

419. Ulrich L, Wernike K, Hoffmann D, Mettenleiter TC, Beer M. Experimental infection of cattle with SARS-CoV-2 [Internet]. bioRxiv; 2020 [cited 2022 Sep 30]. p. 2020.08.25.254474. Available from: https://www.biorxiv.org/content/10.1101/2020.08.25.254474v1

420. Pusterla N, Chaillon A, Ignacio C, Smith DM, Barnum S, Lawton KOY, et al. SARS-CoV-2 Seroconversion in an Adult Horse with Direct Contact to a COVID-19 Individual. Viruses. 2022 May 14;14(5):1047.

421. Kuchipudi SV, Surendran-Nair M, Ruden RM, Yon M, Nissly RH, Vandegrift KJ, et al. Multiple spillovers from humans and onward transmission of SARS-CoV-2 in white-tailed deer. Proc Natl Acad Sci [Internet]. 2022 Feb 8 [cited 2022 Aug 15];119(6):e2121644119. Available from: https://www.pnas.org/doi/abs/10.1073/pnas.2121644119

422. Palmer MV, Martins M, Falkenberg S, Buckley A, Caserta LC, Mitchell PK, et al. Susceptibility of White-Tailed Deer (Odocoileus virginianus) to SARS-CoV-2. J Virol

[Internet]. 2021 May 10 [cited 2022 Sep 16];95(11):e00083-21. Available from: https://journals.asm.org/doi/full/10.1128/JVI.00083-21

423. Porter SM, Hartwig AE, Bielefeldt-Ohmann H, Bosco-Lauth AM, Root JJ. Susceptibility of wild canids to severe acute respiratory syndrome coronavirus 2 (SARS-CoV-2) [Internet]. bioRxiv; 2022 [cited 2022 Aug 15]. p. 2022.01.27.478082. Available from: https://www.biorxiv.org/content/10.1101/2022.01.27.478082v1

424. Dinnon KH, Leist SR, Schäfer A, Edwards CE, Martinez DR, Montgomery SA, et al. A mouse-adapted model of SARS-CoV-2 to test COVID-19 countermeasures. Nature [Internet]. 2020 Oct [cited 2022 Sep 22];586(7830):560–6. Available from: https://www.nature.com/articles/s41586-020-2708-8

425. Leist SR, Dinnon KH, Schäfer A, Tse LV, Okuda K, Hou YJ, et al. A Mouse-Adapted SARS-CoV-2 Induces Acute Lung Injury and Mortality in Standard Laboratory Mice. Cell [Internet]. 2020 Nov 12 [cited 2022 Sep 22];183(4):1070-1085.e12. Available from: https://www.ncbi.nlm.nih.gov/pmc/articles/PMC7510428/

426. Muruato A, Vu MN, Johnson BA, Davis-Gardner ME, Vanderheiden A, Lokugamage K, et al. Mouse-adapted SARS-CoV-2 protects animals from lethal SARS-CoV challenge. PLOS Biol [Internet]. 2021 Nov 4 [cited 2022 Sep 22];19(11):e3001284. Available from: https://journals.plos.org/plosbiology/article?id=10.1371/journal.pbio.3001284

427. Bao L, Deng W, Huang B, Gao H, Liu J, Ren L, et al. The pathogenicity of SARS-CoV-2 in hACE2 transgenic mice. Nature [Internet]. 2020 Jul [cited 2022 Sep 22];583(7818):830–3. Available from: https://www.nature.com/articles/s41586-020-2312-y%5C

428. Hong W, Yang J, Bi Z, He C, Lei H, Yu W, et al. A mouse model for SARS-CoV-2-induced acute respiratory distress syndrome. Signal Transduct Target Ther [Internet]. 2021 Jan 1 [cited 2022 Sep 22];6(1):1–3. Available from: https://www.nature.com/articles/s41392-020-00451-w

429. Jiang RD, Liu MQ, Chen Y, Shan C, Zhou YW, Shen XR, et al. Pathogenesis of SARS-CoV-2 in Transgenic Mice Expressing Human Angiotensin-Converting Enzyme 2. Cell [Internet]. 2020 Jul 9 [cited 2022 Sep 22];182(1):50-58.e8. Available from: https://www.sciencedirect.com/science/article/pii/S009286742030622X

430. Park JG, Pino PA, Akhter A, Alvarez X, Torrelles JB, Martinez-Sobrido L. Animal Models of COVID-19: Transgenic Mouse Model. In: Chu JJH, Ahidjo BA, Mok CK, editors. SARS-CoV-2: Methods and Protocols [Internet]. New York, NY: Springer US; 2022 [cited 2022 Sep 22]. p. 259–89. (Methods in Molecular Biology). Available from: https://doi.org/10.1007/978-1-0716-2111-0_16

431. Sun SH, Chen Q, Gu HJ, Yang G, Wang YX, Huang XY, et al. A Mouse Model of SARS-CoV-2 Infection and Pathogenesis. Cell Host Microbe [Internet]. 2020 Jul 8 [cited 2022 Sep 22];28(1):124-133.e4. Available from: https://www.sciencedirect.com/science/article/pii/S1931312820303024

432. Winkler ES, Bailey AL, Kafai NM, Nair S, McCune BT, Yu J, et al. SARS-CoV-2 infection of human ACE2-transgenic mice causes severe lung inflammation and impaired function. Nat Immunol [Internet]. 2020 Nov [cited 2022 Sep 22];21(11):1327–35. Available from: https://www.nature.com/articles/s41590-020-0778-2

433. Martina BEE, Haagmans BL, Kuiken T, Fouchier RAM, Rimmelzwaan GF, van Amerongen G, et al. SARS virus infection of cats and ferrets. Nature [Internet]. 2003 Oct [cited 2022 Aug 15];425(6961):915–915. Available from: https://www.nature.com/articles/425915a

434. Ciurkiewicz M, Armando F, Schreiner T, de Buhr N, Pilchová V, Krupp-Buzimikic V, et al. Ferrets are valuable models for SARS-CoV-2 research. Vet Pathol [Internet]. 2022 Jul 1 [cited 2022 Aug 15];59(4):661–72. Available from: https://doi.org/10.1177/03009858211071012

435. Kim YI, Kim SG, Kim SM, Kim EH, Park SJ, Yu KM, et al. Infection and Rapid Transmission of SARS-CoV-2 in Ferrets. Cell Host Microbe [Internet]. 2020 May 13 [cited 2022 Aug 15];27(5):704-709.e2. Available from: https://www.sciencedirect.com/science/article/pii/S1931312820301876

436. Monchatre-Leroy E, Lesellier S, Wasniewski M, Picard-Meyer E, Richomme C, Boué F, et al. Hamster and ferret experimental infection with intranasal low dose of a single strain of SARS-CoV-2. J Gen Virol [Internet]. 2021 Feb 19 [cited 2022 Aug 15];102(3):001567. Available from: https://www.ncbi.nlm.nih.gov/pmc/articles/PMC8515860/

437. McMahan K, Giffin V, Tostanoski LH, Chung B, Siamatu M, Suthar MS, et al. Reduced pathogenicity of the SARS-CoV-2 omicron variant in hamsters. Med [Internet]. 2022 Apr 8 [cited 2022 Aug 15];3(4):262-268.e4. Available from: https://www.sciencedirect.com/science/article/pii/S2666634022001325

438. Sia SF, Yan LM, Chin AWH, Fung K, Choy KT, Wong AYL, et al. Pathogenesis and transmission of SARS-CoV-2 in golden hamsters. Nature [Internet]. 2020 Jul [cited 2022 Aug 15];583(7818):834–8. Available from: https://www.nature.com/articles/s41586-020-2342-5

439. Mulka KR, Beck SE, Solis CV, Johanson AL, Queen SE, McCarron ME, et al. Progression and Resolution of Severe Acute Respiratory Syndrome Coronavirus 2 (SARS-CoV-2) Infection in Golden Syrian Hamsters. Am J Pathol [Internet]. 2022 Feb 1 [cited 2022 Aug 15];192(2):195–207. Available from: https://www.sciencedirect.com/science/article/pii/S0002944021004727

440. Deng W, Bao L, Liu J, Xiao C, Liu J, Xue J, et al. Primary exposure to SARS-CoV-2 protects against reinfection in rhesus macaques. Science [Internet]. 2020 Aug 14 [cited 2022 Aug 15];369(6505):818–23. Available from: https://www.science.org/doi/full/10.1126/science.abc5343

441. Kim Y, Gaudreault NN, Meekins DA, Perera KD, Bold D, Trujillo JD, et al. Effects of Spike Mutations in SARS-CoV-2 Variants of Concern on Human or Animal ACE2-

Mediated Virus Entry and Neutralization. Microbiol Spectr [Internet]. 2022 May 31 [cited 2022 Sep 30];10(3):e01789-21. Available from: https://journals.asm.org/doi/10.1128/spectrum.01789-21

442. Wacharapluesadee S, Tan CW, Maneeorn P, Duengkae P, Zhu F, Joyjinda Y, et al. Evidence for SARS-CoV-2 related coronaviruses circulating in bats and pangolins in Southeast Asia. Nat Commun [Internet]. 2021 Feb 9 [cited 2022 Sep 30];12(1):972. Available from: https://www.nature.com/articles/s41467-021-21240-1

443. Delahay RJ, de la Fuente J, Smith GC, Sharun K, Snary EL, Flores Girón L, et al. Assessing the risks of SARS-CoV-2 in wildlife. One Health Outlook [Internet]. 2021 Apr 7 [cited 2022 Sep 30];3(1):7. Available from: https://doi.org/10.1186/s42522-021-00039-6

444. Hedman HD, Krawczyk E, Helmy YA, Zhang L, Varga C. Host Diversity and Potential Transmission Pathways of SARS-CoV-2 at the Human-Animal Interface. Pathogens [Internet]. 2021 Feb [cited 2022 Sep 30];10(2):180. Available from: https://www.mdpi.com/2076-0817/10/2/180

445. Prince T, Smith SL, Radford AD, Solomon T, Hughes GL, Patterson EI. SARS-CoV-2 Infections in Animals: Reservoirs for Reverse Zoonosis and Models for Study. Viruses [Internet]. 2021 Mar [cited 2022 Sep 30];13(3):494. Available from: https://www.mdpi.com/1999-4915/13/3/494

446. Oude Munnink BB, Sikkema RS, Nieuwenhuijse DF, Molenaar RJ, Munger E, Molenkamp R, et al. Transmission of SARS-CoV-2 on mink farms between humans and mink and back to humans. Science. 2021 Jan 8;371(6525):172–7.

447. van Aart AE, Velkers FC, Fischer EAJ, Broens EM, Egberink H, Zhao S, et al. SARS-CoV-2 infection in cats and dogs in infected mink farms. Transbound Emerg Dis [Internet]. 2022 [cited 2022 Sep 30];69(5):3001–7. Available from: https://onlinelibrary.wiley.com/doi/abs/10.1111/tbed.14173

448. Michelitsch A, Wernike K, Ulrich L, Mettenleiter TC, Beer M. Chapter Three - SARS-CoV-2 in animals: From potential hosts to animal models. In: Kielian M, Mettenleiter TC, Roossinck MJ, editors. Advances in Virus Research [Internet]. Academic Press; 2021 [cited 2022 Sep 30]. p. 59–102. Available from: https://www.sciencedirect.com/science/article/pii/S0065352721000051

449. COVID-19 [Internet]. WOAH - World Organisation for Animal Health. [cited 2022 Sep 30]. Available from: https://www.woah.org/en/what-we-offer/emergency-and-resilience/covid-19/

450. Fritz M, Rosolen B, Krafft E, Becquart P, Elguero E, Vratskikh O, et al. High prevalence of SARS-CoV-2 antibodies in pets from COVID-19+ households. One Health [Internet]. 2020 Dec 20 [cited 2022 Sep 30];11:100192. Available from: https://www.sciencedirect.com/science/article/pii/S2352771420302937

451. Kim YI, Kim SG, Kim SM, Kim EH, Park SJ, Yu KM, et al. Infection and Rapid Transmission of SARS-CoV-2 in Ferrets. Cell Host Microbe [Internet]. 2020 May 13 [cited 2022 Sep 30];27(5):704-709.e2. Available from: https://www.sciencedirect.com/science/article/pii/S1931312820301876

452. Harvey WT, Carabelli AM, Jackson B, Gupta RK, Thomson EC, Harrison EM, et al. SARS-CoV-2 variants, spike mutations and immune escape. Nat Rev Microbiol [Internet]. 2021 Jul [cited 2022 Sep 30];19(7):409–24. Available from: https://www.nature.com/articles/s41579-021-00573-0

453. Otto SP, Day T, Arino J, Colijn C, Dushoff J, Li M, et al. The origins and potential future of SARS-CoV-2 variants of concern in the evolving COVID-19 pandemic. Curr Biol [Internet]. 2021 Jul 26 [cited 2022 Sep 30];31(14):R918–29. Available from: https://www.sciencedirect.com/science/article/pii/S0960982221008782

454. CDC. Coronavirus Disease 2019 (COVID-19) [Internet]. Centers for Disease Control and Prevention. 2020 [cited 2022 Sep 30]. Available from: https://www.cdc.gov/coronavirus/2019-ncov/variants/index.html

455. Letko M, Seifert SN, Olival KJ, Plowright RK, Munster VJ. Bat-borne virus diversity, spillover and emergence. Nat Rev Microbiol [Internet]. 2020 Aug [cited 2022 Sep 16];18(8):461–71. Available from: https://www.nature.com/articles/s41579-020-0394-z

456. Yan R, Zhang Y, Li Y, Ye F, Guo Y, Xia L, et al. Structural basis for the different states of the spike protein of SARS-CoV-2 in complex with ACE2. Cell Res [Internet]. 2021 Jun [cited 2022 Aug 12];31(6):717–9. Available from: https://www.nature.com/articles/s41422-021-00490-0

457. Hoffmann M, Kleine-Weber H, Schroeder S, Krüger N, Herrler T, Erichsen S, et al. SARS-CoV-2 Cell Entry Depends on ACE2 and TMPRSS2 and Is Blocked by a Clinically Proven Protease Inhibitor. Cell [Internet]. 2020 Apr 16 [cited 2022 Sep 16];181(2):271-280.e8. Available from: https://www.sciencedirect.com/science/article/pii/S0092867420302294

458. Piccoli L, Park YJ, Tortorici MA, Czudnochowski N, Walls AC, Beltramello M, et al. Mapping Neutralizing and Immunodominant Sites on the SARS-CoV-2 Spike Receptor-Binding Domain by Structure-Guided High-Resolution Serology. Cell [Internet]. 2020 Nov 12 [cited 2022 Aug 12];183(4):1024-1042.e21. Available from: https://www.sciencedirect.com/science/article/pii/S0092867420312344

459. Ozono S, Zhang Y, Ode H, Sano K, Tan TS, Imai K, et al. SARS-CoV-2 D614G spike mutation increases entry efficiency with enhanced ACE2-binding affinity. Nat Commun [Internet]. 2021 Feb 8 [cited 2022 Sep 30];12(1):848. Available from: https://www.nature.com/articles/s41467-021-21118-2

460. Pandey K, Acharya A, Mohan M, Ng CL, Reid SP, Byrareddy SN. Animal models for SARS-CoV-2 research: A comprehensive literature review. Transbound Emerg Dis [Internet]. 2021 [cited 2022 Sep 30];68(4):1868–85. Available from: https://onlinelibrary.wiley.com/doi/abs/10.1111/tbed.13907

461. Niu Z, Zhang Z, Gao X, Du P, Lu J, Yan B, et al. N501Y mutation imparts cross-species transmission of SARS-CoV-2 to mice by enhancing receptor binding. Signal Transduct Target Ther [Internet]. 2021 Jul 27 [cited 2022 Sep 30];6(1):1–3. Available from: https://www.nature.com/articles/s41392-021-00704-2

462. Chan JFW, Zhang AJ, Yuan S, Poon VKM, Chan CCS, Lee ACY, et al. Simulation of the Clinical and Pathological Manifestations of Coronavirus Disease 2019 (COVID-19) in a Golden Syrian Hamster Model: Implications for Disease Pathogenesis and Transmissibility. Clin Infect Dis [Internet]. 2020 Nov 1 [cited 2022 Sep 30];71(9):2428–46. Available from: https://doi.org/10.1093/cid/ciaa325

463. Imai M, Iwatsuki-Horimoto K, Hatta M, Loeber S, Halfmann PJ, Nakajima N, et al. Syrian hamsters as a small animal model for SARS-CoV-2 infection and countermeasure development. Proc Natl Acad Sci [Internet]. 2020 Jul 14 [cited 2022 Sep 30];117(28):16587–95. Available from: https://www.pnas.org/doi/abs/10.1073/pnas.2009799117

464. Rosenke K, Meade-White K, Letko M, Clancy C, Hansen F, Liu Y, et al. Defining the Syrian hamster as a highly susceptible preclinical model for SARS-CoV-2 infection. Emerg Microbes Infect [Internet]. 2020 Jan 1 [cited 2022 Sep 30];9(1):2673–84. Available from: https://doi.org/10.1080/22221751.2020.1858177

465. Matsuyama S, Nao N, Shirato K, Kawase M, Saito S, Takayama I, et al. Enhanced isolation of SARS-CoV-2 by TMPRSS2-expressing cells. Proc Natl Acad Sci [Internet]. 2020 Mar 31 [cited 2022 Sep 30];117(13):7001–3. Available from: https://www.pnas.org/doi/abs/10.1073/pnas.2002589117

466. Bosco-Lauth AM, Root JJ, Porter SM, Walker AE, Guilbert L, Hawvermale D, et al. Survey of peridomestic mammal susceptibility to SARS-CoV-2 infection [Internet]. bioRxiv; 2021 [cited 2022 Sep 30]. p. 2021.01.21.427629. Available from: https://www.biorxiv.org/content/10.1101/2021.01.21.427629v1

467. Francisco R, Hernandez SM, Mead DG, Adcock KG, Burke SC, Nemeth NM, et al. Experimental Susceptibility of North American Raccoons (Procyon lotor) and Striped Skunks (Mephitis mephitis) to SARS-CoV-2. Front Vet Sci [Internet]. 2022 Jan 12 [cited 2022 Sep 30];8:715307. Available from: https://www.ncbi.nlm.nih.gov/pmc/articles/PMC8790025/

468. Griffin BD, Chan M, Tailor N, Mendoza EJ, Leung A, Warner BM, et al. SARS-CoV-2 infection and transmission in the North American deer mouse. Nat Commun [Internet]. 2021 Jun 14 [cited 2022 Sep 30];12(1):3612. Available from: https://www.nature.com/articles/s41467-021-23848-9

469. Mykytyn AZ, Lamers MM, Okba NMA, Breugem TI, Schipper D, van den Doel PB, et al. Susceptibility of rabbits to SARS-CoV-2. Emerg Microbes Infect [Internet]. 2021 Jan 1 [cited 2022 Sep 30];10(1):1–7. Available from: https://doi.org/10.1080/22221751.2020.1868951

470. Newman A, Smith D, Ghai RR, Wallace RM, Torchetti MK, Loiacono C, et al. First Reported Cases of SARS-CoV-2 Infection in Companion Animals — New York, March–April 2020. Morb Mortal Wkly Rep [Internet]. 2020 Jun 12 [cited 2022 Sep 30];69(23):710–3. Available from: https://www.ncbi.nlm.nih.gov/pmc/articles/PMC7315787/

471. Patterson EI, Elia G, Grassi A, Giordano A, Desario C, Medardo M, et al. Evidence of exposure to SARS-CoV-2 in cats and dogs from households in Italy. Nat Commun [Internet]. 2020 Dec 4 [cited 2022 Sep 30];11(1):6231. Available from: https://www.nature.com/articles/s41467-020-20097-0).

472. Sailleau C, Dumarest M, Vanhomwegen J, Delaplace M, Caro V, Kwasiborski A, et al. First detection and genome sequencing of SARS-CoV-2 in an infected cat in France. Transbound Emerg Dis [Internet]. 2020 [cited 2022 Sep 30];67(6):2324–8. Available from: https://onlinelibrary.wiley.com/doi/abs/10.1111/tbed.13659

473. Liu K, Tan S, Niu S, Wang J, Wu L, Sun H, et al. Cross-species recognition of SARS-CoV-2 to bat ACE2. Proc Natl Acad Sci [Internet]. 2021 Jan 5 [cited 2022 Sep 30];118(1):e2020216118. Available from: https://www.pnas.org/doi/abs/10.1073/pnas.2020216118

474. Li Q, Nie J, Wu J, Zhang L, Ding R, Wang H, et al. SARS-CoV-2 501Y.V2 variants lack higher infectivity but do have immune escape. Cell [Internet]. 2021 Apr 29 [cited 2022 Sep 30];184(9):2362-2371.e9. Available from: https://www.sciencedirect.com/science/article/pii/S0092867421002312

475. Wang C, Zheng Y, Niu Z, Jiang X, Sun Q. The virological impacts of SARS-CoV-2 D614G mutation. J Mol Cell Biol [Internet]. 2021 Oct 1 [cited 2022 Sep 30];13(10):712–20. Available from: https://doi.org/10.1093/jmcb/mjab045

476. Yurkovetskiy L, Wang X, Pascal KE, Tomkins-Tinch C, Nyalile TP, Wang Y, et al. Structural and Functional Analysis of the D614G SARS-CoV-2 Spike Protein Variant. Cell [Internet]. 2020 Oct 29 [cited 2022 Sep 30];183(3):739-751.e8. Available from: https://www.sciencedirect.com/science/article/pii/S0092867420312290

477. Hou YJ, Chiba S, Halfmann P, Ehre C, Kuroda M, Dinnon KH, et al. SARS-CoV-2 D614G variant exhibits efficient replication ex vivo and transmission in vivo. Science [Internet]. 2020 Dec 18 [cited 2022 Sep 30];370(6523):1464–8. Available from: https://www.science.org/doi/full/10.1126/science.abe8499

478. Plante JA, Liu Y, Liu J, Xia H, Johnson BA, Lokugamage KG, et al. Spike mutation D614G alters SARS-CoV-2 fitness. Nature [Internet]. 2021 Apr [cited 2022 Sep 30];592(7852):116–21. Available from: https://www.nature.com/articles/s41586-020-2895-3

479. Hu J, He CL, Gao QZ, Zhang GJ, Cao XX, Long QX, et al. D614G mutation of SARS-CoV-2 spike protein enhances viral infectivity [Internet]. bioRxiv; 2020 [cited 2022 Sep

30]. p. 2020.06.20.161323. Available from: https://www.biorxiv.org/content/10.1101/2020.06.20.161323v2

480. Johnson MC, Lyddon TD, Suarez R, Salcedo B, LePique M, Graham M, et al. Optimized Pseudotyping Conditions for the SARS-COV-2 Spike Glycoprotein. J Virol [Internet]. 2020 Oct 14 [cited 2022 Sep 30];94(21):e01062-20. Available from: https://journals.asm.org/doi/full/10.1128/JVI.01062-20

481. Li Q, Wu J, Nie J, Zhang L, Hao H, Liu S, et al. The Impact of Mutations in SARS-CoV-2 Spike on Viral Infectivity and Antigenicity. Cell [Internet]. 2020 Sep 3 [cited 2022 Sep 30];182(5):1284-1294.e9. Available from: https://www.sciencedirect.com/science/article/pii/S0092867420308771

482. Zhang L, Jackson CB, Mou H, Ojha A, Peng H, Quinlan BD, et al. SARS-CoV-2 spike-protein D614G mutation increases virion spike density and infectivity. Nat Commun [Internet]. 2020 Nov 26 [cited 2022 Sep 30];11(1):6013. Available from: https://www.nature.com/articles/s41467-020-19808-4